UNIVERSITÉ D'OTTAWA
UNIVERSITY OF OTTAWA

A thesis submitted to the
School of Graduate Studies and Research

In partial fulfillment of the requirement
for the degree of
Philosophical Doctor of Science

In the Ottawa-Carleton Chemistry Institute
Department of Chemistry
University of Ottawa
Ottawa, Ontario
Canada

May 1996

Candidate	Supervisor
Seán Thomas Barry	Professor Darrin Richeson

Compounds with Mixed Ligand Systems as Precursors for Thermal Synthesis of III-V Extended Solids: Halo-Pnictido, Alkyl-Pnictido, and Siloxo-Pnictido Complexes of Gallium and Indium

Seán Thomas Barry

A 350 word abstract for the thesis entitled

"Compounds with Mixed Ligand Systems as Precursors for Thermal Synthesis of III-V Extended Solids: Halo-Pnictido, Alkyl-Pnictido, and Siloxo-Pnictido Complexes of Gallium and Indium"

by: Seán Thomas Barry

The compounds $MN(SiMe_3)_2Cl_2$.base (**1**: M = Ga, base = thf; **2**: M = In, base = pyridine) were synthesised. Compound **1** disproportionated to gallium trichloride while **2** did not show any thermal reactivity.

The compounds $[Ga(R)_2N(SiMe_3)_2]_2$ (**3**: R = ^{n}Bu, **4**: R = ^{t}Bu) were synthesised. Complex **4** decomposed into several products at 400°C, while **3** thermolysed to form hexagonal GaN at 400°C, after annealing at 900°C.

Phosphido analogues of these, $[Ga(^nBu)(R)P(SiMe_3)_2]_2$ (**5**: R = ^{n}Bu, **6**: R = Cl) as well as $[(^nBu)_2InP(SiMe_3)_2]_2$ (**7**) were synthesised. Complex **5** thermally rearranged to GaP at 250°C.. NMR studies determined that although the side product Me_3SiCl was formed in the thermolysis of **6**, several products resulted and the desired phosphinido was isolated. The thermolysis of **7** at 400°C produced both InP and In^0.

A series of primary amido gallium alkyl complexes: $[^tBu_2Ga(\mu\text{-}N(H)^tBu)]_2$ (**8**), $[^nBu_2Ga(N(H)^tBu)]_2$ (**9**), $^nBu_2Ga[NH(2,6\text{-}Me_2C_6H_3)]py$ (**10**) and $^nBu_2Ga[NH(2,6\text{-}Me_2C_6H_3)]_2[Li(Et_2O)]$ (**11**) were synthesised.. Thermolysis of **8** at 120°C gave a compound which ^{1}H NMR characterisation suggested was $[^tBuGaN^tBu]_x$ but the extreme air sensitivity of this compound precluded characterization. Compound **9** was robust to

thermolysis. Compounds **10** and **11** formed many products upon thermolysis at 170°C and 155°C respectively.

The siloxide compounds $M(OSiMe_3)_{3-x}Cl_x.py$ (**12**: M = Ga, X = 0; **13**: M = Ga, X = 1, **14**: M = In, X = 0; **15**: M = In, X = 1) were synthesised. All demonstrated elimination of $(Me_3Si)_2O$ as determined by ^1H NMR and MS, with only **12** forming any undesirable side-products. Thermolysis products were not isolated.

A series of trimethylsilylamido-siloxo complexes: $Ga(N(SiMe_3)_2)(OSiMe_3)_2py$ (**17**), $[Li(thf)_2][Ga(N(SiMe_3)_2)(OSiMe_3)_2Cl]$ (**16**), $[Li(py)_2][In(N(SiMe_3)_2)(OSiMe_3)_2Cl]$ (**18**), and $[Li(py)_2][In(N(SiMe_3)_2)(OSiMe_3)_3]$ (**19**) were synthesised. **17** thermolised to a grey powder, which evolves into hexagonal GaN upon heating at 900°C. Thermolysis experiments of compounds **16**, **18**, and **19** indicate a more complex rearrangement process than for **17**; they do not proceed smoothly to yield the III-V nitride.

Lastly, $[In(N(SiMe_3)_2)(\mu^2\text{-}O)]_x$ (**20**) was prepared from hexane in the absence of coordinating base. It was characterised by ^1H NMR, elemental analysis and MS, but its crystallinity precluded a single-crystal XRD to establish the extent of oligomerisation.

Dedicated to my father:

Thomas Harold Barry
July 30, 1941-April 2, 1981

In memoriam

Acknowledgments

First and foremost, I would like to acknowledge Darrin Richeson, who has taught me more than any other one person I have known. His expert knowledge and inventive nature are enhanced by an enthusiasm that is heart-warming and infectious. He *is* the best supervisor; and a good friend.

I have also had the honour to know Sandro Gambarotta during my time at the University of Ottawa. His professionalism and dedication have encouraged me and his sense of humour sets him apart.

I owe both Susanah Scott and Christian Detellier a large debt of gratitude for their encouragement and tutelage over the years I have spent here. I am glad to have had the input of these scientists on the present work.

I also thank the support staff, particularly Corinne Bensimon for the great amount of work she did in helping to characterise all of the compounds I present herein. I also specially thank Glen Facey for excellent help and suggestions concerning NMR.

I thank the coworkers who have made our lab both a distinctive and enjoyable place to work. In particular, I thank Stéphanie Belhumeur. Her cursory work on the phosphide chemistry presented herein launched that work. As well, Yuanlin Zhou, Irina Kargina, Frédéric Guerin and Stephen Foley have lent aspects to the way I work and think about chemistry that I consider invaluable.

My family has given me the love and support necessary to continue: My mother, Nancy, has my undying love and gratitude. My step-father Sterling, who I love and thank for everything he has done for me. My twin Steven, who means more to me than I can ever say; whom I could not live without. My errant sister Kathleen, for continually challenging what I accept, and being an open and loving person. My very best friend Erin, who is not a member of my immediate family in name alone, who has been on my mind and in my heart from the day I met her. And Cameron, who lives on in my thoughts.

My friends provided support, interpretation and challenge that helped me grow into myself. Shirin Lal, my sweet love, who has helped and supported me, without condition. Jason Copple, who continually demonstrates the difference between being strong and acting strong. David O'Meara, for his willing and provoking input into my work, his support and help are measureless. Andrea Skillen, for assuring and reassuring me that it could be done. I would also like to thank Paul Griffin, Leigh Irvine, James Torck, Kelly Torck, Annette Lee, Jeff Hardill, Leona McCharles and Nicholas Higgs. Finally, the staff of Boko Bakery, for keeping my strength up.

Abstract

The compounds $MN(SiMe_3)_2Cl_2$.base (**1**: M = Ga, base = thf; **2**: M = In, base = pyridine) were synthesised and found to not produce for GaN and InN respectively, at the temperatures studied. Compound **1** disproportionated to allow isolation of gallium trichloride while **2** did not show any reactivity.

The compounds $[Ga(R)_2N(SiMe_3)_2]_2$ (**3**: R = ^{n}Bu, **4**: R = ^{t}Bu) were synthesised and characterised by NMR, IR and EA. These complexes showed different thermal behaviour. Complex **4** decomposed into several products above 400°C which were not readily characterisable, while **3** thermolysed to form hexagonal GaN at 400°C, after annealing at 900°C.

Phosphido analogues to these, $[Ga(^nBu)(R)P(SiMe_3)_2]_2$ (**5**: R = ^{n}Bu, **6**: R = Cl) were synthesised and characterised by NMR, IR and EA. Complex **5** thermally rearranges to GaP at a temperature as low as 250°C. Attempts to make a phosphinido to mimic the intermediate of this transformation by thermolysing **6** was not successful. NMR studies determined that although the appropriate side product (Me_3SiCl) was formed in the thermolysis of **6**, several other products formed and separation of these was not possible. As well, the compound $[(^nBu)_2InP(SiMe_3)_2]_2$ (**7**) was synthesised and characterised by NMR, IR and EA. Its thermolysis at 400°C produced both InP and In^0. NMR studies of the side-products of this reaction show formation of isobutene, suggesting that β-hydrogen elimination had occurred.

A series of primary amido gallium alkyl complexes that includes the base-free dimers, $[^tBu_2Ga(\mu\text{-}N(H)^tBu)]_2$ (**8**) and $[^nBu_2Ga(N(H)^tBu)]_2$ (**9**), the Lewis base stabilized monomeric complex, $^nBu_2Ga[NH(2,6\text{-}Me_2C_6H_3)]py$ (**10**) and an anionic complex, $^nBu_2Ga[NH(2,6\text{-}Me_2C_6H_3)]_2[Li(Et_2O)]$ (**11**) were synthesised. Complex **8** crystallizes in the triclinic space group P-1 (a=10.265(5)Å, b=15.752(6)Å, c=8.932(4)Å, α=90.32(3), β=105.61(3), γ=88.24(4))with two molecules, each residing on an inversion center, in the asymmetric unit. Thermolysis of this species at 120°C gave a compound which NMR characterization suggests is $[^tBuGaN^tBu]_x$ but the extreme air sensitivity of this compound and its tetrahydrofuran adduct precluded full characterization.

The use of excess amido ligand allowed the isolation and crystallization of **11**. Complex **11** crystallized in the monoclinic space group $P2_1/n$ (a=8.666(2)Å, b=22.305(3)Å, c=15.570(3)Å, β=103.47(2))with Z = 4. A bridging interaction of the lithium cation with the lone pair of electrons on each of amido nitrogen atoms generates a molecular core which is made up of a planar Ga-N1-Li-N2 distorted square (N1-Ga1-N2 94.4°, Ga1-N2-Li1 86.2°, N1-Li1-N2 92.2°, Ga1-N1-Li1 87.1).

As well, a series of siloxide compounds of indium and gallium were synthesised to test their thermal reactivity. The series of compounds $M(OSiMe_3)_{3-x}Cl_x.py$ (**12**: M = Ga, X = 0; **13**: M = Ga, X = 1, **14**: M = In, X = 0; **15**: M = In, X = 1) all demonstrated elimination of $(Me_3Si)_2O$ as determined by ^1H NMR and MS, with only **12** forming any undesirable side-products.

A series of mixed trimethylsilylamido-siloxo complexes of gallium and indium have been prepared as potential precursors to GaN and InN. The complex $Ga(N(SiMe_3)_2)(OSiMe_3)_2py$ (**17**) undergoes a smooth thermolysis to yield a grey powder, $(Me_3Si)_2O$, and free pyridine. Although the grey powder initially produced in the thermolysis is amorphous by X-Ray diffraction, the powder pattern evolves into that of hexagonal GaN upon heating at 900°C.

A related complex, $[Li(thf)_2][Ga(N(SiMe_3)_2)(OSiMe_3)_2Cl]$ (**16**), is reported and characterized by single crystal X-Ray diffraction. Analogous anionic indium derivatives, $[Li(py)_2][In(N(SiMe_3)_2)(OSiMe_3)_2Cl]$ (**18**), $[Li(py)_2][In(N(SiMe_3)_2)(OSiMe_3)_3]$ (**19**), have also been prepared and their characterization is reported. Thermolysis experiments of compounds **16**, **17**, and **18** indicate a more complex rearrangement process than for **17**; they do not proceed smoothly to yield the III-V nitride.

Lastly, $[In(N(SiMe_3)_2)(\mu^2\text{-}O)]_x$ (**20**) was prepared from hexane in the absence of coordinating base. It was characterised by ^1H NMR, elemental analysis and MS, but its crystallinity precluded a single-crystal XRD to establish the extent of oligomerisation.

Publications

Barry, S. T. Bellehumer, S., and Richeson, D. S.,"Thermally Induced Transformations of Alkyl Gallium and Indium Phosphido Complexes: Dealkylsilylation Routes to MP (M = Ga, In)", *Chem. Mater.*,submitted for publication July 1996.

Barry, S. T. and Richeson, D. S., "Preparation and Characterization of Mixed Alkyl Amido Complexes of Gallium", *J. Orangomet. Chem.*, **1995**, *510*, p. 103.

Barry. S. T. and Richeson, D. S., "Designated Molecular Deconstruction: The Facile Transformation of $GaN(SiMe_3)_2(OSiMe_3)_2py$ (py=pyridine) to GaN", *Chem. Mater.*, **1994**, *6*, p. 2220.

Conference Presentations

Barry. S. T. and Richeson, D. S., "Elimination of Hexamethyldisiloxane: From Molecular Species to Solid State Compounds", 78th Canadian Society for Chemistry Conference and Exhibition, Guelph, Ontario, May 1995.

Barry. S. T. and Richeson, D. S., "Preparation and Characterization of Mixed Alkyl Amido Complexes of Gallium", 78th Canadian Society for Chemistry Conference and Exhibition, Guelph, Ontario, May 1995.

Barry. S. T. and Richeson, D. S., "Amides, Imides and Nitrides: From Discrete Molecules to Extended Solids", Inorganic Discussion Weekend, Guelph, Ontario, November 1994.

Barry. S. T. and Richeson, D. S., "Rare-Earth and Transition Metal Pnictide Precursors for CVD", Inorganic Discussion Weekend, Ottawa, Ontario, November 1992.

Table of Contents

Table of Contents(continued)

List of abbreviations

eV .....Electron Volts

LEDs .....Light Emitting Diodes

CVD .....Chemical Vapour Deposition

Pn .....Pnictide; the family of elements containing N, P, As, Sb, Bi

MPn.....Metal Pnictide extended solid; in this case the metal is from the family of elements containing B, Al, Ga, In, Th

NMR .....Nuclear Magnetic Resonance

XRD .....X-Ray Diffraction

PXRD.....Powder X-Ray Diffraction

XPS .....X-Ray Photoelectron Spectroscopy

EA .....Elemental Analysis; used to describe combustion analysis of C, H, and N.

TGA .....Thermogravimetric Analysis

SIMS .....Secondary Ion Mass Spectrometry

TEM .....Transmission Electron Microscopy

SEM .....Scanning Electron Microscopy

XRF.....X-Ray Fluorescence

ppm .....parts per million

thf.....Tetrahydrofuran

py.....pyridine

IR.....Infra-red

List of Figures

List of Figures (continued)

List of Tables

Axis Mundi

Mid-August and on the lawn
children are hopping the length
of a wooden ladder found lying
in a depth of uncut grass.
They stretch out their arms, one
foot pointed and poised to geiger
for gravity's center as they size
up the square between the slats
of each jump. Kicked, the rungs and
uprights stiffly squeak with rusted joints.
The children stare hard in tensed
concentration, all of them together
but each alone in their turn, the *there*
and here of being smack-dab - nothing
to worry about, just the tilt of the ground
and the thick air that's cooling. For them
and at this particular time of day, as
light and sound quiver, sponged by
hay bales, the movement of evening slows
so twenty steps might feel like years
and the slippery longitudes of their passage
balance a chill across every backbone.

-from "Among the Months"
by David O'Meara

Chapter 1: Introduction to Group III-V semiconductors

Elements from the main groups IIIA and VA can be mixed in a 1:1 stoichiometric ratio to form binary extended solids with extremely useful characteristics.[1] These materials all have high melting points and can form crystalline semiconducting lattices with high thermal conductivity. They are also extremely inert and hard materials; they are not volatile due to their nature as extended solids. These materials usually exhibit either a wurtzite (hexagonal) or a zinc blende (cubic) lattice.

Binary group III-V compounds have been extensively studied because of their use as semiconductors.[1,2] The band-gaps for these semiconductors span a range of energies in the visible spectrum (Table 1), making them useful materials for applications from infrared to ultraviolet wavelengths. This allows their employment in imaging and graphics, as these materials can be tailored (through doping) to emit wavelengths of light throughout the visible spectrum. GaAs is perhaps the most well-studied member of this family and is used today in modern computer architecture, while its cousin GaN, with a band-gap of 3.4 eV (for the wurtzite polytype) has potential application to blue-light technologies such as LEDs and blue-UV detectors.

Table 1: Binary III-V semiconductors and their corresponding band-gaps[3]

Binary Solid	Band-gap (eV)
AlAs	2.2
GaAs	1.4
InAs	0.4
AlN	6.2
GaN	3.4
InN	1.9
AlP	3.0
GaP	2.3
InP	1.3

Like many wide band-gap semiconductors, these materials are extremely resistant to fatigue, wear and thermal conditions. This inertness bolsters their utility as semiconductors as they can be used in more caustic environments and subjected to harsher treatment than many materials.

One fundamentally important step in the technological application of these materials is the ability to prepare them as very thin layers over complex surfaces.[1] These layers should be epitaxial and uniform over a large area. In order to achieve these characteristics, chemical vapour deposition (CVD) techniques have been exploited.

CVD is a modern technique used for the synthesis of thin films. It relies on volatile precursors meeting in the gas phase at a substrate and subsequently reacting on that substrate to produce the required semiconductor. This necessitates the starting materials be furnished with ligand systems which can interreact without incorporating into the lattice of the solid material that is formed.[1]

A key factor in this technique is the stability of the material. The precursors should be volatile enough to be transported in the gas phase at a temperature where the material is stable, but not so robust as to not react when the material reaches the substrate. Currently, GaN thin films are prepared from a well-mixed stream of trimethyl gallium and ammonia passed over the desired substrate, which is held at a particular temperature by resistive heating. Although this results in a high-quality gallium nitride sample on the substrate surface, there are a few undesirable characteristics inherent to this technique.[2] The first and foremost is the high temperature of the reaction, making the process energy-intensive. Secondly, the mixing process is complex and any flow problems can cause formation of a material which does not contain the elements in a 1:1 ratio. Even sub-stoichiometric changes will greatly affect the band-gap, which in turn will lead to electronic devices with irreproducible properties.

A solution to these two problems is the design of single source molecular precursors for the deposition of III-V semiconductors. These precursors would start with an intact bond between the group III and group V elements and would have an attendant ligand system which would promote volatility at a low temperature, while ultimately producing unreactive and volatile side-products which do not become incorporated in the formed solid. In the synthesis of such precursors, an understanding of the bonding between group III metals and group V "pnicogens" is imperative.[2]

The available literature on this topic is vast, and a survey of it in its entirety would not accent prominently the features appropriate for this thesis. This introduction will focus on two main categories of metal-pnictide (M-Pn) bond formation:

1. Dehalosilation: typically Me_3SiX (X = halide) is eliminated, where the halide group originates on the metal centre and the trimethylsilyl group comes from the ligand. The resulting strong silicon-halide bond is the driving force for the reaction.

Firstly, reactivity which leads to the formation of complexes with M-Pn bonds will be addressed, followed by an examination of the chemistry of some existing precursors to form MPn (rnetal-pnictide) materials.

2. Alkane elimination: if the metal centre and pnictide both bear alkyl groups (or protons), sufficient thermal excitation can promote alkane elimination which results in an increased M-Pn bond order. The unreactive nature of the resultant alkane side-products makes this a particularly attractive method.

The first part of this section will deal with alkyl eliminations seen in the literature, and the latter part is concerned with transformations which partially or completely eliminate their ligand systems to produce clusters or extended MPn materials, respectively.

Hand-in-hand with the initial M-Pn bond formation comes the question of further reactivity of these compounds to ultimately produce MPn. In many cases , the same reaction which initially formed the M-Pn bonds can be repeated to produce a binary, solid state material. Often, similar dehalosilation or alkane elimination reactions may occur to produce the appropriate extended solid. To this end, an effort will be made to summarize melting point or other thermolysis data to demonstrate the general ability of these types of compounds to undergo thermolysis.

It should be noted that M-Pn bond formation is by no means limited to the two possibilities outlined above. For instance, it is common to eliminate a salt (e.g. LiCl) from an alkali pnictide and metal halide in order to generate the M-Pn bond. Many of these reactions are employed in the synthesis of starting materials which undergo subsequent reactions which fit into either dehalosilation and alkane elimination. Thus, these methods will be discussed implicitly as they arise.

The last section of this introduction will deal with metal-alkoxide compounds. Although these compounds are not directly useful in the formation MPn materials, they have a rich and well-explored reactivity. The ease of synthesis of these compounds, coupled with their volatility and thermal lability suggests that alkoxide ligands may be useful ligands for interreaction and elimination in MPn precursors. A survey of literature highlighting the elimination of alkoxide ligands will be presented in order to demonstrate their potential as candidates for a MPn precursor's ligand environment.

Chapter 2: Literature concerning halo-pnictides of gallium and indium

1. Examples of Halosilane Elimination to promote M-Pn bond formation

The relative stability of the Si-Cl bond compared to Si-E bonds (E = Br, I, N) is favourable for the elimination of a chlorosilane to form a MPn centre (Table 2). A search of the literature reveals this to be a well-explored concept.

Table 2: Selected bond strengths which involve silicon[4]

Bond Between	Bond Energy (kcal/mol)
Si-Cl	85.7
Si-Br	69.1
Si-I	50.9
Si-N	76.4

For example, elimination of Me_3SiCl from an aluminum amide complex has been reported for $Al[N(SiMe_3)_2]_2Cl$, which was formed by LiCl elimination between $AlCl_3$ and 2 equivalents of $LiN(SiMe_3)_2$.[5] This dehalosilation occurred at 150°C, but Me_3SiCl was a minor side-product compared to methane. This suggests formation of an aluminum hydride intermediate which subsequently (and undesirably) eliminates with a silyl methyl group.

Nutt and coworkers found that $GaCl_3$ would react with $RN(SiMe_3)_2$ in the following manner:[6]

$GaCl_3 + RN(SiMe_3)_2 \rightarrow SiMe_3Cl + Cl_2GaN(R)(SiMe_3)$ (1)

where R = H, Me

Although there were no thermolyses attempted, both the methyl and the proton derivatives appeared volatile at low temperatures according to melting-point data, and $Cl_2GaNH(SiMe_3)$ was said to "decompose slightly" under sublimation. Unfortunately, this decomposition product was not characterised and it could not be determined if the material reacted further to yield an imide or a nitride.

Halosilane elimination from an arsenic starting material was demonstrated in 1986 and this reactivity has been well-explored subsequently by Richard Wells and coworkers.[7] The starting materials were a series of silyl arsines which were synthesised by a variety of methods, with the common step:

$R_{3-n}PnLi_n + n\ Me_3SiCl \rightarrow R_{3-n}Pn(SiMe_3)_n + n\ LiCl$ (2)

where n = 1, 2, 3
R = Me_3SiCH_2, Mes
Pn = As, P

This methodology made for easy adaptation of the ligand which allowed tuning of its reactivity, steric congestion and the number of possible halosilane. Dimers and trimers were common products of these eliminations between group III metals and the pnictides phosphorus and arsenic:

$$n\ R_2PnSiMe_3 + R_{3-n}MX_n \rightarrow R_{3-n}M(PnR_2)_n + n\ Me_3SiX \quad (3)$$

$$n\text{-}1\ R_2PnSiMe_3 + R_{3-n}MX_n \rightarrow R_{3-n}M(X)(PnR_2)_{n-1} + n\text{-}1\ Me_3SiX \quad (4)$$

where $n = 1, 2, 3$
$X = Cl, Br$
$R = Me_3SiCH_2, Mes$
$Pn = As, P$
$M = Al, Ga, In$

The extent of oligomerisation of these compounds was measured by cryoscopic methods and crystallography. As well, a $^{13}C\{^1H\}$ dynamic NMR experiment on the compound $\{[(Me_3SiCH_2)_2As]_2GaBr\}_2$ determined that there was a dimer-trimer equilibrium in solution, and it was put forth that this is a common condition for all compounds of this family.

Two examples which follow from equations 3 and 4 are $[(Me_3Si)_2AsGa(CH_2SiMe_3)_2]_2$ and $(CH_2SiMe_3)_2GaAs(SiMe_3)_2Ga(CH_2SiMe_3)_2Cl$ and these demonstrate possible ligand bridge ensembles.[7] The first of these compounds exhibited a Ga-As-Ga-As planar ring comprising the centre of a dimeric structure, a feature typical of homoleptic compounds of this nature, and found in many such compounds where steric crowding is not a factor. In the second, the dimer is centered on a

Ga-As-Ga-Cl ring (a "mixed bridge core") which is non planar (Figure 1). This connectivity is common for compounds where steric congestion is too great to accommodate two pnictide-containing ligands as bridges.

Similar indium-containing dimeric compounds are also well-characterised According to single crystal X-ray diffraction (XRD), the compounds of the formula $(CH_2SiMe_3)_2InAs(SiMe_3)_2InCH_2SiMe_3)_2Cl$ have the mixed-bridge core (Figure 1B) where both a chloride and a pnictide (in this case arsenic) bridge. Both the gallium and indium analogues seemed to have some interesting thermochemistry according to the melting point determinations. Indeed, $[(Me_3Si)_2AsIn(CH_2SiMe_3)_2]_2$ decomposed to a " black powder" at 210°C. However, these reactions were not explored further.

Reaction of $As(SiMe_3)_3$ with diethyl aluminum chloride gave the adduct $Et_2(Cl)AlAs(SiMe_3)_3$.[8] This suggests that the initial step in these reactions is coordination of the pnicogen lone pair to the metal centre. This compound was shown to undergo halosilane elimination to form the bridging dimer $[Et_2AlAs(SiMe_3)_2]_2$, but subsequent reactivity toward forming the binary solid state compound was left unexplored and no evidence of thermoreactivity was indicated by the melting point determination.

The starting material $P(SiMe_3)_3$ also shows loss of a trimethylsilyl group when reacted with $(Me_3SiCH_2)_2InCl$ to form the compounds $[(Me_3SiCH_2)_2InP(SiMe_3)_2]_2$ and $(Me_3SiCH_2)_2InP(SiMe_3)_2In(CH_2SiMe_3)_2Cl$ (reactions 3 and 4).[9] Both of these materials were structurally characterised by XRD and found to be dimers. The latter is yet another example of

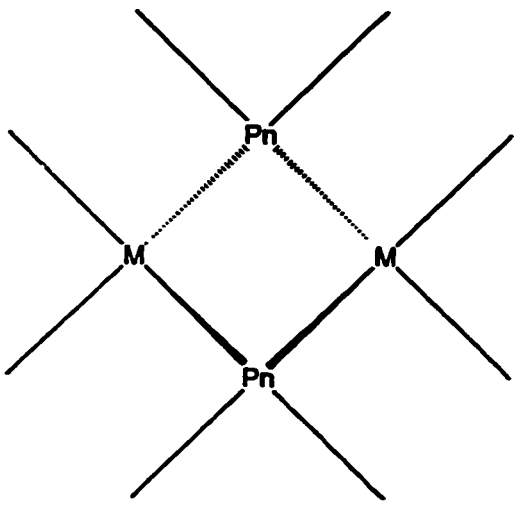

A

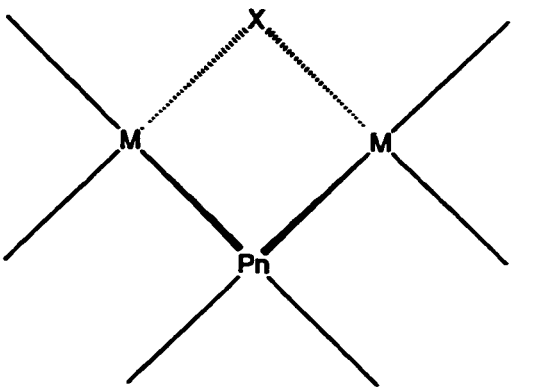

B

Figure 1: Two possible configurations of a dimeric core of a Group III-V dimer showing (A) a double pnictide (Pn) bridge and (B) a mixed-bridge pnictide-halide (X) core.

the mixed bridge core shown in Figure 1. Unlike the previous materials, the melting points of these In-P dimers were sharp and there were no sign of thermolysis.

A similar reaction with Ph_2GaCl and $LiP(SiMe_3)_2$ gave the compound, $Ph_2GaP(SiMe_3)Ga(Ph)_2Cl$, complete with a structure exhibiting the mixed bridge core.[10] An interesting facet of this work is the isolation and structural characterisation of the adduct of the same gallium starting material and $P(SiMe_3)_3$, namely $Ph_2(Cl)Ga{\cdot}P(SiMe_3)_3$. This confirms the natural suspicion that the first step in the Me_3SiCl elimination is indeed dative bonding of the pnictide compound to the metal centre. This compound does not eliminate trimethylsilyl chloride when heated; an NMR tube experiment showed that there was more than one compound formed, but not $Ph_2GaP(SiMe_3)Ga(Ph)_2Cl$.

The arsinide starting material $RAs(SiMe_3)_2$ was used to form bridging "arsinido" compounds:[7]

$$Me_3SiCH_2As(SiMe_3)_2 + RGaCl_2 \rightarrow [RGaAsCH_2SiMe_3]_2 + 2\ SiMe_3Cl \qquad (5)$$

where R = Cl, Ph

However, these materials were not characterised fully and further reactivity or structural determination remains unexplored.

2. Examples of Halosilane Elimination to produce M-Pn extended solids

One need not stop after formation of a single bond between the metal and the pnictide. Indeed, most of the focus in this field in the late 1980s and early 1990s was to produce MPn from single-molecule precursors in low-temperature (i.e. room temperature) reactions. There are several excellent reviews on the topic.[2,7,11]

Wells et al. have exploited the chemistry in reaction 6 to produce an array of interesting chemistry. GaP, InP, GaAs and InAs can all be synthesised according to the following general scheme:[12]

$$MX_3 + Pn(SiMe_3)_3 \rightarrow 3\ SiMe_3X + MPn \qquad (6)$$

where X = Cl, Br, I
Pn = As, P
M = Ga, In

In this transformation, the reactants were heated *in vacuo* overnight at 300°C and annealed "in a cold flame". This leaves the unanswered question of whether the reaction occurred at the reported 300°C or during the annealing process. According to the powder X-ray crystal diffractogram (PXRD), the resulting GaP was not very crystalline, showing only broad features centered at expected GaP peaks. This might be expected for a precipitate formed in solution, and

the subsequent annealing step is likely to have produced the small amount of crystallinity that was detected.

The above general reaction was initially discovered with $As(SiMe_3)_3$, and this research was done concurrently in two research groups,[13,14] A typical reaction showed that GaAs was formed after a series of thermolyses at increasing temperatures.[13] The initial volatile products were collected from a stoichiometric solution reaction between $GaCl_3$ and $As(SiMe_3)_3$ and titrated to determine the chlorosilane content. Initially, 2.5 equivalents of chlorosilane were collected, and after 330°C, no further volatiles were evolved and the product exhibited the PXRD pattern of GaAs. $GaBr_3$ also gave GaAs when reacted in the same manner except with an ultimate reaction temperature of 410°C and InAs was formed using $InCl_3$ in this manner with a final reaction temperature of 150°C.

Interestingly, it was shown that the size of the particles formed in this reaction was dependent on the solvent in which they were produced.[14] Indeed, if the reaction between $GaCl_3$ and $As(SiMe_3)_3$ was carried out in quinoline, the crystallites formed were about 4.5 nm at their major diameter and soluble in both quinoline and pyridine. Annealing these crystallites both increases the crystallinity and destroys their solubility, thus indicating a coalescence of the particles.

Subsequent work on the reaction of $GaCl_3$ and $As(SiMe_3)_3$ found a reaction intermediate which was not structurally characterised but which has the empirical formula $AsCl_3Ga_2$.[15] The reaction required two equivalents of $GaCl_3$, and direct combination of these materials led to the aforementioned product within 16 days time. Heating of this material over the temperature range

40-410°C produced microcrystalline GaAs and $GaCl_3$, the latter of which was sublimed out of the reaction vessel.

Perhaps the series of reactions which achieve the preparation of binary III-V extended solids most directly are the reactions of $InCl_3$ with $P(SiMe_3)_3$ and $As(SiMe_3)_3$ respectively.[16,17] Wells and coworkers ultimately produced InAs and InP through this thermolysis, without characterisation of the reaction intermediates or side-products.[16] These reactions were done in sealed tubes using ultrasonic radiation to get intermediates of allegedly known composition, although the elemental analyses reported for these intermediates in no way support the proposed formulations. These materials are subsequently reacted at 350°C to produce either InP or InAs. This seemingly inelegant procedure works with $InBr_3$ and $P(SiMe_3)_3$ to produce InP as well. In all cases, some manner of uncharacterised material is sublimed out of the reaction mixture during the "annealing" step, which can suggest a reaction is occurring or purification taking place. According to the report, the sublimed side-product was not identified or characterised in any way. Such characterisation might have led to a valuable insight about the mechanism of the process.

Work by Barron *et al.* sheds some light on these reactions.[17] InX_3 (where X = Cl, Br, I) was reacted with $P(SiMe_3)_3$ at -78°C and allowed to warm to room temperature, where an orange material formed in each case. These materials were analysed by X-ray photoelectron spectroscopy (XPS) and elemental analysis (EA) and each material gave the elemental formula $X_2InP(SiMe_3)_2$, and were assumed to be polymeric due to their insolubility. All of these materials were shown to give the appropriate MPn material between 540-600°C. In the case of

$[Cl_2GaP(SiMe_3)_3]_n$, thermogravimetric analysis (TGA) showed a weight loss consistent with 2 equivalents of chlorosilane.

It should be noted that a contradictory report for the reaction of InI_3 with $P(SiMe_3)_3$ in toluene was reported by Wells et al.[16] It was found that, under the same reaction conditions as described above (except for the inclusion of 3 mL of diethylether in the reaction mixture), the phosphine adduct of the indium starting material was formed in good yield. This well-characterised intermediate is reported to be stable under an inert atmosphere at room temperature. Thermolysis of this adduct ultimately led to the formation of InP in high yield.

Chapter 3: Literature concerning alkyl-pnictides of gallium and indium

1. Examples of Alkyl Elimination to promote M-Pn bond formation

Aside from the abundance of methods and materials which capitalise on the strong Si-X bond, there have been several attempts to increase the M-Pn bond order by eliminations involving alkyl groups.[18] Much of this work has been centred on the idea of decreasing the toxicity of the materials used industrially for the synthesis of MPn extended solids (e.g. AsH_3) as well as stabilising them with respect to reactions with the atmosphere.

Several examples of possible precursors for alkyl elimination were discussed previously due to the method of their synthesis (i.e. dehalosilylation),[7-11] but Wells et al. have exploited alkyl elimination to synthesise a possible precursor for further alkyl elimination to GaAs.[19] A reaction between the secondary arsine $HAs(CH_2SiMe_3)_2$ and Ph_3Ga produced $[(Me_3SiCH_2)_2AsGaPh_2]_2$. The yield of the reaction was quite low and benzene was not detected nor investigated as a side-product of the reaction, suggesting that the reaction is more complicated than a simple alkyl elimination. This compound melts with decomposition at 181-183°C, suggesting some further thermochemistry for this compound.

An interesting family of potential MPn precursors are the pnictide adducts of R_3M (M = Al, Ga, In). Adduct formation between group III metal complexes and pnictide bases is a well-explored area, and the first characterisation of trialkyl gallium pnictides were done in the gas

phase in 1976.[20] Since that time, several compounds have been synthesised and studied in solution or solid states.

For instance, Bradley et. al. synthesised a series of trimethyl indium adducts with a variety of amines.[21] The synthesis involved generation of trimethyl indium in solution and subsequent addition of the appropriate base. Of these, the compounds $Me_3InN(H)(C_6H_{11})_2$, Me_3In(2,6-dimethylpiperidine), Me_3In(2,2,6,6-tetramethylpiperidine), and $Me_3InN(H)(Me)CH_2CH_2NHMeInMe_3$ (Figure 2) showed the ability to eliminate methane and form the appropriate alkyl indium amides. Although further reaction of these compounds seems unlikely, compounds like $Me_3InN(H)(C_6H_{11})_2$, where the nitrogen is not incorporated into the ring, might be suitable for imide or nitride formation.

The same group reported adducts and pnictide compounds of gallium using many of the same bases.[22] The synthesis entailed the substitution of either diethylether or bisdiphenyl phosphinoethane with the appropriate pnictide, and subsequent characterisation were carried out using NMR or XRD. These base adducts are stable, sublimable compounds, showing no degradation nor elimination which would suggest low-temperature reactivity suitable for CVD. It is interesting to note that for the compound $Me_3GaN(H)(C_6H_{11})_2$, the corresponding amide ($Me_2GaN(C_6H_{11})_2$) was not synthesised by thermolysis of the adduct, but by the reaction of Me_2GaCl and $LiN(C_6H_{11})_2$.

A good example of this class of adduct compounds are the H_2N^tBu adducts of trimethyl-gallium and indium.[23] These were synthesised by the addition of this amine to a solution of

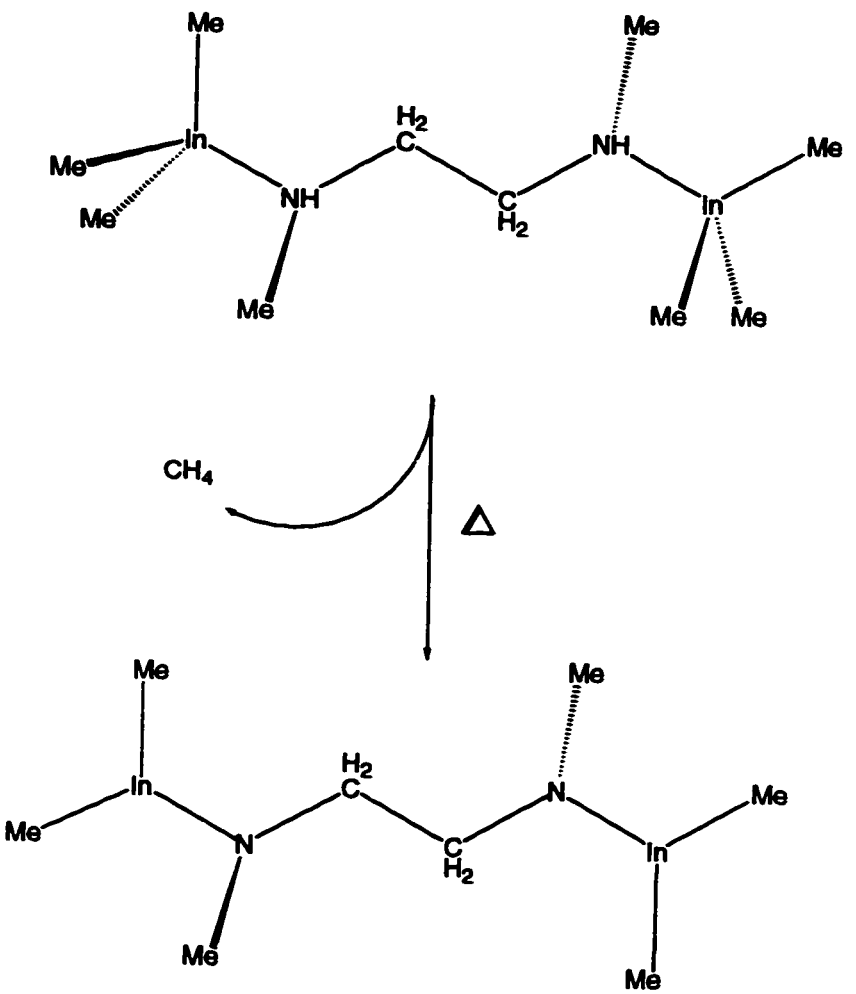

Figure 2: Dinuclear indium complex $Me_3InN(H)(Me)CH_2CH_2N(H)(Me)InMe_3$ demonstrating a bridging ligand showing alkyl elimination to form the corresponding amide, $Me_2InN(Me)CH_2CH_2N(Me)InMe_2$.

the appropriate trimethyl metal complex. Both of the gallium and indium derivatives were characterised by XRD and no thermolysis studies were reported for either. The compound $Me_3InNH_2{}^tBu$ sublimes at 80°C, and the analogous gallium complex merely melted at 65-67°C without sublimation or decomposition. Oddly enough, the compound $[Me_2GaN(H)^tBu]_2$ was also reported and structurally characterised by XRD,[23] but it was synthesised by the reaction of Me_2GaCl and $LiN(H)^tBu$ in diethylether. There was no mention of an alternate synthesis for this dimer involving alkane elimination from the adduct, and further thermolysis was also left unexplored.

Thermolysis of molecular precursors containing Pn-H bonds to increase the M-Pn bond order has also been demonstrated at low temperature. For example, reaction of $(^tBu)_3Ga$ and either PH_3 or AsH_3 occurred at below room temperature, to give the trimers $[^tBu_2Ga(\mu\text{-}PnH_2)]_3$ (where Pn = As, P) in quantitative yield.[24] $[^tBu_2Ga(\mu\text{-}PH_2)]_3$ was characterised crystallographically to determine the extent of oligomerisation, while $[^tBu_2Ga(\mu\text{-}AsH_2)]_3$ was shown to be a trimer by mass spectrometry. Both compounds thermolysed to produce the appropriate binary extended solid at 200°C ($[^tBu_2Ga(\mu\text{-}PH_2)]_3$) and 155°C ($[^tBu_2Ga(\mu\text{-}AsH_2)]_3$), with isobutane and isobutylene detected as the side-products.

It is interesting to note that the same reaction using NH_3 produced the adduct $^tBu_3GaNH_3$ at slightly above room temperature.[25] When this compound was heated to 170°C in the presence of ammonia, it quantitatively converted to the trimer $[^tBu_2Ga(\mu\text{-}NH_2)]_3$, whether reacted in the solid state or in solution. This trimer was also synthesised by addition of $LiNH_2$ to *in situ* generated

$^tBu_2GaCl$ and shown to be a trimer by single crystal XRD. No further thermolysis data was given for this compound.

The synthesis of the analogous aluminum compounds $[^tBu_2Al(\mu\text{-}PH_2)]_3$, $[^tBu_2Al(\mu\text{-}AsH_2)]_3$[25], and $[^tBu_2Al(\mu\text{-}NH_2)]_3$[26] has also been reported. All of these compounds were prepared between 55-115°C and the characterised as trimers by XRD. Although the thermal chemistry of these compounds was not explored, the As and P derivatives showed decomposition at their melting points, while the N derivative did not show this reactivity. The trimer $[Me_2Al(\mu\text{-}NH_2)]_3$ was prepared by this method as well, in refluxing benzene, and characterised as a trimer by XRD.[26] It showed no reactivity at the melting point, and thermal reactivity was not explored in this work. However, the authors make the interesting observation that the $[Me_2Al(\mu\text{-}NH_2)]_3$ trimer has a skew-boat conformation, similar to that of any given six-membered fragment of the AlN wurzite structure. It was suggested that there is relatively little structural reorganisation necessary between this possible precursor and bulk AlN.

In 1990, Gladfelter et al. reported the synthesis of the trimer $[H_2GaNH_2]_2$, by passing NH_3 over H_3GaNMe_3 for one hour.[27] It was characterised by MS and XRD, and showed a chair conformation for the six-member ring. It was reported that this material thermolised above 200°C with evolution of hydrogen to produce GaN, which became more crystalline upon heating to 600°C. The product was the cubic form of GaN and showed no indication of containing or converting to the hexagonal structure.

An analogous trimer $[Me_2GaNH_2]_2$, formed at 120°C from H_3NGaMe_3 was characterised by XRD.[28] A mass spectrogram of the compound contained the $[Me_2GaNH_2]_2^+$ ion (m/z = 345). There was no reported EA, melting point nor thermolysis for this compound.

The analogous aluminum compound $[Me_2AlNH_2]_2$ formed from H_3NAlMe_3 at room temperature over several days with release of methane.[29] Subsequent reaction occurred at 125°C with the evolution of methane and the eventual production of AlN was seen at elevated temperatures. Kinetic data indicated a monomer-dimer-trimer equilibrium for this compound in solution. This work also assesses the kinetics of the methane elimination and compares several possible mechanisms to the experimental data.

The ammonia adduct of trimethyl indium, which was first described by Coates and Whitcombe in 1956,[30] shows similar reactivity to its cousins.[31] The original synthesis proceeded by the co-condensation of Me_3In and NH_3. The compound was only characterised by a melting point. Methane was found to evolve slowly from this compound at room temperature, and heating the compound to 80°C readily produced Me_2InNH_2 and one equivalent of methane which was collected with a Töpler pump. It has been conjectured that the transformation of this compound to InN follows the same mechanism as discovered for aluminum.

Another aspect of alkyl elimination chemistry is the loss of two groups, to form the M=Pn double bond without continuing all the way to a MPn semiconductor. For example, The first instance of a main-group imide was observed in 1962 and was structurally characterised in 1972.[32] It was found to have a cubic skeleton of four aluminum-nitrogen monomers and was termed a "pseudo-cubane".

Since that time, there have been a great many group III metal imides with orders of aggregation of anywhere from 2 to 16. Roesky et al. found that addition of a primary amide to a solution of R_3M could ultimately lead to a series of metal imido complexes[33]:

$$2\ C_5F_6NH_2 + 2\ MR'_3 \rightarrow [R'_2MN(H)C_5F_6]_2 + 2\ R'H$$

$$[R'_2MN(H)C_5F_6]_2 \rightarrow 1/2\ [R'MNC_5F_6]_4 + 2\ R'H \qquad (7)$$

where M = Al, Ga, In
R' = Me, Mes

When M = Al, and R = Me, the intermediate amido compound was not isolated, but the pseudo-cubane was formed from refluxing hexane and characterised by XRD. When M = Al, and R = Mes, the elimination to the amido species occurred in good yield in refluxing hexane, but the subsequent imide formation was not reported. It was conjectured that steric congestion does not allow this subsequent reaction.

In the case of trismesityl gallium, a dimeric amido complex was isolated from refluxing hexane and structurally characterised. Subsequent heating of this dimer in the solid state resulted in a pseudo-cubane in good yield, but with one strange feature. One of the gallium centres in the cube bore an amide group ($N(H)C_6F_5$), suggesting elimination of two equivalents of Mes from the metal centre, and requiring one extra equivalent of primary amine per cubane cluster. This reaction is not stoichiometric with respect to the starting material. The yield was reported as 71%, and it is therefore possible that 1/5 of the starting material was depleted of its amido group.

If this is an accurate description of the reaction, the mechanism of imido formation cannot be as straightforward as step-wise elimination of RH, as purported by this work. Unfortunately, no effort was made to explain or investigate this anomaly.

In the cases M = In, Ga and R = Me,[33] the reaction was found to continue in a stepwise fashion to the expected metal imides. X-ray crystallography showed that the metal imido compounds are both pseudo-cubane, with slight distortions of the $[MN]_4$ cube. Characterisation of the intermediate amido complex demonstrated clearly that this reaction is stepwise. The second elimination occurred in a solid state reaction at 200°C (Ga compound) and 220°C (In compound), while the initial elimination occurred in refluxing toluene in both cases. It is unfortunate for this series of reactions that the final products were not subjected to harsher conditions in order to determine if the corresponding metal nitrides would result.

2. Examples of Alkyl Elimination to produce M-Pn extended solids

The final stage in alkyl elimination is to eliminate all three groups on both the metal and pnictide, resulting in MPn extended solid formation. Precursors for these compounds are synthesised by different methods, but as this section will demonstrate, salt elimination is the most prevalent.

Precursors with the general formula $[R_2MPn^tBu_2]_n$ were synthesised by one of two general reaction schemes. The first was a typical salt elimination:

$$n\ GaCl_3 + n\ ^tBu_2PnLi + 2n\ RLi \rightarrow [R_2GaPn^tBu_2]_n + 3n\ LiCl \qquad (8)$$

and the second a comproportionation between homoleptic metal-pnictide complex and metal-alkyl starting materials :

$$1/3n\ M(Pn^tBu_2)_3 + 2/3n\ R_3M \rightarrow [R_2MPn^tBu_2]_n \qquad (9)$$

where M = Ga, In,
Pn = P, As
R = ^{n}Bu, ^{t}Bu, Me

These compounds were found to deposit MPn films at temperatures up to 780°C. The films were characterised by: XPS in order to determine their elemental composition; secondary ion mass spectrometry (SIMS) to identify impurities; and scanning electron microscopy (SEM) to provide a view of the surface morphology. Generally, films from these precursors exhibited correct elemental composition and impurity levels which were comparable to electronic grade samples of the appropriate semiconductor. Although important, this work relies on very high reaction temperatures to construct the thin MPn layer and holds no advantage over the modern industrial synthesis in this respect.

An elegant example of MPn formation from the corresponding adduct was found in 1991 by Steigerwald and group.[34] At -70°C, addition of $P(SiMe_3)_3$ to $InMe_3$ gave the phosphine adduct. However, when the reaction was performed at 110°C, there was elimination of tetramethylsilane (TMS) and formation of $[Me_2InP(SiMe_3)_2]_2$, a dimer bridged through phosphorus. The compound proceeds to lose TMS and eventually forms InP at 400°C. The InP was characterised by PXRD and found to be polycrystalline, while the elemental composition was determined using X-ray fluorescence (XRF). Thorough characterisation of evolved TMS complemented the verification of the formation of InP.

Interestingly, $^tBu_3In$ and PH_3 were used to synthesize InP "whisker crystals" in toluene.[35] This low-temperature synthesis found a black precipitate from the refluxing solution contained both InP and In^0 and transmission electron microscopy (TEM) showed that these crystals seemed to grow from an In^0/InP "flux droplet" at the tip of the crystal. This phenomenon was also

demonstrated for the formation of InAs and GaAs, from with $^tBu_3In/AsH_3$ and $^tBu_3Ga/AsH_3$ mixtures, respectively.

Reaction of Me_2InCl and $LiNR_2$ (R = Et, ^{i}Pr, $SiMe_3$) resulted in a facile reaction which formed the indium amido compounds $Me_2In(NR_2)_2$ and loss of LiCl.[36] All of these compounds were characterised as dimers by XRD and the molecular ions of the dimers were detected by MS. Also, all sublimed at less than 100°C and showed no signs of decomposition at these temperatures, although thermolysis was not attempted.

Bradley and coworkers reported two other possible precursors for CVD: $Me_2GaPn(Me)_2$ (where Pn = P, As).[22] The phosphorus adduct was synthesised by elimination of LiCl from Me_2GaCl and $LiPn(Me)_2$, while the arsenic analogue was prepared by elimination of methane from $Me_3GaAs(H)Me_2$. Both of these materials were trimers, and the arsenic derivative sublimes at 100-110°C. Thermolysis data for these compounds was not reported.

A similar compound $^iPr_2In(NH^tBu)_2$ was prepared from $^iPr_2In$ Cl and $Li(NH^tBu)_2$.[37] This material was shown to be dimeric (cryoscopic methods and XRD). Thermolysis of this compound was not reported, but it decomposed at its melting point, with reported gas evolution. Considering that there is an available amido proton, there is a likelihood of imide or nitride formation.

The following example fits the criteria for this chapter only by being absolutely inappropriate as an example of a dehalosilation reaction. A series of mixed-alkyl lithium amides were reacted

to produce a series of disubstituted gallium amidochlorides.[38] Subsequent reaction of these amides with NaN_3 gave a series of bisamido gallium azides:

$$(R_1R_2N)_2GaCl + NaN_3 \rightarrow (R_1R_2N)_2GaN_3 + NaCl \qquad (10)$$

The resulting gallium azides were structurally characterised and shown to produce GaN films on a variety of substrates at temperatures as low as 260°C, with the crystallinity varying as a function of temperature. Unfortunately, the side-products were not characterised, leaving the question of mechanism unanswered.

An interesting precursor for formation of GaAs was synthesised by Ekherdt and coworkers in 1994.[39] $Ga(As(^tBu)_2)_3$, synthesised from $LiAs^tBu_2$ and $GaCl_3$, was transformed to GaAs using chemical-beam epitaxy. This system does not have the desired metal-pnictide stoichiometry, and the side-products would have to be arsenic-containing in order to produce GaAs. The reactions occurred between 415-600°C and resulted in reasonably pure, crystalline GaAs. There were some detectable impurities of silicon and carbon, which were attributed to impurities present in the starting material. Indeed, the reaction is likely far more complicated than simple ligand elimination, and impurities could possibly be produced during the reaction, but this question is not addressed in the work cited.

Other examples of homoleptic M-Pn complexes were reported by Jones, Cowley and coworkers.[40] Preparative routes for these compounds follow the general synthesis:

$$GaCl_3 + 3R_1R_2NLi \rightarrow Ga(NR_1R_2)_3 + 3\ LiCl \qquad (11)$$

where $R_1 = {}^tBu$, $R_2 = H$, $SiMe_3$
$R_1 = SiMe_3$, $R_2 = SiMe_3$

The compound $[Ga(N(H)^tBu)_3]_2$ is a structurally characterised dimer and the geometry of the N atoms suggest the presence of N-H functions. This compound melts with decomposition. The other two compounds are monomers, and again decomposition was seen for $Ga(N(SiMe_3)^tBu)_3$, suggesting similar possible reactivity. However, $Ga(N(SiMe_3)_2)_3$ showed no such tendency for decomposition as reported in the original synthesis for this compound.[41] The homoleptic gallium amide $Ga(tmp)_3$ (where tmp = 2,2,6,6-tetramethylpiperidide), was synthesised by elimination HCl from $GaCl_3$ and 2,2,6,6-tetramethylpiperidine. It showed no decomposition at its melting point.

Another such possible precursor was unearthed by Power et al. in 1993.[42] $In[N(SiMe_3)_2]_3$ was synthesised in a manner similar to the gallium derivative (Equation 11). This paper discussed another possible precursor material, $^tBuInN(SiPh_3)(2,6\text{-}i\text{-}Pr_2C_6H_3)$, which was structurally characterised by XRD and upon heating decomposed to a yellow oil at 158-163°C. No further thermolysis data was offered.

Thermolysis of homoleptic amides of group III metals can also lead to MPn solids.[39] Beyond the examples already discussed, there are examples in which the pnictide bears only proton groups for further reactivity. For instance, $In(NH_2)_3$ was formed at -33°C when InI_3 and KNH_2 were

dissolved in liquid ammonia.[43] This compound is claimed to be a monomer, although characterisation in this respect is incomplete. Thermolysis of this compound at 207°C produced a black powder, which showed a characteristic PXRD for InN when annealed at 400°C, and eliminated 1.8 eq. of ammonia, suggesting the main decomposition pathway is deprotonation of one amide group by the other two.

Chapter 4: Literature concerning alkoxides of gallium and indium

The previously-discussed reactivity is of course not limited to pnictide compounds, and these type of eliminations (dehalosilation, dealkylation etc.) from group III metals involving alkoxide ligands have been studied at length and for many years. An excellent review by Mehrotra covers the extensive chemistry of aluminum and the various synthetic routes to its alkoxides.[44]

A synthesis of MPn which appears to be unique in the literature is the reaction of In(acetylacetonate)$_3$ with As(SiMe$_3$)$_3$.[45] This reaction was carried out at 126°C in refluxing triethylene glycol dimethyl ether (triglyme), the resulting InAs was characterised by XRF. It is interesting to note that this work does not address the reaction in any way, and does not attempt to describe or even to predict the nature of the side-products.

In 1989, Douglas and Theopold reported the synthesis of two MPn precursors which contain the pentamethylcyclopentadienyl (Cp*) ligand.[46] The first of these Cp*$_2$GaAs(SiMe$_3$)$_2$, was prepared from [Cp*$_2$GaCl]$_2$ and Li(thf)$_2$As(SiMe$_3$)$_2$. The product was shown to be a monomer by XRD. It reacted with ^{t}BuOH to produce ^{t}BuOSiMe$_3$, Cp*H and GaAs. Although not free of impurities, the GaAs was formed at ambient temperatures. The reaction of Cp*$_2$GaAs(SiMe$_3$)$_2$ with HCl formed Cp*Ga(Cl)As(SiMe$_3$)$_2$, and this new material also reacted at room temperature with ^{t}BuOH to form GaAs.

The second precursor reported was [Cp*In(Cl)As(SiMe$_3$)$_2$]$_2$, which was formed by reacting [Cp*$_2$InCl]$_2$ and Li(thf)$_2$As(SiMe$_3$)$_2$, with the surprising elimination of LiCp*. This material also reacted readily with ^{t}BuOH and formed ^{t}BuOSiMe$_3$, Cp*H and a yellow powder. The yellow

powder was almost amorphous but exhibited a broad peak in the PXRD centered at the main peak of InP.

Theopold and Douglas showed that addition of methanol to a solution of $R_2InP(SiMe_3)_2$ (R = Me_3SiCH_2 or CH_3CCH_2) gave InP as well as protonated forms of the ligands (including return of methanol).[47] ^1H NMR studies demonstrated the existence of dialkyl indium methoxide and PH_3, which then reacted to produce InP and regenerate MeOH. The InP produced was found to be free of impurities, but when the same procedure was followed using alkyl chloride complexes of the type $R(Cl)InP(SiMe_3)_2$ (R = Me_3SiCH_2, Cp^*), there was chloride remaining in the InP produced.

Compounds of the general formula $[Me_2Al(\mu\text{-}OR)]_n$ can be formed through alkyl eliminations by the following route, termed alcoholysis:[48]

$$AlMe_3 + ROH \rightarrow Me_2Al(OR) + MeH \qquad (12)$$

where R = Me, Et, ^{n}Pr, ^{i}Pr, ^{n}Bu, ^{i}Bu, ^{s}Bu, ^{t}Bu, C_5H_{11}, $CH_2CH_2{}^i$Pr, $CH_2{}^t$Bu, C_6H_{13}, C_8H_{17}, $C_{10}H_{21}$, $C_{12}H_{25}$

The compounds are consistently measured by cryoscopy to be dimers, with the exception of $[Me_2Al(\mu\text{-}OMe)]_3$, which is been shown to be a trimer by XRD. Compounds of this nature show a dynamism of oligomerisation in solution, as was extensively studied by Barron and coworkers.[49]

This reaction scheme even works with very bulky R groups, such as 2,6-di-*tert*-butyl-4-methylphenyl. It should be noted that these reactions occur at room temperature and side-products can be easily detected. It is also interesting to note that the original method of preparing $[Me_2Al(\mu\text{-}OMe)]_3$ was not by the mechanism of reaction 12, but by comproportionation between $AlMe_3$ and $Al(OMe)_3$ in the appropriate stoichiometric mixture.[50]

The same group (Barron et al.) showed -with a typical thoroughness and invariance- that almost any compound of the general fomula $[^tBu_2Ga(\mu\text{-}OR)]_n$ could be synthesised by a scheme similar to reaction 12.[51] This is not a new idea,[52] and has been utilised by several workers to prepare compounds which show the typical oligomerisation to dimers and trimers. Indeed, most methods described by Mehrotra in his review of aluminum chemistry can be used with gallium to varying degrees of success.[44]

The alcoholysis method was used by Schmidbaur and Schindler in 1966 to prepare $[Me_2M(\mu\text{-}OR]_2$)where M = Al, Ga, In and R = $SiMe_3$, $SiPh_3$, and ^tBu) which were found to be dimers by molecular weight determination and showed a planar ring according to IR.[53] The compounds $[Me_2M(\mu\text{-}OSiMe_3)]_2$ also reacted with both Ph_3SiOH and ^tBuOH to eliminate silanol and result in the appropriate dimer.

Very little in this regard has been done with indium. Aside from the groundbreaking work of Schmidbaur and Schindler,[53] there are few examples.

Power et al. have used this alcoholysis method to synthesise gallium monomers with bulky aryl groups on the oxygen.[54] The compounds $^tBu_2AlO(2,6\text{-}^tBu\text{-}4\text{-}R\text{-}C_6H_2)$ (where R = H, Me,

^{t}Bu) were characterised by XRD and found to be monomers. It is interesting that the analogous gallium compound ^{t}Bu$_2$GaO(2,6-^{t}Bu-4-Me-C$_6$H$_2$) was not synthesised by alcoholysis but by LiCl elimination from ^{t}Bu$_2$GaCl and LiO(2,6-^{t}Bu-4-Me-C$_6$H$_2$).

In contrast, Barron and Cleaver showed that alcoholysis could indeed be utilised to make a similar monoalkoxide ^{t}Bu$_2$GaOCPh$_3$ in fairly good yield.[55] Through XRD, a short Ga-C interaction was seen, which suggested an agostic interaction between one phenyl proton and gallium, which may help stabilise the reaction of ^{t}Bu$_3$Ga with Ph$_3$OH.

An interesting compound formed by the alcoholysis reaction is the oxygen-centred, indium-containing cluster (InO^{i}Pr)(μ_2-O^{i}Pr)$_4$(μ_3-O^{i}Pr)$_4$(μ_5-O) (figure 3),[56] which was synthesised by refluxing InCl$_3$ in an isopropyl alcohol/benzene solution with NaO^{i}Pr. Although the stoichiometry was not stated, it can be assumed from the context of the paper that the intended product was In(O^{i}Pr)$_3$. The authors suggest partial hydrolysis as the mechanism for the formation of the cluster, although partial thermolysis and subsequent loss of O(^{i}Pr)$_2$ could also explain this observation.

A cluster with similar architecture was reported by Eaborn et al. in 1986, and is shown in figure 3.[57] In this case the compound [O{(Me$_3$Si)$_3$CIn}$_4$(OH)$_6$] was synthesised by a multi-step reaction, as follows:

$$InCl_3 + LiC(SiMe_3)_3 \rightarrow Li(thf)_3(\mu\text{-}Cl)InCl_2(C(SiMe_3)_3$$

$$Li(thf)_3(\mu\text{-}Cl)InCl_2(C(SiMe_3)_3) + \text{excess } LiAlH_4 \rightarrow ((SiMe_3)_3C)In(H)(\mu\text{-}H)Li(thf)_2(\mu\text{-}H)In(\mu\text{-}H)(H)(C(SiMe_3)_3)$$

$$((SiMe_3)_3C)In(H)(\mu\text{-}H)Li(thf)_2(\mu\text{-}H)In(\mu\text{-}H)(H)(C(SiMe_3)_3)$$

$$+ \text{excess MeOH} + \text{Excess } H_2O \rightarrow [O\{(Me_3Si)_3CIn\}_4(OH)_6] \qquad (13)$$

These two clusters were structurally characterised by XRD. No additional characterisation or reactivity was reported, although it is assumed the material is stable to reaction with water, as it was used in excess in the final step of the reaction.

Except that one compound has an overall four-fold cluster ($(InO^iPr)_5(\mu_2\text{-}O^iPr)_4(\mu_3\text{-}O^iPr)_4(\mu_5\text{-}O)$) and one a three-fold ($[O\{(Me_3Si)_3CIn\}_4(OH)_6]$), their structures are remarkably similar. Both clusters are centered around an oxygen atom and have μ_2 alkoxo ligands in the "skirt" of the cluster. Also, both compounds have each indium supported by a non-bridging alkoxo group. The compound $(InO^iPr)_5(\mu_2\text{-}O^iPr)_4(\mu_3\text{-}O^iPr)_4(\mu_5\text{-}O)$ has μ_3 alkoxo ligands bridging the indium centres, while they are μ_2 in ($[O\{(Me_3Si)_3CIn\}_4(OH)_6]$, giving a staggered and eclipsed arrangement respectively.

Barron and coworkers used alcoholysis with one equivalent of water in the place of alcohol to synthesise the trimer $[^tBu_2Ga(\mu\text{-}OH)]_3$.[58] This compound can also be synthesised by KCl elimination from $^tBu_2GaCl(thf)$ and KOH in refluxing thf. Thermolysis and thermogravimetric data for this compound suggest (but do not confirm) the elimination of one equivalent of isobutane to form a white solid which was examined by NMR. The authors concluded that an insoluble polymer $[^tBuGaO]_n$ was formed. This work also provided the synthesis of a peroxogallium product $[^tBu_2Ga(\mu\text{-}O(O^tBu))]_2$. This compound, when mixed in the appropriate stoichiometry with $^tBu_3Ga$ will make the previously described $[^tBu_2Ga(\mu\text{-}O^tBu)]_2$.

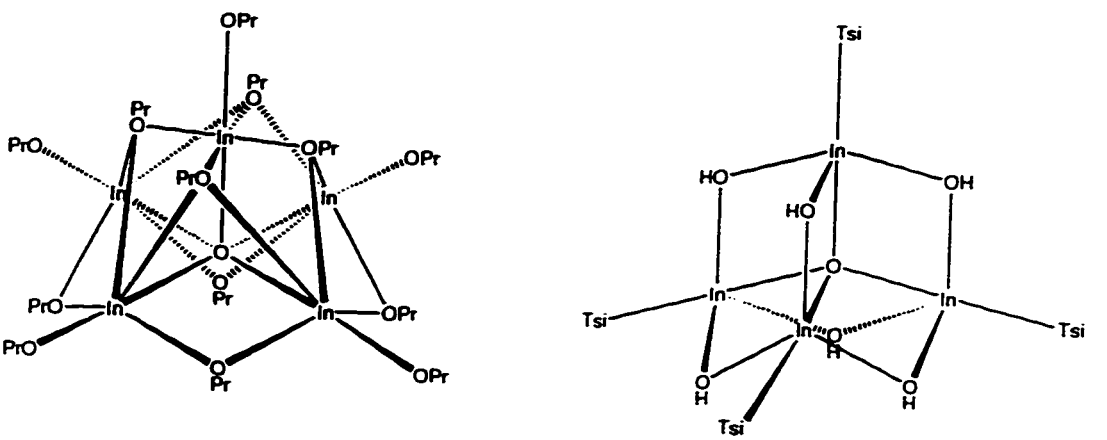

Figure 3: Two alkoxoindium compounds with similar structure and a central oxo ligand : $In(O^iPr)_5(\mu_2\text{-}O^iPr)_4(\mu_3\text{-}O^iPr)_4(\mu_5\text{-}O)$ and $In(C(SiMe_3)_3)(\mu_2\text{-}OH)_6(\mu_4\text{-}O)$.

The peroxide compound $[(^tBu)_2In(OO^tBu)]_2$ was synthesised by bubbling dry O_2 through a solution of $In(^tBu)_3$.[59] It was said to be stable to both oxidation and thermolysis. However, there is no reported melting point or other thermolysis data, and this work was discontinued due to the difficulty of handling $In(^tBu)_3$. The chemistry of peroxo species containing group III metals is well-studied but is beyond the scope of this thesis.[60]

In an aside which touches back on the idea of extended solid synthesis, GaS has been prepared by Barron and group using $[^tBuGaS]_4$ as a CVD precursor.[61] This tetramer was earlier synthesised by reaction of $^tBu_3Ga$ with H_2S at -10°C in pentane.[62] The resultant dimer $[^tBu_2GaSH]_2$ was structurally characterised by XRD. When this dimer was heated above 45°C, it was found to transform into the pseudo-cubane tetramer $[^tBuGaS]_4$. Films of cubic GaS were synthesised from this species on a variety of resistively heated substrates in the range 380-550°C. According to this report, this film "relaxes" to hexagonal GaS with time. It was argued that the compound maintains its cubane form from the molecular species and forms a kinetically stable cubic GaS. This converts slowly to the thermodynamically stable hexagonal form of GaS with time.

Mehrotra et al. were the first to isolate homoleptic trisalkoxides of indium.[63] $In(O^iPr)_3$ was synthesised in a benzene/isopropanol mixture using a stoichiometric ratio of sodium isopropoxide. This alkoxide group was shown to be labile to replacement by other alkoxides (Me, Et, ^{n}Bu, ^{s}Bu, and ^{n}Pentyl) when reacted with the respective alcohols in benzene. The number of groups replaced at the indium centre was controlled by stoichiometry. It was also

shown that the adducts $InCl_3.XROH$ (R = Et, X = 3; R = ^{i}Pr, X = 2) were stable when synthesised in refluxing benzene.

In 1965, Scmidbaur found that the diethylether adduct of MMe_3 (where M = Al, In, Ga) would react with Me_3SiOH to free diethylether and methane and produce the dimer $[Me_3SiOMMe_2]_2$.[64] These materials were characterised by NMR and EA and found to be dimers by the symmetry demonstrated by IR. Further reaction of these compounds with ^{t}BuOH eliminated Me_3SiOH and gave the dimers $[^{t}BuOMMe_2]_2$.

One example of surprising reactivity was described by Bradley, Hurthouse and coworkers.[65] $(^{t}Bu_2InCl)_2$ was allowed to stir in diethylether which contained 2 eq. of ^{n}BuLi and 2.6 eq. of tetramethylpiperidine to yield $^{t}Bu_2In(\mu\text{-}OEt)]_2$. The yield with respect to indium was good and no other side-products were isolated, leaving the mechanism of this reaction highly suspect. This synthesis was described as "not optimal" due to the surprising rending of ether to form ethoxide and the inactivity of the tetramethylpiperidine. However, the reaction was not attempted using either EtOLi -the logical lithium alkoxide- nor without the tetrametylpipridine present. The compound was said to sublime at 90°C and its connectivity was determined by XRD.

Chapter 5: Hypothesis

An attempt to focus the literature search on materials which have possible thermochemistry resulting in formation of MPn solids clearly shows that this field is under current and intense scrutiny. It is also evident that if a metal-pnictide bond is to be maintained and the bond order increased to the ultimate end of forming MPn, the key to successful precursors results from a logical and planned choice of ligand system. These ligand systems should meet several criteria from reactivity and synthetic standpoints. For reactivity purposes, a ligand is desired to have the following characteristics:

- the capability to impart volatility to the molecular precursor
- steric hindrance to protect the M-Pn core
- the ability to maintain small (i.e. mono-, di or trimeric) molecular clusters
- thermal reactivity at relatively low temperatures
- convenient reactivity to form a leaving group
- the ability to form stable and volatile side products
- lack of incorporation of the ligand system in the extended solid

and for synthetic purposes:

- ease of detection by characterisation techniques
- enhancement of the crystallinity and solubility of the molecular precursor
- easily characterised side-products

Success in dehalosilation and dealkylsilation reactions depends on the strength of the resulting bonds compared to the relatively weak starting bonds. The Me_3Si group can be used to good advantage, and contains many attractive features which an appropriate ligand system requires, such as bulk and volatility. As well, the presence of silicon allows X-ray techniques (e.g. XRF) for partial (qualitative) elemental analysis.

Dealkylation reactions also conform to many of these requirements. Reaction temperature is typically higher in these reactions, but the stability of the side products as well as the fact that they tend to be gases under reaction and standard conditions make them attractive as precursors. Moreover, the side products of these reactions are bound to be well-characterised materials, allowing for easy assessment.

The long history of alkoxide chemistry of the group III metals demonstrates that OR groups are susceptible to replacement and reaction. Although oxygen is not a desirable nucleus for inclusion in a leaving group due to the fear of oxide formation, alkoxide compounds nonetheless show suitable reactivity and can be as easily detected and characterised as their alkyl cousins.

In the pursuit of precursors for MPn semiconductors, the main concern is to increase the bonding between the metal and the pnictide. Ideally, if this is done with enough control, isolation of intermediate products may be possible. This in turn would lead to a better understanding of both the mechanism of the reaction as well as the factors concerned with optimising the reaction in terms of temperature and yield.

There are several pathways which could be envisioned for the loss of a ligand system and the creation of M-Pn bonds. This work centres on the reactivity of the trimethylsilyl group, and three types of elimination were explored for gallium and indium (Figure 4).

To this end, the following materials will be reported and their thermal chemistry investigated:

$Ga(Pn(SiMe_3)_2X_2$	where Pn = N and X = Cl, $OSiMe_3$, ^nBu, ^tBu where Pn = P and X = ^nBu
$In(Pn(SiMe_3)_2X_2$	where Pn = N and X = Cl, $OSiMe_3$ where Pn = P and X = ^nBu

As a side-branch of this chemistry, the synthesis and thermal reactivity of the following series of siloxide compounds was also examined, to determine the reactivity of the $OSiMe_3$ moiety:

$Ga(OSiMe_3)_xCl_{3-x}$	where X = 2, 3
$In(OSiMe_3)_xCl_{3-x}$	where X = 2, 3

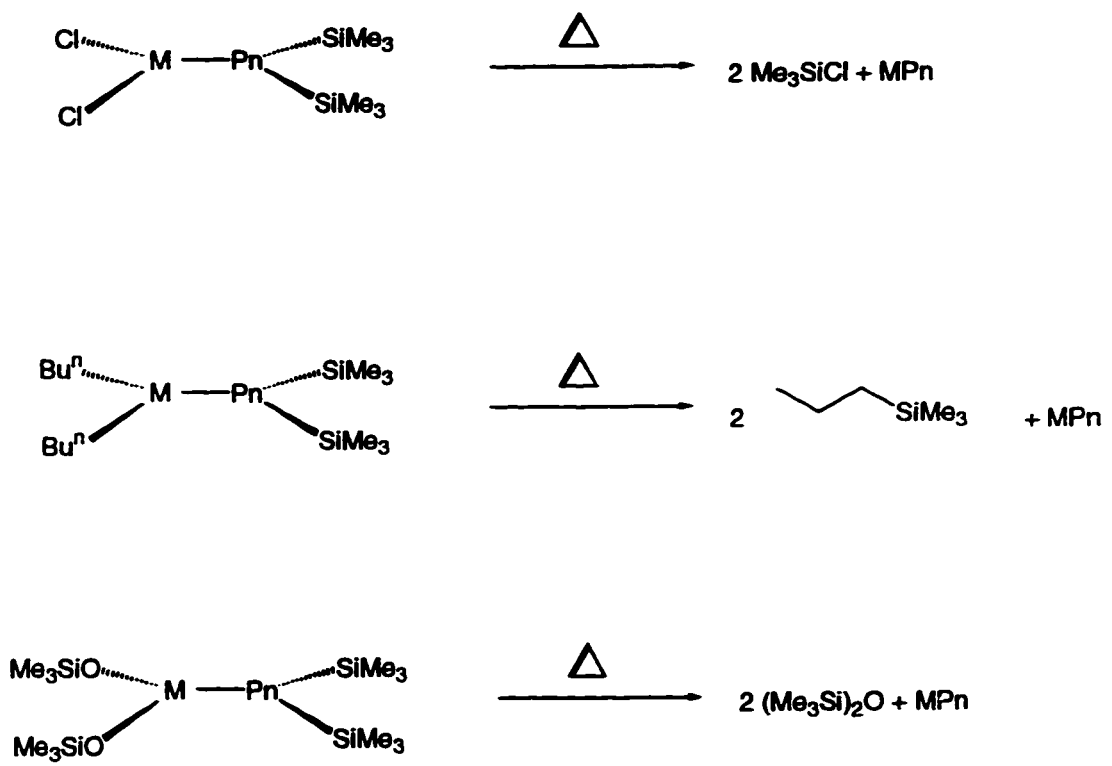

Figure 4: Three possible ligand environments and their thermolysis to eliminate a volatile side-product and produce MPn.

Another aspect of this chemistry is the possibility to probe the mechanism of MPn synthesis. This could allow some insight into the formation of oligomers and their influence on the resulting lattice of the extended solid. Since these materials exhibit either cubic or hexagonal lattices, it is interesting to investigate the oligomerisation of these materials to see if their structures correspond to the lattice arrangement.

One avenue which this work exploits is the synthesis of primary pnictides which contain a bulky and relatively unreactive alkyl group. This allows the possibility of elimination of an alkane or silane from the precursor without the material "continuing all the way" to an extended solid (Figure 5). Indeed, an example of meta-stable cubic gallium nitride resulting from a precursor with a cubane structure has been examined previously.[27] Exploitation of this avenue may allow synthesis of previously inaccessible polytypes of many MPn semiconductors which would undoubtedly afford different electronic properties.

In an effort to study oligomerisation, a series of gallium alkyl amides were prepared using primary amides. The synthesis, characterisation and preliminary thermal reactivity of the following compounds were investigated:

$Ga(R)_2N(H)(R')$ where R = ^{n}Bu and R' = 2,5-dimethylaniline, ^{t}Bu
where R = ^{t}Bu and R' = ^{t}Bu

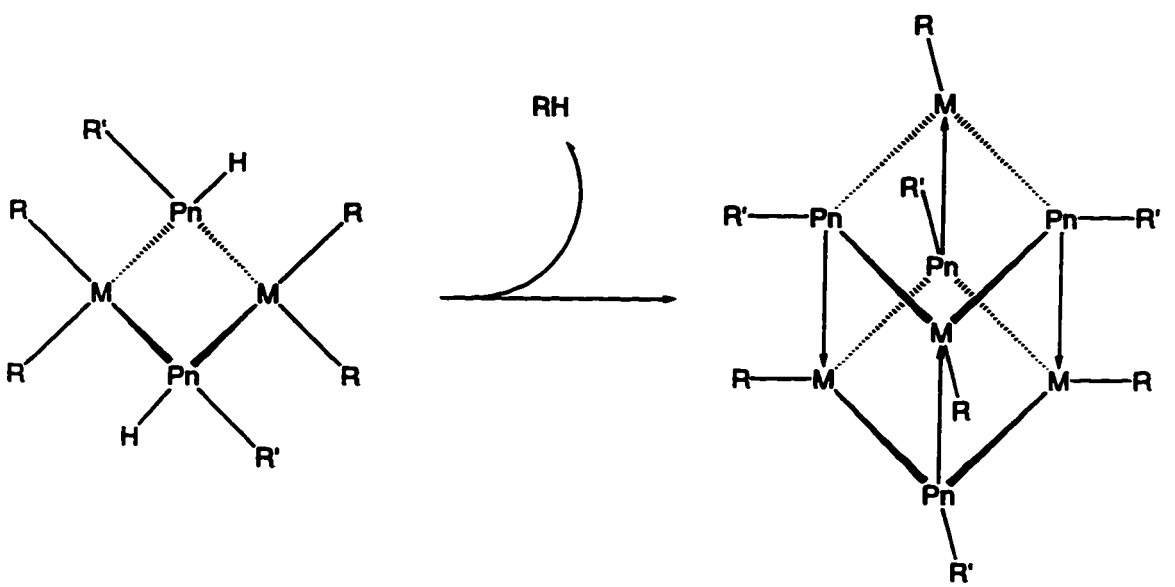

Figure 5: Possible alkane elimination from primary amido compounds resulting in an increased oligomerisation of the complex.

Finally, the general synthesis of gallium and indium compounds as precursors for MPn materials utilises salt elimination to a great degree. The Lewis acidity associated with Ga and In (III) complexes cause incorporation of LiCl in the primary coordination of the sphere and this is largely dependent on the solvent used in the synthesis. Effect of solvent in the preparation of the above-mentioned compounds will be discussed as well as stabilisation with other lithium salts. The synthesis and reactivity of the following compounds will be examined:

$Li(base)_2M(N(SiMe)_3)_2(OSiMe_3)_2Cl$

where M = Ga and base = thf
M = In and base = pyridine

$[Li(py)_2][In(N(SiMe_3)_2(OSiMe_3)_3]$

$[Li(Et_2O)_2][Ga(^nBu)_2(NH(Ph(Me)_2))_2]$

Chapter 6: The amido-chlorides and alkyl-pnictides

1. The amido-chloride compounds

The substitution reaction of lithium bis(trimethylsilyl)amide and a metal chloride is well-precedented in the literature for the synthesis of the corresponding metal amido complex.[66] The preparation of lithium bis(trimethylsilyl)amide can be carried out in either a hydrocarbon, in which case the product is base-free,[67] or in a coordinating solvent such as diethylether of thf, in which case one equivalent of base is incorporated by the salt. This versatility of the lithium salt can be exploited when the amount of coordinating base needs to be controlled in a reaction.

When one equivalent of lithium bis(trimethylsilyl)amide was added at room temperature to a hexane solution of $GaCl_3$, there was immediate precipitation of a white solid, which was shown to be lithium chloride by qualitative tests. When the solvent was removed from the reaction mixture, a slightly yellow oil remained, which showed a single peak at 0.31 ppm with respect to TMS in the ^1H NMR. No amount of drying under vacuum nor heating of this compound could convince it to become crystalline; the idea being that some small amount of impurity might be preventing solidification of this compound. An attempt at microdistillation of this material with a top temperature of approximately 150°C resulted in the decomposition of this compound into several intractable products by NMR.

However, it was found that addition of excess thf followed by evaporation of the solvent under vacuum produced microcrystalline $GaN(SiMe_3)_2Cl_2$.thf (**1**). Given the acidity of the three-coordinate Ga centre and the ample literature precedent for bridging chloride groups in such systems, it is conjectured that the oil isolated in the above reaction is a collection of oligomers or a polymer of $GaN(SiMe_3)_2Cl_2$. When a coordinating base is added, this oligomerisation is broken down to form the monomeric unit $GaN(SiMe_3)_2Cl_2$·thf.

An alternate route to this base adduct is provided by addition of the thf adduct of the lithium salt: $Li(thf)N(SiMe_3)_2$. Addition of $Li(thf)N(SiMe_3)_2$ to a dilute hexane solution of $GaCl_3$, gave precipitation of lithium chloride. Subsequent filtration and evaporation of solvent from the mother liquor afforded **1** in good yield. Although structural analysis of this compound was not done, it is speculated that this compound is a monomer due to the steric bulk at the metal centre. Indeed, the resonances for thf protons in the NMR spectrum of **1** at 3.61 and 1.00 ppm are shifted from their "free" positions (3.56, 1.41 ppm) , which is a strong indication that the thf is bound to the Ga centre. This relatively small shift is in accord with the shielding effect of gallium on the attendant ligand system.

This material was found to sublime between 90 -105°C under oil-pump vacuum and the sublimed solid was shown by NMR to be **1**, with the coordinated thf intact and in a 1:1 equivalent ratio with the amide group.

Thermolysis of this compound was attempted by two different methods, both with similar results. Initially, thermolysis of this compound was performed in toluene at approximately 200°C. Although the goal of this thermolysis was to effect the elimination of

trimethylsilylchloride and produce gallium nitride, there was no precipitate formed. After reaction, cooling the toluene solution caused the recrystallisation of $GaCl_3$, obviously the result of disproportionation of the starting material. This $GaCl_3$ was characterised by a single crystal XRD study, and was found to have a different unit cell (monoclinic, a = 6.61 Å, b = 13.08 Å, c = 11.03 Å, $\beta = 103.93^{\circ}$) and packing geometry than the literature example (triclinic, a = 6.94 Å, b = 6.84 Å, c = 6.82 Å, $\alpha = 119.5^{\circ}$, $\beta = 103.93^{\circ}$, $\gamma = 118.6^{\circ}$).[68] This observation was attributed to an effect of the solvent on the crystallisation, in this case toluene. In an effort to characterise the side-products of this thermolysis, this reaction was performed in an NMR tube. No peak was observed at 0.09 ppm, which would have been evidence of trimethylsilylchloride formation. Instead, a plethora of trimethylsilyl signals (all between 0.0 and 0.4 ppm) were found, and characterisation of these peaks proved to be an impossible task.

An alternate thermolysis of this material was carried out at 400°C in the solid state under a slightly positive pressure of N_2, and yielded a volatile liquid in the reaction vessel. This volatile liquid was collected and caught fire when exposed to air. Given the above data, it seems likely that this liquid was a mixture of thf and $GaCl_3$ ($GaCl_3$ causes the ignition of the pyridine), as well as some other possibly volatile side-products. There was no evidence of a precipitated solid in the reaction vessel.

With respect to indium trichloride, the insolubility of this compound in hydrocarbon solvents limits room temperature reactions to a coordinating solvent in order for appreciable reaction to occur.

Addition of one equivalent of $LiN(SiMe_3)_2$ to a diethyl ether slurry of $InCl_3$ at room temperature causes no discernible change, but since both $InCl_3$ and LiCl are white powdery solids at room temperature, it was difficult to differentiate between the two. The mixture was allowed to stir for three days to ensure full reaction of the starting material and comproportionation of any species. The remaining white solid was removed by filtration and XRF showed a trace amount of indium compared to chloride. This suggested that all of the $InCl_3$ had reacted and that the solid was LiCl polluted with a small amount of $InCl_3$. Reducing the volume of the mother liquor allowed isolation of a crystalline material. This material showed a singlet in the NMR at 0.41 ppm and two diethylether signals at 3.24 and 0.92 ppm. (cf. free diethylether 3.25 and 1.10 ppm) Unfortunately, further characterisation of this compound by EA or XRD was not possible due to the extreme air sensitivity of this compound. In an attempt to both quench the acidity of the metal centre and to replace diethylether with a potentially less labile ligand, the synthesis was repeated with addition of excess pyridine to the reaction mixture after the LiCl was removed. Evaporation to dryness and subsequent crystallisation from hexane gave $InN(SiMe_3)_2Cl_2.py$ (**2**) in excellent yield.

For the reasons put forth for **1**, the bulkiness of the ligands and the obviously four-coordinate metal centre describe a monomer. However, attempted sublimation of this material up to 150°C was unsuccessful.

Thermolysis of this compound was attempted in a sealed NMR tube using a sand-filled glass tube furnace. This technique, although somewhat unrefined, allowed temperatures of 200+°C to be reached, without bursting the NMR tube The subsequent NMR of the material kept at 200°C

overnight showed no thermal decomposition. The thermal stability of this compound dissuaded further thermolysis attempts.

The thermal reactivity of compounds **1** and **2** demonstrate that they are not good candidates for synthesis of MPn extended solids, but their remaining chloride groups present a chance to alter their reactivity and explore the effect of substitution on thermolysis. These materials have potential as starting materials for complexes with more promising reactivity.

2. The alkyl-pnictide compounds

When $GaN(SiMe_3)_2Cl_2$.thf (**1**) was stirred in hexane with 2 eq. of ^nBuLi , followed by filtration to remove LiCl and evaporation of the volatiles *in vacuo*, a clear and only slightly yellow oil was isolated. As was the case for **1**, this oil could only be rudimentarily characterised. A strongly coordinating base was added in order to facilitate crystallisation of the monomer.

The same reaction procedure and work-up, except with the addition of pyridine after filtration of LiCl, provided crystalline $^nBu_2GaN(SiMe_3)_2$.py (**3**) in good yield. This material is likely a four-coordinate, monomeric gallium complex. Firstly, the material was recrystallised in toluene after addition of pyridine and removal by an oil pump vacuum, demonstrating that the pyridine is coordinated by the gallium complex. Secondly, the pyridine peaks in the ^1H NMR (8.34, 6.78 , 6.46 ppm) are shifted with respect to free pyridine (8.53, 7.03, 6.71 ppm). Lastly, the integrated

intensities of pyridine compared to the silyl peak were 5:18 (py:silyl), demonstrating the presence of one pyridine per metal centre.

The ^{1}H NMR for **3** clearly illustrates the presence of the ^{n}Bu groups by the presence of three signals between 0.7 and 1.6 ppm (Figure 6). The multiplet at 1.55 ppm is due to the two central CH_2 proton signals from the butyl chain. The triplet at 1.05 ppm results from CH_3 and the misshapen triplet at 0.81 ppm is from the CH_2 bonded to the metal. It is the proximity to the metal that accounts for this chemical shift. It should be noted that the NMR peak widths for the ^{n}Bu groups are quite a bit larger than that observed for the Me_3Si signal. This again points to a constrained environment for these groups.

Thermolysis of **3** proved to be quite interesting; when heated in a Schlenk tube at 400°C in a tube furnace, a liquid was evolved which refluxed over the top of the reaction. The white, crystalline **3** present in the tube began to melt, but rapidly blackened into a small kernel of solid material.

A powder XRD pattern of this solid after drying under vacuum showed some broad features which -although not diagnostic- could be attributed to amorphous GaN (Figure 7). This lack of crystallinity was not a wholly unexpected result as the GaN was formed at a relatively low temperature (400°C). Since the material did not have an opportunity to crystallise, it is expected to be finely-divided and amorphous.

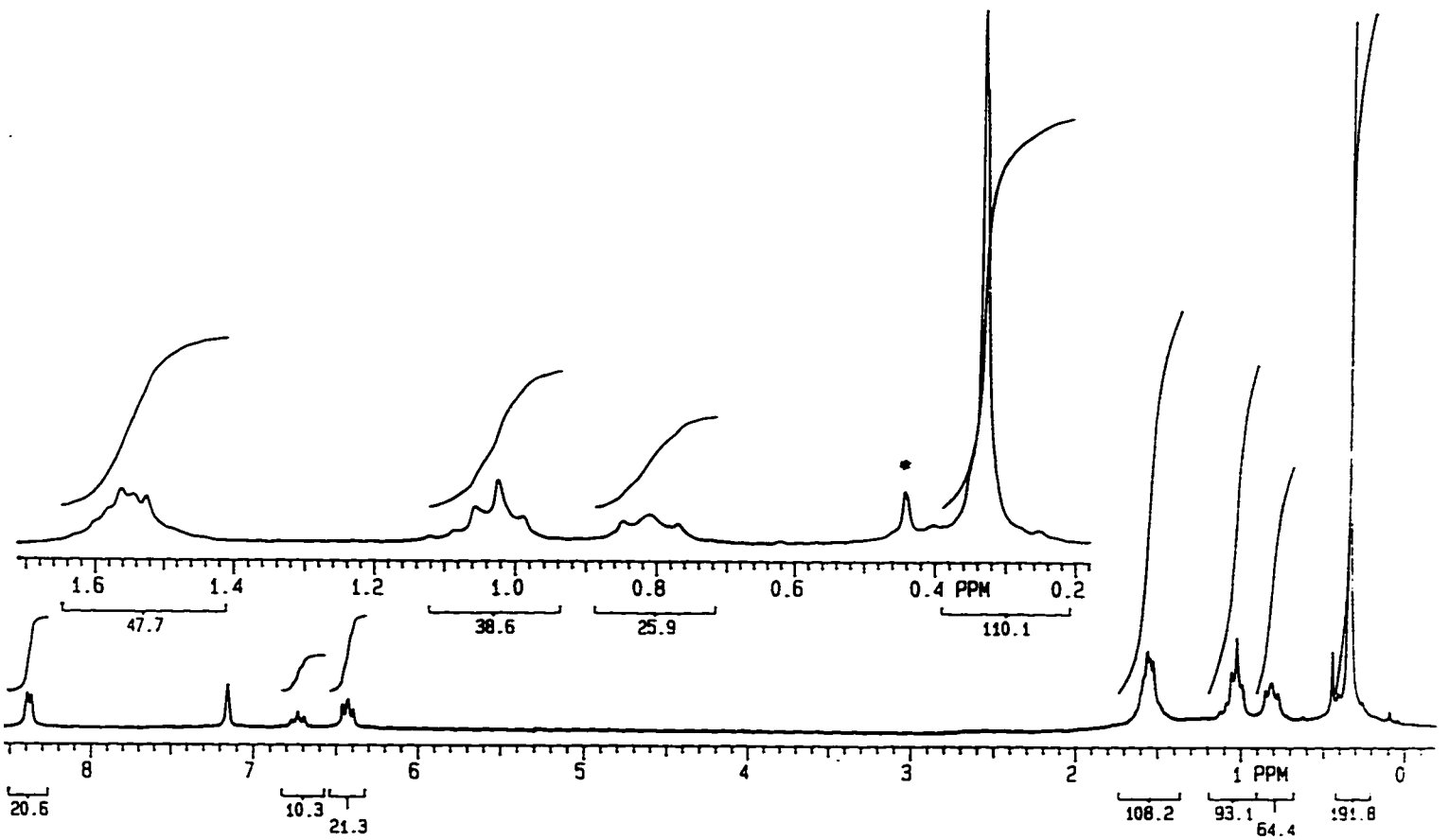

Figure 6: The ^{1}H NMR of $^{n}Bu_2GaN(SiMe_3)_2.py$ (3) with an inset detailing the butyl and trimethylsilyl proton signals. (* marks an impurity of silicone grease.)

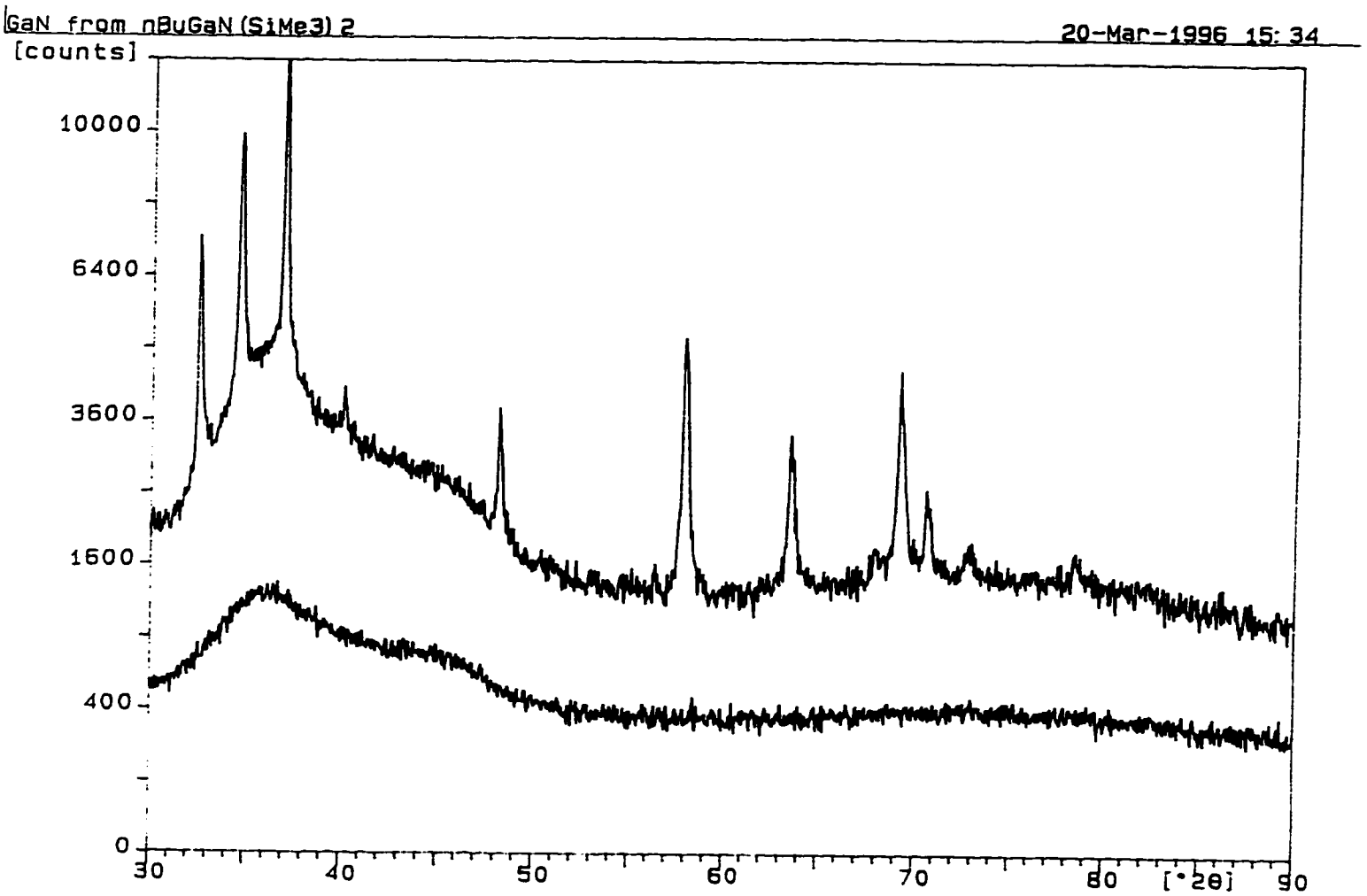

Figure 7: The PXRD for $^{n}Bu_2GaN(SiMe_3)$ (3) showing the amorphous material resulting from the reaction mixture at 400°C (lower diffractogram) and the resultant crystallinity after annealing at 900°C (upper diffractogram).

Initial attempts at annealing this compound under air found evidence of Ga_2O_3 formation by PXRD, due to reaction with atmospheric oxygen. This reaction is greatly enhanced in the present case due to the finely-divided nature of the compound.

A subsequent reaction was performed and this time the amorphous solid was transferred to a quartz tube and sealed in vacuum. This sealed tube was then heated to 900°C for 48 hr and a PXRD clearly showed formation of GaN alone (Figure 7).[69] An XRF corroborated the presence of gallium in the material. There were no other side products, nor any Ga_2O_3 detected.

Table 3 displays the correspondence between the literature[69] and experimental values of d-spacing and intensity found for GaN. An interesting aspect of the data highlighted in this table is the difference in relative intensities of the peaks. This anomaly has a few sources.

Firstly, the experimental data for the gallium nitride comes from a sample annealed at 900°C. Although annealed overnight, this material was not perfectly crystalline, by any means. If there was a preferred orientation of the sample crystals (i. e. the material crystallises in one orthogonal direction in preference to another) then this would manifest itself in the relative intensity of the peaks, and not in peak position.

Second, it can be seen from Figure 7 that there is a large background of amorphous GaN, even at 900°C. This background will obviously affect the reported intensities.

Table 3: The literature d-spacings and intensities for GaN as compared to those from a GaN sample resulting from thermolysis of **3**.

GaN (literature) d-spacing in Å	Intensity (%)	h k l	GaN (experimental) d-spacing in Å	Intensity (%)
2.76	70	1 0 0	2.76	61
2.59	50	0 0 2	2.59	85
2.43	100	1 0 1	2.43	100
1.88	60	1 0 2	1.89	14
1.59	90	1 1 0	1.59	29
1.46	80	1 0 3	1.46	13
1.38	20	2 0 0	1.38	2
1.36	80	1 1 2	1.36	20
1.33	70	2 0 1	1.33	7
1.30	20	0 0 4	1.30	2
1.22	50	2 0 2	1.22	2
1.17	40	1 0 4	1.17	1

Lastly, the nature of the detector determines that higher angle peaks (lower d-spacing) show less intensity as they are harder to detect. Data treatment can correct for this, and the literature values for GaN have been adjusted to account for this instrumental error. However, the experimental data was not so treated, and it is obvious from Figure 7 that higher angle peaks drop off rapidly in intensity. It is important to point out that the same trend in intensity of the peaks with respect to one another can be seen between the theoretical and experimental values; with the exception of the 0 0 2 peak in the experimental case. This indicates that the crystallinity is uniform in all cardinal directions, and enhanced intensity of the 0 0 2 peak is attributed to the background of the spectrum.

Subsequent reactions allowed collection of the liquid side-products, which were shown by ^1H NMR and MS to contain butane, pyridine and butylsilane. Although butylsilane and pyridine are expected side-products of this reaction, butane is surprising as it requires the presence of a proton in order to be produced. Since there is neither presence of butene in the MS or NMR, and there is no evidence of Ga^0 or Ga_2O_3 in the PXRD, it seems unlikely that this proton comes from β-hydrogen elimination. It is possible that some impurity allowed the formation of a minute quantity butane which was detected by the MS.

The analogous compound $[^tBu_2GaN(SiMe_3)_2]_2$ (**4**) can be made from the addition of $LiN(SiMe_3)_2$ to $^tBu_2GaCl$. Although $^tBu_2GaCl$ can be made using ^{t}BuLi, a far better yield can be achieved using ^{t}BuMgCl. For this reason, the Grignard reagent ^{t}BuMgCl was stirred with $GaN(SiMe_3)_2Cl_2$.thf (**1**) in diethylether at 0°C. As this material crystallised nicely upon filtration and removal of solvents, there was no reason to add base to it. The resulting crystalline **4**

showed no diethylether in the NMR, and is therefore likely a dimer if the gallium is to be coordinatively saturated. The lack of incorporation of diethylether as a coordinating solvent is likely due to the steric protection afforded the metal centre by the ^{t}Bu groups.

Thermolysis of this material was attempted in degrees. An NMR tube sealed with a Teflon stopcock was heated for 24 hr. at 30°C intervals. At the end of each interval, an NMR spectrum was collected to determine the extent of thermolysis (by loss of peaks) and to identify any products. Since the system was sealed, any soluble, proton-bearing products could be seen. By 200°C, no discernible change had taken place. As in the thermolysis of **1**, temperatures above 200°C were not attained because of concerns about cracking the NMR tube.

Solid-state thermolysis of this compound at 400°C was found to produce an uncharacterisable liquid (NMR showed a glut of peaks in both the butyl and silyl regions) and although a mirror of black material was deposited in the flask, the yield was so poor that characterisation was impossible. It seems obvious from the lack of deposited solid that most of this material sublimed away, either as starting material or as partially-reacted intermediate. By any measure, the confusing NMR made it clear that more than one process was under way in the thermolysis, and this material was not an appropriate candidate for GaN production. It seems likely that this multiple reactivity , which contrasts with the clean reactivity of the ^{n}Bu analogue **3**, is caused by the abundance of available β-hydrogens.

The phosphorus analogue of **3** - $[^{n}Bu_2GaP(SiMe_3)_2]_2$ (**5**) - was easily synthesised by Me_3SiCl elimination from a mixture of $P(SiMe_3)_3$ and $^{n}Bu_2GaCl$ in diethylether. Compound **5** was highly

crystalline and, in this state, even moderately air-stable. This stability is attributed more to the crystallinity of the material than any other factor since subsequent syntheses of microcrystalline **5** as a powder did not show the same stability.

Several indications suggest that this material is also a dimer. An NMR tube reaction of the material showed no reaction when the material was stirred in thf and dried *in vacuo*. For the compound to be coordinatively saturated and unable to react with thf, there should be a bridging ligand. This suggests an oligomer of some variety.

The ^{1}H NMR also suggested that the material is a dimer in solution (Figure 8). The signal for the trimethylsilyl peak (0.43 ppm) should be split by the adjacent ^{31}P nucleus. This spin 1/2 nucleus should produce a doublet, yet a triplet is found ($J_{PH} = 0.005$ Hz), suggesting that there are two ^{31}P nuclei affecting the centre. A $^{1}H\{^{31}P\}$ spectrum showed a singlet for the trimethylsilyl protons at 0.43 ppm, demonstrating that this splitting indeed comes from the phosphorus. If the material were dimeric, there would be an $^{3}J_{PH}$ and an $^{5}J_{PH}$ splitting. Although chemically equivalent, they are separated from the silyl group protons by a different number of bonds and therefore are inequivalent to the proton being split, resulting in a triplet. This "virtual splitting has been documented in the literature.[70].

Crystals of **5** exhibited air-stability to the extent that they could be left over-night air without obvious degradation (as probed by ^{1}H NMR). Due to the size and air-stability of these crystals, it was possible to perform a single-crystal XRD study to determine the connectivity of the material.

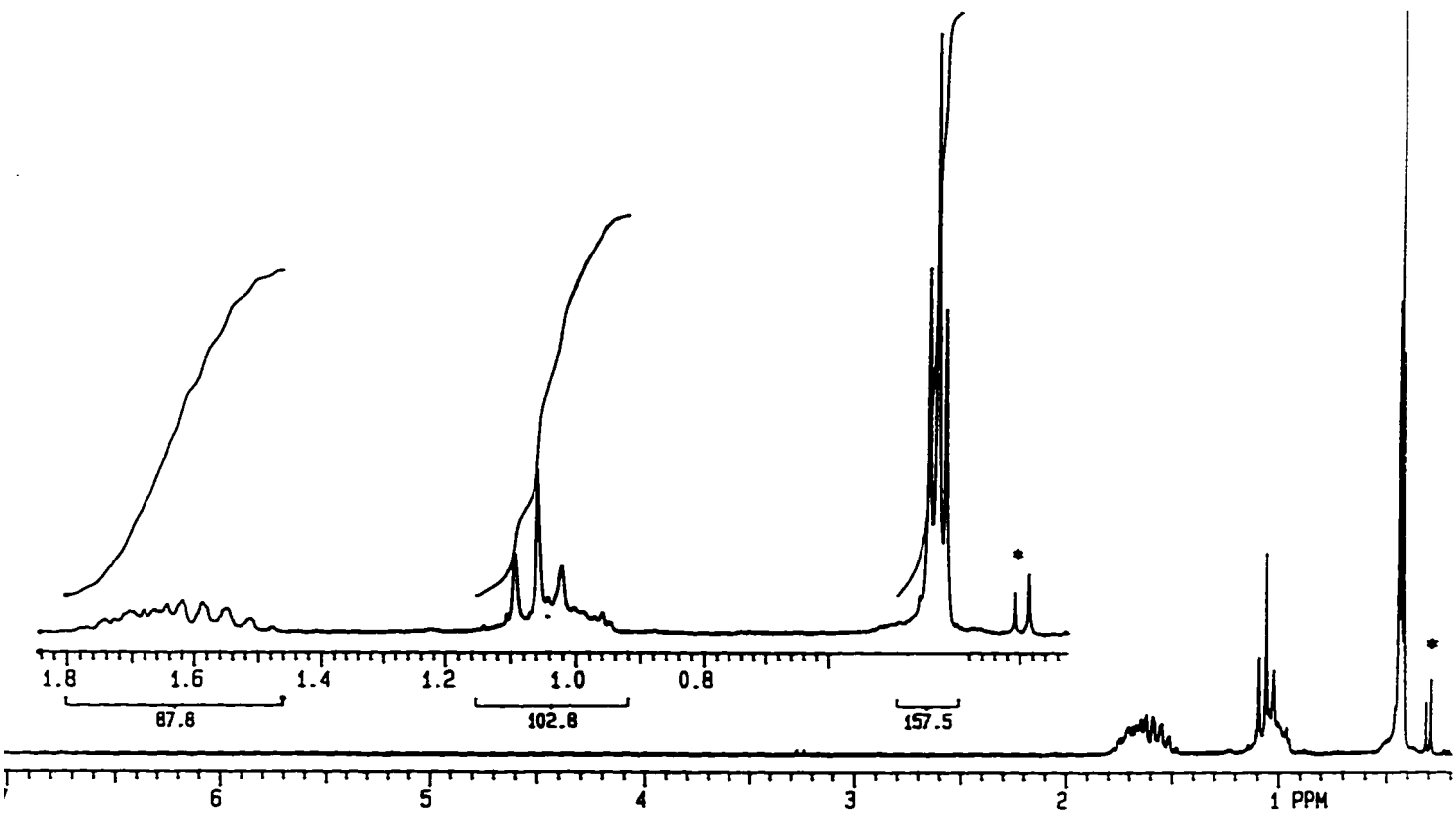

Figure 8: The ^{1}H NMR of $[^{n}Bu_2GaP(SiMe_3)_2]_2$ (**5**) with an inset detailing the butyl signals and the triplet from the splitting between the trimethylsilyl protons and the two phosphorus of the dimer (* marks an impurity of $P(SiMe_3)_3$).

The result showed a dimeric material with a distorted square centre (Figure 9, full crystal data in Appendix 1).The complex crystallises in the triclinic space group P-1(bar) (#2) with no anomalously short intermolecular contacts. Selected bond distances and angles for the molecule are presented in Table 4.

The structural analysis revealed a Ga_2P_2 core which deviates from planarity by .2° (the sum of the internal angles for the core is 359.8°), and the angles within this core are somewhat strained. For example, the angle P1-Ga2-P2 angle is 88.5°. Both the bridging P and the Ga centres are in distorted tetrahedral environments with a range of bond angles (Figure 9).

Since **5** exhibited some air-stability, it was possible to perform a thermogravimetric analysis (TGA) (Figure 10). This analysis showed two main weight losses at 200 and 275°C, which result in a total mass loss of 77%. Based on the formation of GaP with a ceramic yield of 28% from **5**, the expected weight-loss for the compound which is 72%. These numbers are self-consistent, considering the material is somewhat air sensitive and may have begun to react with O_2 and water in the atmosphere. This could result in the loss of some phosphide as $HP(SiMe_3)_2$ and cause the percent weight lost to be higher than expected.

When the thermolysis of **5** was carried out on a large scale and the side-products collected, it was evident from the ^1H NMR and MS that butylsilane was produced, as was expected for the dealkylsilation of **5** to produce GaP. The reason *two* weight-losses were seen in the TGA might be due to the low volatility of the butylsilane produced. The first weight loss results from the elimination reaction and the second small weight loss is the vapourisation of butylsilane adhered

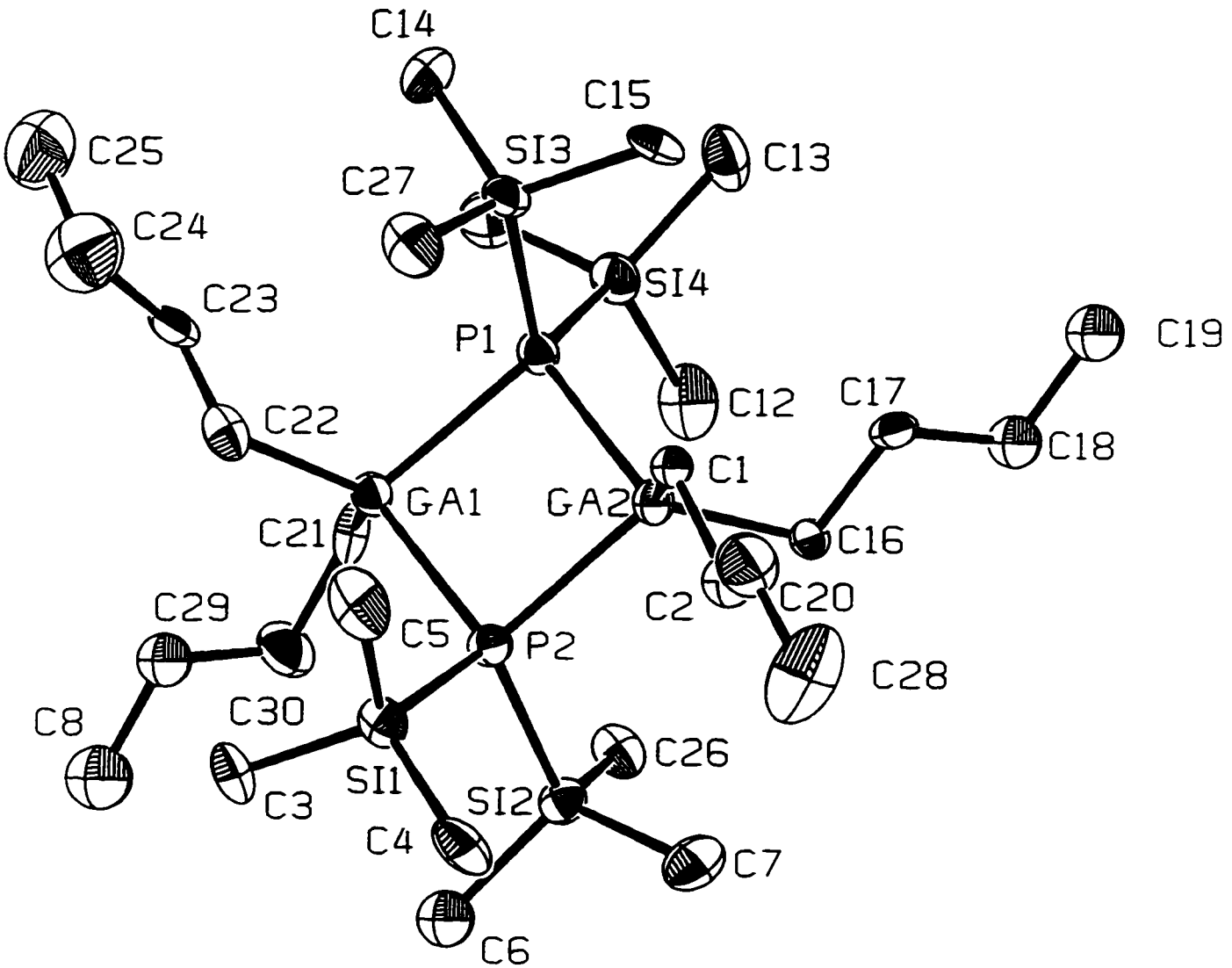

Figure 9: The single crystal XRD ORTEP diagram of $[^{n}Bu_2GaP(SiMe_3)_2]_2$ (**5**) confirming its dimeric nature.

Table 4: Selected bond lengths and angles from the single crystal XRD of **5**.

Bond	Length in Å	Vertices	Angle in°
Ga1-P1	2.463(3)	P1-Ga1-P2	88.1(1)
Ga1-P2	2.451(3)	P1-Ga1-C21	113.1(3)
Ga1-C21	2.00(1)	P1-Ga1-C22	106.8(3)
Ga1-C22	1.99(1)	P2-Ga1-C21	112.7(3)
Ga2-P1	2.445(3)	P2-Ga1-C22	115.9(3)
Ga2-P2	2.454(3)	C21-Ga1-C22	116.5(4)
Ga2-C1	2.010(9)	P1-Ga2-P2	88.5(1)
Ga2-C16	1.99(1)	P1-Ga2-C1	113.8(3)
P1-Si3	2.254(4)	P1-Ga2-C16	111.6(3)
P1-Si4	2.265(4)	P2-Ga2-C16	112.6(3)
P2-Si1	2.258(4)	P2-Ga2-C16	114.8(3)
P2-Si2	2.244(4)	C1-Ga2-C16	113.3(4)
Si1-C3	1.85(1)	Ga1-P1-Ga2	91.6(1)
Si1-C4	1.85(1)	Ga1-P1-Si3	119.7(1)
Si2-C5	1.85(1)	Ga1-P1-Si4	111.7(1)
Si2-C6	1.86(1)	Ga2-P1-Si3	108.3(1)
Si2-C7	1.86(1)	Ga2-P1-Si4	119.0(1)
Si2-C26	1.86(1)	613-P1-Si4	106.7(2)
Si3-C14	1.84(1)	Ga1-P2-Ga2	91.7(1)
Si3-C15	1.85(1)	Ga1-P2-Si1	111.0(1)
Si3-C27	1.87(1)	Ga1-P2-Si2	118.8(1)
Si4-C11	1.85(1)	Ga2-P2-Si1	119.6(1)
Si4-C12	1.85(1)	Ga2-P2-Si2	109.9(1)
Si4-C13	1.85(1)	Si1-P2-Si2	106.1(2)
		Ga2-C1-C2	105.9(6)
		Ga2-C16-C17	109.0(6)
		Ga1-C22-C23	108.5(7)

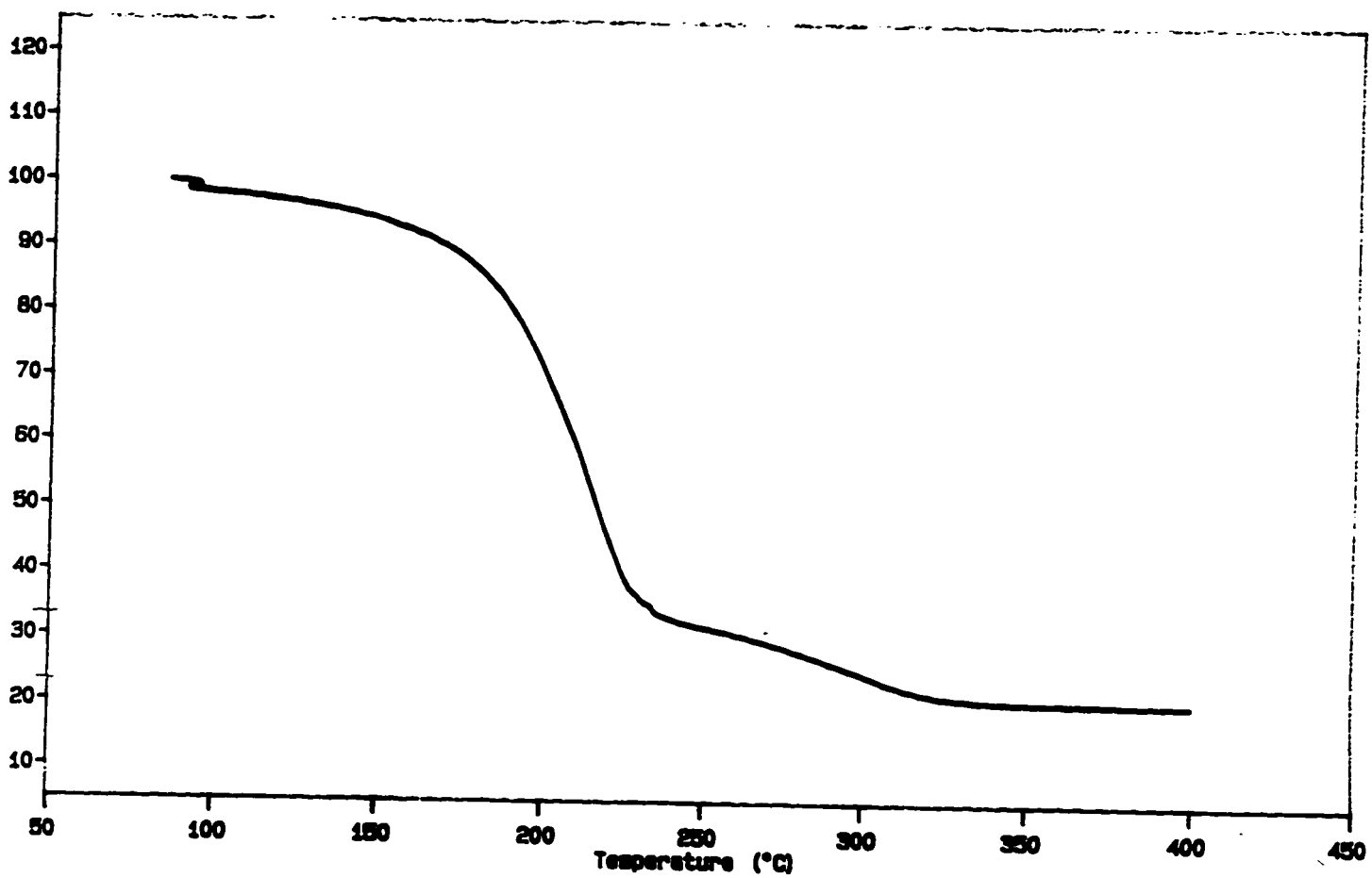

Figure 10: The TGA of $[^{n}Bu_2GaP(SiMe_3)_2]_2$ (5) showing a 77% weight loss due to GaN formation. (ceramic yield = 28%)

to the solid state product of the reaction. Reaction of the compound in the solid state at 400°C produced a grey-black material within a matter of minutes. The thermolysis was done under nitrogen, and a clear liquid was seen to reflux above the hot-zone of the furnace. This clear liquid appeared viscous at room temperature and was soluble in benzene. ^{1}H NMR of this compound showed the presence butylsilane, which was confirmed by MS.

The PXRD of the grey-black material identified it as GaP, which was produced in a 97% yield (Figure 11). The material showed crystallinity without annealing, which was unexpected due to the relatively high melting-point of GaP (1465°C).[2] It seems that there is some crystallisation mechanism at work, perhaps similar to that conjectured by Buhro, where an In^0 flux allows crystallisation of the refractory material.[35]

Table 5 shows the correspondence between the literature[71] and experimental spectra for GaP. As before, the relative intensities are not the same as literature values but follow the same trends. Likely, the reasons for this are the same as discussed previously for GaN.

XRF analysis confirmed the ratio of Ga:P as 1:1. A small (10 mole%) impurity of silicon was also detected. Since there is no evidence of any other crystalline material by PXRD, appears that the silicon-containing impurity was amorphous in nature. The liquid side product of the reaction was found to be viscous and was difficult to vacuum transfer at room temperature, so some of it might have remained with the solid through the attempted purification steps.

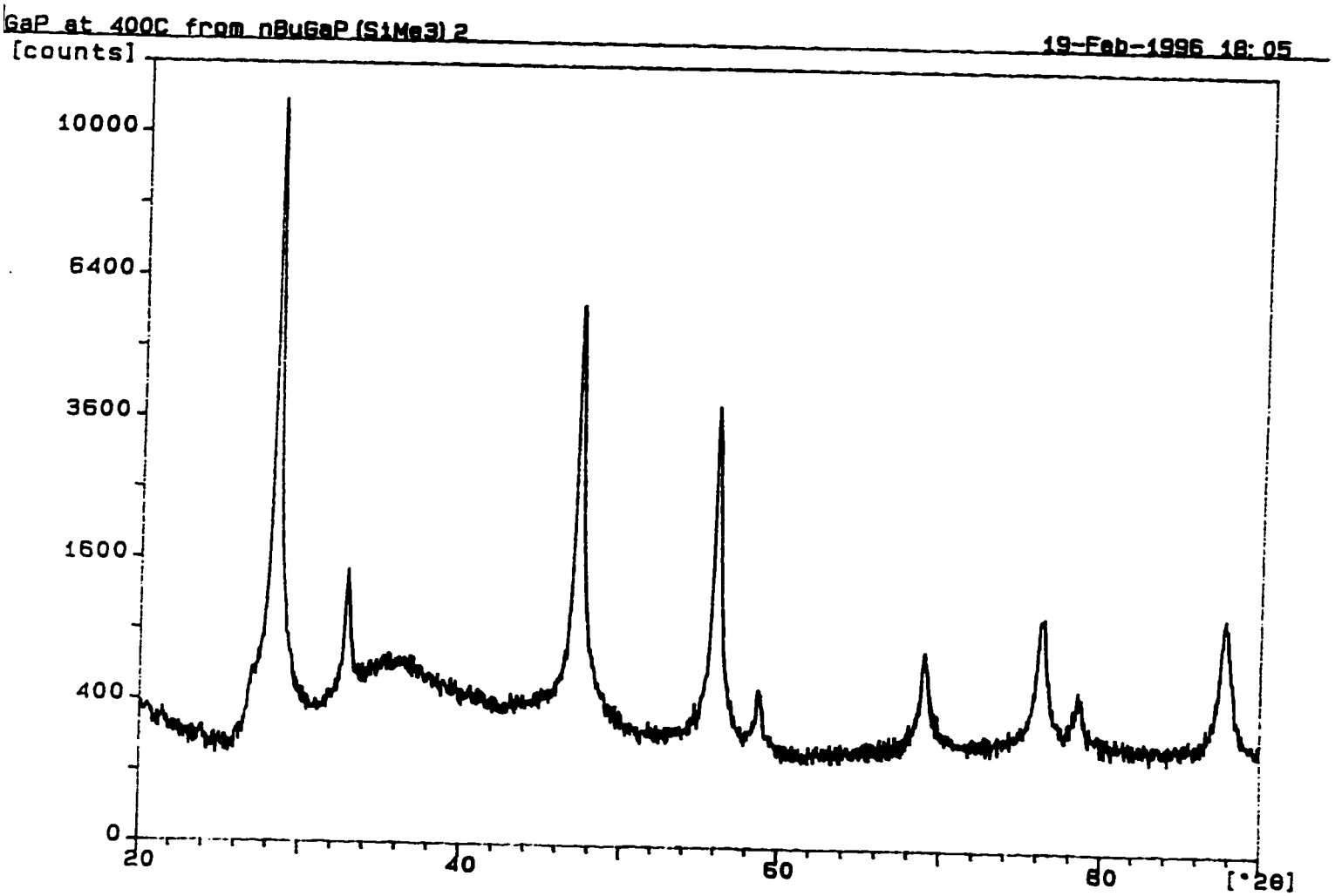

Figure 11: The PXRD of GaP from $[^{n}Bu_2GaP(SiMe_3)_2]_2$ (**5**) at 400°C without annealing.

Table 5: The literature d-spacings and intensities for GaP as compared to those from a GaP sample resulting from thermolysis of **5**.

GaP (literature) d-spacing in Å	Intensity (%)	h k l	GaP (experimental) d-spacing in Å	Intensity (%)
3.15	100	1 1 1	3.14	100
2.73	13	2 0 0	2.72	8
1.93	88	2 2 0	1.93	31
1.64	13	3 1 1	1.64	17
1.57	1	2 2 2	1.57	1
1.36	3	4 0 0	1.36	2
1.25	8	3 3 1	1.25	3
1.22	6	4 2 0	1.22	1
1.11	4	4 2 2	1.11	2

The silicon impurity might also be from the glass of the reaction vessel, as the vessel was cut in order to allow removal of the GaP. It is possible that glass fragments fell in with the GaP before it was removed, and were not detected by PXRD due to the amorphous nature of glass.

Since the above reactivity suggested that the trimethylsilychloride elimination may occur more easily than alkyl group elimination, $^{n}BuGaCl_2$[72] was stirred in diethylether with $P(SiMe_3)_3$. The idea was to eliminate both chlorides as Me_3SiCl and form a phosphinido moiety at the gallium centre. However, the room temperature reaction between these two produced $Ga(^{n}Bu)(Cl)P(SiMe_3)_2$ (**6**) in mediocre yield due to its solubility, and no other product could be isolated. The NMR of this compound is understandably similar to that of **5**, also exhibiting a triplet for the trimethylsilyl protons. This indicates that the material is a stable phosphorus-bridged dimer in solution. These results are in perfect accord with what is expected when the relative basicities of the phosphorus and chloride centres are considered.

Subsequent thermolysis of **6** in an NMR tube at a mere 90°C in an oil bath showed formation of a peak at 0.09 ppm, indicating elimination of trimethylsilylchloride, as was desired. Unfortunately, five other trimethylsilyl signals evolved, implying that several other reactive pathways are open to this compound at such a temperature. All of these signals appeared between 1.50 and 0.50 ppm and were split by phosphorus. Isolation of these product was not attempted as the thermolysis was not distinct enough to pursue.

When a stoichiometric amount of $(^{n}Bu)_2InCl$ was added to a stirred solution of $P(SiMe_3)_3$ in diethylether, an almost immediate reaction occured, as indicated by a slight yellowing of the solution. After allowing the material to comproportionate

overnight, the volatiles were removed under vacuum and the resulting white solid was recrystallised in toluene, begetting $[(^nBu)_2InP(SiMe_3)_2]_2$ (**7**) in good yield.

The lack of diethylether in the ^1H NMR and the fact that, as with **5**, the trimethylsilyl signal is split into a triplet by the phosphorus, is evidence that this complex is a dimer. The ^1H NMR of **7** is similar to that of **5**, with only the multiplet for the α-CH_2 coming in at a lower field than the signal for the CH_3 triplet, due to the deshielding effect of the indium nucleus.

The thermolysis of this compound at 400°C under nitrogen in a Schlenk tube produced a liquid side-product and a dark grey solid. When the solid was washed with acetone and air-dried, small crystals could be seen in it, indicating a high degree of crystallinity. A PXRD revealed two distinct products: InP and metallic indium (Figure 12).

Table 6 demonstrates the agreement between the literature spectra of both InP and In^0 and the spectrum resulting from the thermolysis of **7**. An XRF analysis showed a ratio of In:P of 2:1 and a large silicon impurity. Since no XRD reflections for possible silicon products appeared, the nature of the silicon impurity is still unclear and suspected to be contamination from the reaction vessel.

The metallic indium presumably resulted from a β-hydrogen elimination from the butyl group; this was confirmed by the presense of butene in the ^1H NMR as well as in a MS of the side-products. Butane was also found, indicating a reductive elimination which eventually leads to the fomation of In^0. (Figure 13)

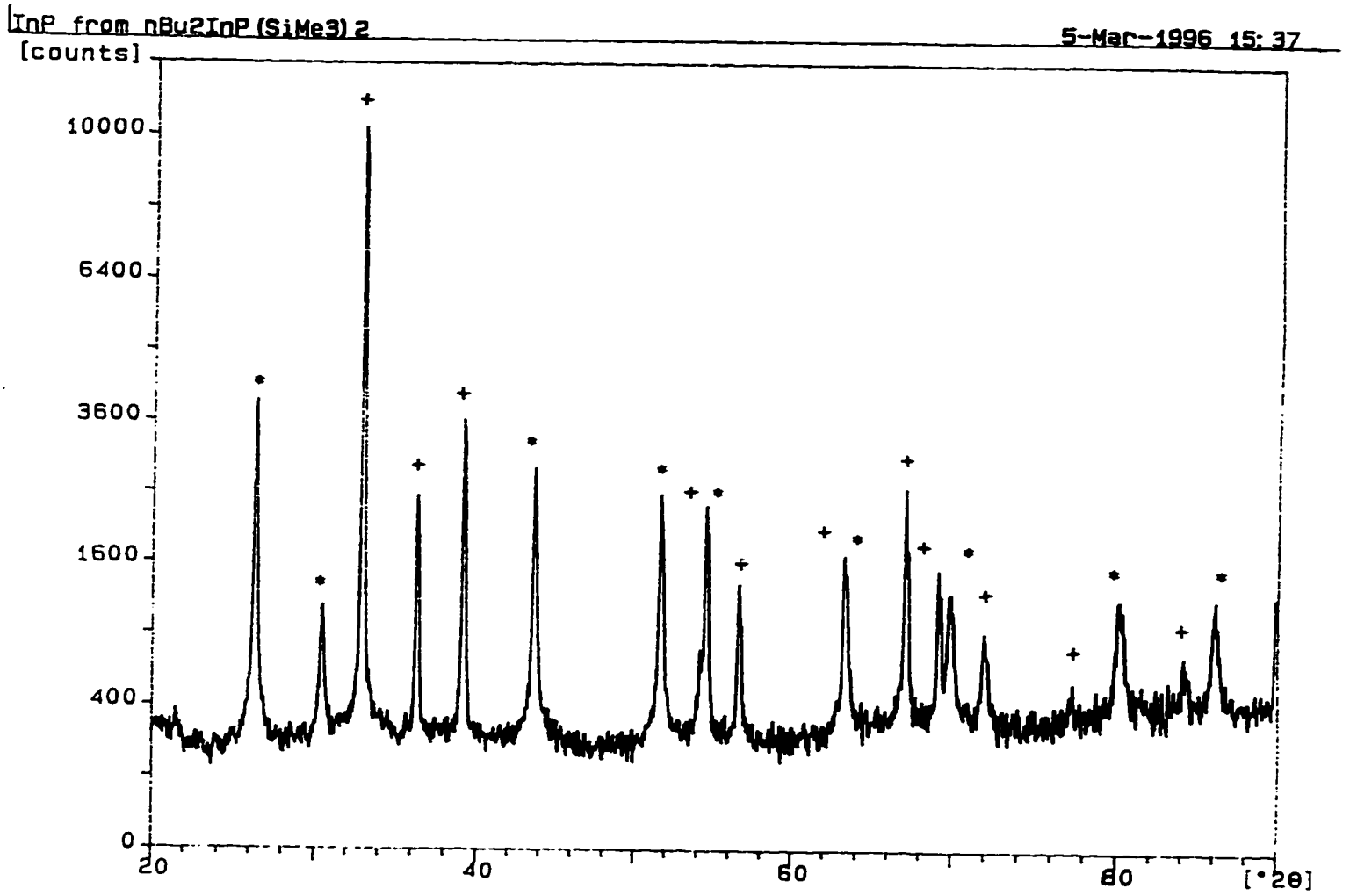

Figure 12: The PXRD of a physical mixture of In and InP from $[(^nBu)_2InP(SiMe_3)_2]_2$ (7) at 400°C (where * are InP reflections and + are In^0 reflections).

Table 6: The literature d-spacings and intensities for InP and In^0 as compared to those from a solid sample resulting from thermolysis of **7**.[73,74] The starred peaks are indistinguishable from each other in the spectrum.

InP and In^0 d-spacing in Å		(literature) Intensity (%)	h k l		InP and In^0 d-spacing in Å		(experimental) Intensity (%)
InP	In^0		InP	In^0	InP	In^0	
3.39		100	1 1 1		3.40		71
2.94		35	2 0 0		2.94		16
	2.72	100		1 0 1		2.71	100
	2.47	21		0 0 2		2.47	32
	2.30	21		0 0 2		2.30	46
2.07		50	2 2 0		2.07		32
1.77		35	3 1 1		1.77		21
1.69		10	2 2 2		1.68		19*
	1.68	24		1 1 2		1.68	19*
	1.63	12		2 0 0		1.63	12
1.47		10	4 0 0		1.47		12*
	1.47	16		1 0 3		1.47	12*
	1.40	23		2 1 1		1.39	15
	1.36	11		2 0 2		1.36	8
1.35		10	3 3 1		1.34		8
	1.31	8		4 2 0		1,31	5
	1.24	3		0 0 4		1.23	1
1.20		10	4 2 2		1.20		5
	1.15	5		2 2 0		1.15	1
1.13		15	5 1 1		1.13		5

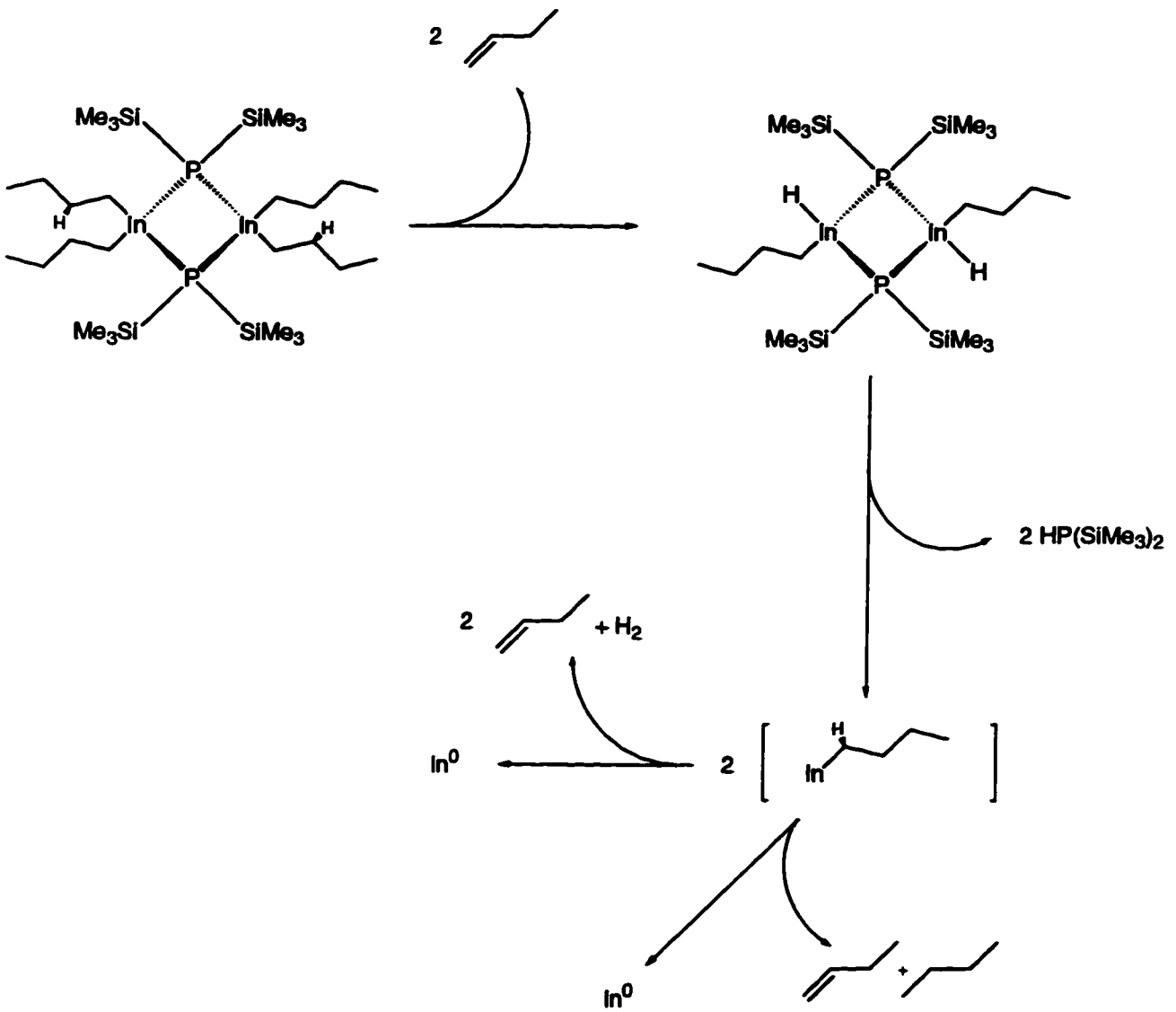

Figure 13: A mechanism for In^0 from $[(^nBu)_2InP(SiMe_3)_2]_2$, (7) demonstrating first β-hydrogen elimination and subsequent reductive elimination of In^{3+} to In^+.

The alkyl-silyl elimination from **7** motivated the exploration of similar reactivity from the $P(SiMe_3)_3$ adduct of $In(^nBu)_3$. When $In(^nBu)_3$[75] was stirred in hexane with $P(SiMe_3)_3$, a viscous liquid product resulted. The ^1H NMR for this compound confirmed that the phosphido moiety was present and the integration showed the presence of one butyl group for every trimethylsilyl group (Figure 14). As well, the trimethylsilyl signal was a doublet ($J_{PH} = 0.03$ Hz), as one would expect for the compound $(^nBu)_3InP(SiMe_3)_3$. Due to the air-sensitive nature of this material, full characterisation to confirm this formula was not possible as elemental analysis results were inconclusive. The thermolysis of $(^nBu)_3InP(SiMe_3)_3$ was performed under the same conditions (400°C under N_2) as used for **7**. Liquid side-products and a grey solid were produced and a PXRD of the grey solid again showed the presence of both In metal and InP. An XRF of the grey solid gave an In:P ratio of 3:1. An amorphous silicon impurity was again present, but its formulation and source is unknown.

In order to explore the effects of temperature on the reaction product ratio, $(^nBu)_3InP(SiMe_3)_3$was heated in a sealed NMR tube under nitrogen. At 110°C and over a 24 hr. period, the adduct $(^nBu)_3InP(SiMe_3)_3$ showed no reactivity whatsoever. When it was heated to 130°C overnight by an oil bath in a sealed NMR tube, a grey solid precipitated from the reaction mixture. The PXRD pattern of this material showed indium metal as the only obvious phase. The appearance of an extremely small set of resonances in the ^1H NMR at 5.00 ppm indicated the presence of butene, as expected from the reaction sequence in Figure 14. It appears that production of indium metal can occur at fairly low temperatures and thus both **7** and the adduct $(^nBu)_3InP(SiMe_3)_3$ are not suitable for the production of pure InP.

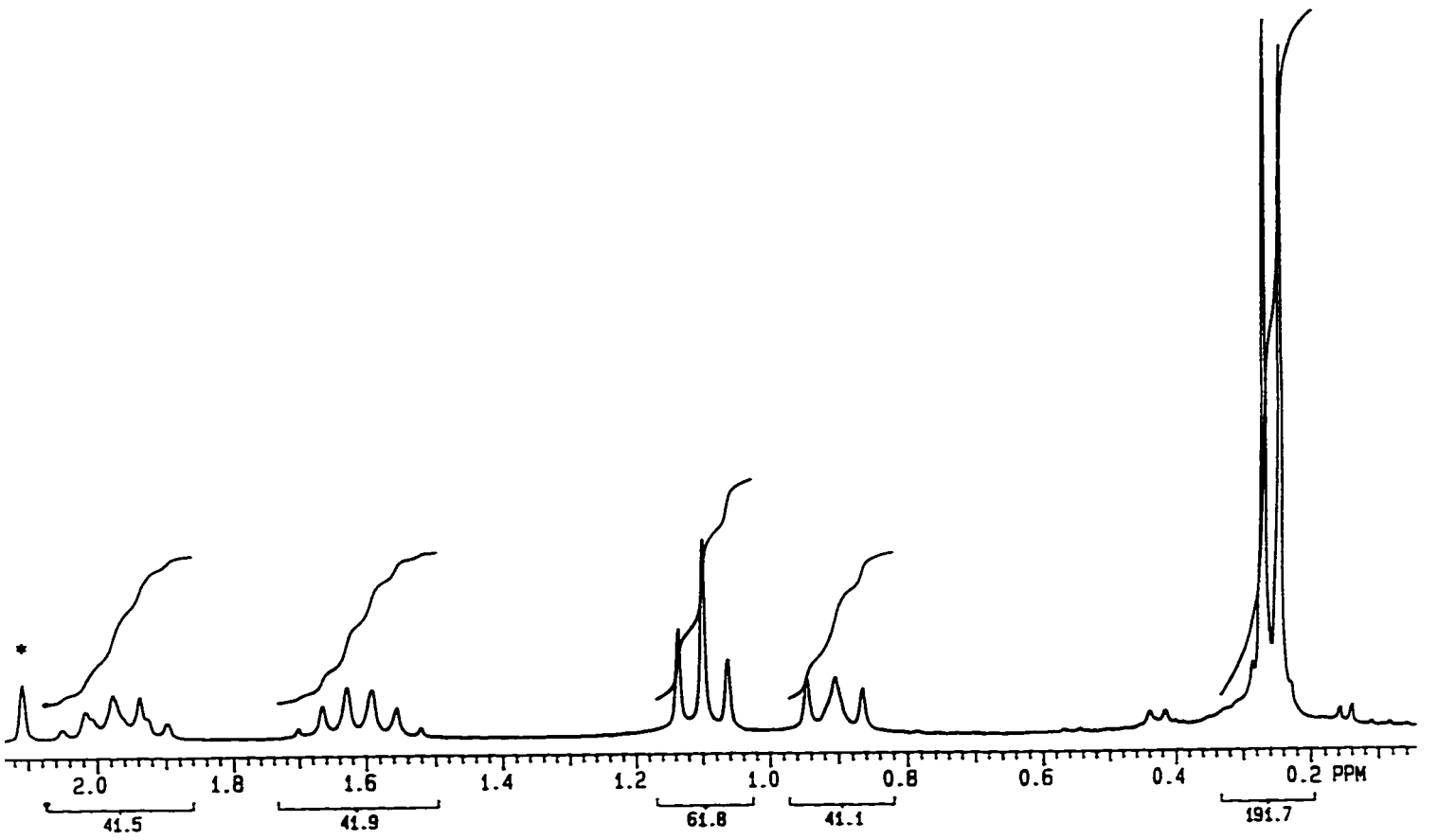

Figure 14: The ^{1}H NMR of $(^{n}Bu)_3InP(SiMe_3)_3$ demonstrating the doublet from the trimethylsilyl protons being split by the one phosphorus of the monomer. (* marks an impurity of toluene).

The reaction mixture for the NMR tube boil-up of $(^nBu)_3InP(SiMe_3)_3$ also contained **7**. Side-products of this reaction are not evident in the ^1H NMR, but **7** is plainly apparent and obviously the result of elimination of an alkylsilane ($^nBuSiMe_3$). Unfortunately, these two reactions seem to occur at similar temperatures, and thus pure **7** cannot be produced from the adduct.

The differences in the reactivity between the indium and gallium complexes of the general formula $[^nBu_2MP(SiMe_3)_2]_2$ is striking and can be attributed to the following facts:

1. Stability of a higher coordination number around indium compared to gallium.

2. The relative acidity of gallium versus indium.

Although both metal centres can form complexes with either four or six ligands in their coordination spheres, due to the difference in radius, gallium prefers four ligands while indium is able to easily accommodate six. As a result indium has more freedom - even in a moderately sterically congested environment - to coordinate ligands for the purposes of reaction, where gallium is more constrained by the steric demands of its surroundings. This may partially account for $^n(Bu)_2InP(SiMe_3)_2$ reacting by several different pathways while thermolysis of $^n(Bu)_2GaP(SiMe_3)_2$ proceeds by one pathway.

The higher charge to radius ratio for gallium results in it being a more acidic metal centre than indium. This may allow the ligands attached to indium to associate and dissociate more freely. Particularly in the case of the adduct $(^nBu)_3InP(SiMe_3)_3$, and even in the case of $^n(Bu)_2InP(SiMe_3)_2$, this may result in a homoleptic alkyl indium species, which can undergo

intramolecular β-H eliminations and alkyl reductive eliminations. This would allow the indium species access to a second reaction pathway which is denied the gallium species.

The varying successes of the compounds **3-7** in the generation of MPn demonstrate the utility of this class of compounds for the synthesis of extended solids, as well as possible pitfalls (*e.g.* β-hydrogen and reductive elimination) which can be avoided by careful choice of ligand system.

Chapter 7: The alkyl-amides with primary amides

The tendency of gallium and indium amido complexes to oligomerise and thus increase the coordination number of the metal centre is expected to manifest itself for imido complexes of these metals. The aggregation of these species may divulge useful information about the mechanism and formation of MPn from molecular precursors.

Elimination of an alkane from an alkyl gallium complex containing a primary amide is one inroad to an imido complex; therefore a series of gallium compounds containing primary amido groups were synthesised and the thermolysis of these compounds was studied. Since steric effects are likely to play an important role in the level of aggregation of these species, we have chosen both alkyl groups (^{n}Bu and ^{t}Bu) and amido groups (^{t}BuNH and [2,6-$Me_2C_6H_3$]NH) of intermediate steric bulk.

The reaction of $(^t Bu)_2GaCl$ and $LiN(H)^tBu$ in hexane resulted in the immediate formation of LiCl. After filtration and removal of the solvent under vacuum, recrystallisation in a thf/hexane solution resulted in the isolation of $[Ga(^tBu)_2(NH^tBu)]_2$ (**8**) as colourless crystals in 49% yield. The ^{1}H NMR spectrum of this complex indicated the appropriate ratio of ^{t}Bu groups for the formula $[(^tBu)_2Ga(N(H)^tBu)]_n$ along with a broad singlet at 2.12 ppm which was assigned to the amido proton. However, there was no evidence of ν_{NH} in the IR spectrum for this complex. This is not an unusual feature as coordination of the amido group to a metal centre will often cause the N-H absorbance to fall into, and subsequently be masked by, the broad C-H found between 2800-3000 cm^{-1}. This compound does not coordinate ancillary ligands such as thf or pyridine; indeed

the crystallisation of this base-free compound occured from thf. Since, unlike the with the $N(SiMe_3)_2$ moiety, the amide does not share a bond with silicon, the amido lone pair is much more basic. This feature manifests itself by forming a bond which supercedes that of a possible dative thf interaction.

Crystals of **8** are stable in air for several hours. This is likely due to the presence of the bulky substituents, and this stability allowed characterisation by single-crystal XRD. In order to confirm the nuclearity of complex **8**, a single crystal X-ray diffraction study was performed and it confirmed the dimeric nature of this primary amido-bridged complex: $[(^tBu)_2Ga(\mu\text{-}N(H)^tBu)]_2$ (Figure 15, full crystal data in Appendix 2).

The complex crystallises in the triclinic space group P-1 with two molecules in the asymmetric unit and no anomolously short intermolecular contacts. Selected bond distances and angles for the two molecules are presented in Table 7.

The structural analysis revealed a planar Ga_2N_2 core, with each of the molecules residing on an inversion centre. The angles within this core are quite strained. For example, the angle N1-Ga1-N1A is 81.7° and that for Ga1-N1-Ga1A is 98.3° (the sum of the internal angles for both molecules is 360°). Both the bridging N and the Ga centres are in distorted tetrahedral environments with a range of bond angles. The structural parameters including Ga-C (range = 2.052(3)Å to 2.065(3)Å) and Ga-N (range = 2.060(3)Å to 2.069(3)Å) distances are in accord with those observed for similar compounds in the literature.[76]

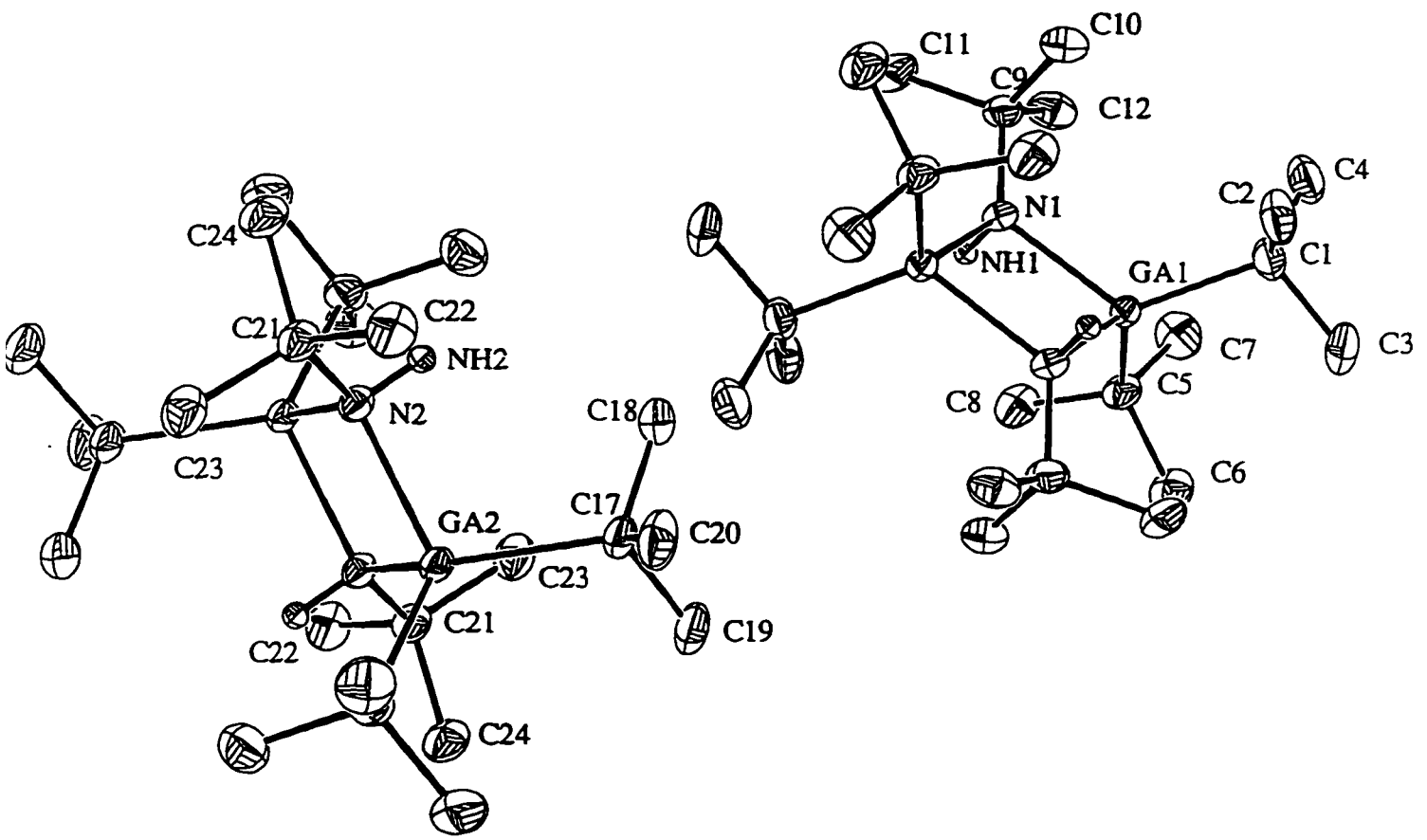

Figure 15: The single crystal XRD ORTEP diagram of [^{t}Bu$_2$Ga(μ-N(H)^{t}Bu)]$_2$, (**8**) showing the two orientations of the molecule in the unit cell and confirming its dimeric nature.

Table 7: Selected bond lengths and angles from the single crystal XRD of **8**.

Bond	Length in Å	Vertices	Angle in°
Ga1-N1	2.068(3)	N1-Ga1-N1a	81.7(1)
Ga1-N1a	2.060(3)	N1-Ga1-C1	120.1(1)
Ga1-C1	2.065(3)	N1-Ga1-C5	108.2(1)
Ga1-C5	2.055(3)	N1a-Ga1-C1	108.7(1)
Ga2-N2	2.062(3)	N1a-Ga1-C5	120.2(1)
Ga2-N2b	2.069(3)	C1-Ga1-C5	114.5(1)
Ga2-C13	2.052(3)	Ga1-N1-Ga1a	98.3(1)
Ga2-C17	2.054(3)	Ga1-N1-C9	125.9(2)
N1-C9	1.511(4)	Ga1a-N1-C9	124.9(2)
N2-C21	1.503(4)	Ga1-C1-C2	112.9(2)
C1-C2	1.522(6)	Ga1-C1-C3	107.6(2)
C1-C3	1.548(6)	Ga1-C1-C4	113.8(3)
C1-C4	1.539(5)	Ga1-C5-C6	114.2(2)
C5-C6	1.537(5)	Ga1-C5-C7	107.1(2)
C5-C7	1.530(5)	Ga1-C5-C8	113.4(2)
C5-C8	1.531(5)	N2-Ga2-N2b	82.3(1)
C9-C10	1.528(5)	N2-Ga2-C13	120.7(1)
C9-C11	1.532(5)	N2-Ga2-C17	107.5(1)
C9-C12	1.522(5)	N2b-Ga2-C13	108.8(1)
		N2b-Ga2-C17	120.2(1)
		C13-Ga2-C17	114.1(1)
		Ga2-N2Ga2b	97.7(1)
		Ga2-N2-C21	126.2(2)
		Ga2b-N2-C21	124.2(2)
		Ga2-C17-C18	113.3(2)
		Ga2-C17-C19	115.3(2)
		Ga2-C17-C20	107.0(2)

Thermolysis of this compound at 120°C under nitrogen in toluene allowed isolation of a clear crystalline material. ^{1}H NMR showed two singlets at 1.29 and 0.86 ppm of equal integration. An IR of this compound also was found to lack the NH absorption, but as previously described, this is by no means indicative of an absence of a amido proton. However, there was a notable absence of a NH resonance in the ^{1}H NMR as well, which contrasts with the spectrum of the starting material. Extreme reactivity of this compound with air and water precluded a meaningful elemental analysis or mass spectral analysis, but the available spectroscopy suggests the formulation $[^t$BuGaN^{t}Bu$]_x$. This assignment was supported by the reactivity of this complex with thf. When it was stirred in toluene with thf and subsequently recrystallised, the ^{1}H NMR showed thf resonances at 3.47 and 1.31 ppm, which is shifted from the free thf resonances. The ^{1}H NMR spectrum also contained two singlets (equal by integration) at 1.47 and 1.27 ppm, and integration also showed one thf molecule per gallium ^{t}Bu group. Again the extremely reactive nature of this compound did not allow full and proper characterisation, but the most likely formulation is $[^t$BuGaN^{t}Bu(thf)$]_2$.

A similar reaction of $(^n$Bu$)_2$GaCl and LiN(H)^{t}Bu in hexane gave an oily, non-crystalline solid. A crude NMR of this compound showed it to be impure; the complex $[^n$Bu$_2$Ga(N(H)^{t}Bu)$]_2$ (**9**) could be isolated as colourless crystals in approximately 40% overall yield by crystallisation in thf. This material is a dimeric primary amido dialkyl species as shown through ^{1}H and ^{13}C NMR spectral analysis, and elemental analysis confirmed the formulation of **9**. Complex **9** can be sublimed under oil pump vacuum at 90°C.

The ^{1}H NMR of **9** did show one odd feature. The butyl α-C*H*$_2$ is split into two multiplets at 0.73 and 0.55 ppm. Each of these resonances integrate as four protons per dimer, and a 2 dimensional COSY ^{1}H NMR spectrum determined their connectedness, as well as relating them to the β-C*H*$_2$ peak. A 2 dimensional heteronuclei correlation spectrum attributed both proton resonances to the same ^{13}C resonance (16.2 ppm) which was found to be a CH_2 by a DEPT experiment. This splitting is likely due to the constrained environment in which the protons find themselves. A variable temperature NMR did not confirm nor deny this claim, as the peaks did not show coalescence at the high-temperature threshold of the solvent.

[^{n}Bu$_2$Ga(N(H)^{t}Bu)]$_2$ (**9**) did not demonstrate any thermal activity when heated in a sealed NMR tube up to 200°C in an oil bath. Compared to [Ga(^{t}Bu)$_2$(NH^{t}Bu)]$_2$ (**8**), this material is remarkable stable. Complex **9** has only two α-hydrogens which have a particular spatial orientation, where **8** has nine such protons and these are arrayed around the alkyl group. Thus, loss of an alkyl group by elimination with the α-hydrogen is less likely within **9** and subject to steric effects.

Similarly, attempts to make a Lewis base-free complex from the reaction of (^{n}Bu)$_2$GaCl and Li[N(H)(2,6-C$_6$H$_3$Me$_2$)] in diethylether were unsuccessful, yielding only an oily intractable material which was not stable enough for characterisation. Addition of pyridine did not facilitate the crystallisation of this material but allowed isolation of an oil that was relatively stable in air (over several hours). This allowed the characterisation of the material as (^{n}Bu)$_2$Ga[NH(2,6-

$C_6H_3Me_2$)]py (**10**) by spectroscopic characterisation and microanalysis. The amido proton in **10** was identified by both IR (3297 cm^{-1}) and ^1H NMR (3.09 ppm).

Again, the stability of this material compared to the other isolated oils is attributed to the steric protection of the gallium centre, which impedes reaction with atmospheric oxygen and water.

Thermolysis of **10** at 170°C in a sealed NMR tube showed degradation of the methyl signal at 2.36 ppm from a singlet to a broad resonance at 2.90 ppm,and a new singlet at 2.65 ppm. The NH resonance at 3.09 ppm decreases significantly and small broad peaks appear at 3.46, 3.77 and 4.04 ppm. Both the butyl signals and the resonance for the aromatic ring remain constant. This reactivity suggested two or more products are the result of the thermolysis, but subsequent experiments on a larger scale failed to yield any charaterisable material. Given the oily nature of **10** and the fact that it is present in the NMR spectrum even after heating at 170°C for several days, it is not surprising that separation and isolation of it or any product of the thermolysis was not forthcoming.

The use of excess anionic ligands also allowed the isolation and crystallisation of alkyl amido complexes from the oily materials produced from the 1:1 reaction of $^nBu_2GaCl$ and lithium amide. For example, the interaction of $\{^nBu_2Ga[NH(2,6\text{-}Me_2C_6H_3)]\}_n$ with an additional equivalent of $LiN(H)(2,6\text{-}C_6H_3Me_2)$ in hexane produced an oil. When this oil was thoroughly dried under vacuum and dissolved in diethylether, crystals of $^nBu_2Ga[NH(2,6\text{-}Me_2C_6H_3)]_2[Li(Et_2O)]$ (**11**) were isolated in mediocre yield. This crystalline material showed reasonable stability in air, surviving for several minutes before clouding to opacity. Therefore,

structural characterisation by single crystal X-ray diffraction was possible and confirmed the molecular connectivity of this complex. (Figure 16, , full crystal data in Appendix 3). Complex **11** crystallised in the monoclinic space group $P2_1/n$ with $Z = 4$. The structure consists of a gallium centre in a pseudotetrahedral coordination sphere composed of two amido ligands (Ga-N1 = 2.011(8)Å, Ga-N2 = 2.006(7)Å), and two ^{n}Bu ligands (Ga-C17 = 2.002(9)Å, Ga-C21 = 1.985(12)Å). A bridging interaction of the lithium cation with the lone pair of electrons on each of amido nitrogen atoms generates a molecular core which is made up of a planar Ga-N1-Li-N2 distorted square (N1-Ga1-N2 94.4°, Ga1-N2-Li1 86.2°, N1-Li1-N2 92.2°, Ga1-N1-Li1 87.1). Additional selected bond distances and angles for **11** are given in Table 8. Consistent with the spectroscopic data is the presence of one diethyl ether ligand completing the unusual, distorted trigonal planar coordination of the Li cation.

Thermolysis of this compound up to 150°C gave no reaction. At 155°C in a sealed NMR tube, **11** showed a similar degradation to the methyl signal as was seen for **10**. In this case, a surfeit of signals resulted in the region between 1.70 and 2.40 ppm. In addition, both the aromatic ring signals at 7.00 and 6.70 ppm produced a great number of signals between 7.4 and 6.5 ppm, and the butyl signals showed the same proclivity. The interesting feature of the ^{1}H NMR of the thermolysis mixture is the presence of butene signals at 4.95, 5.04 and 5.80 ppm, suggesting that β-hydrogen elimination had taken place. Unfortunately, nothing could be isolated from thermolysis reactions of this product, and further thermolysis did not cause a comproportionation of the several products evident in the NMR.

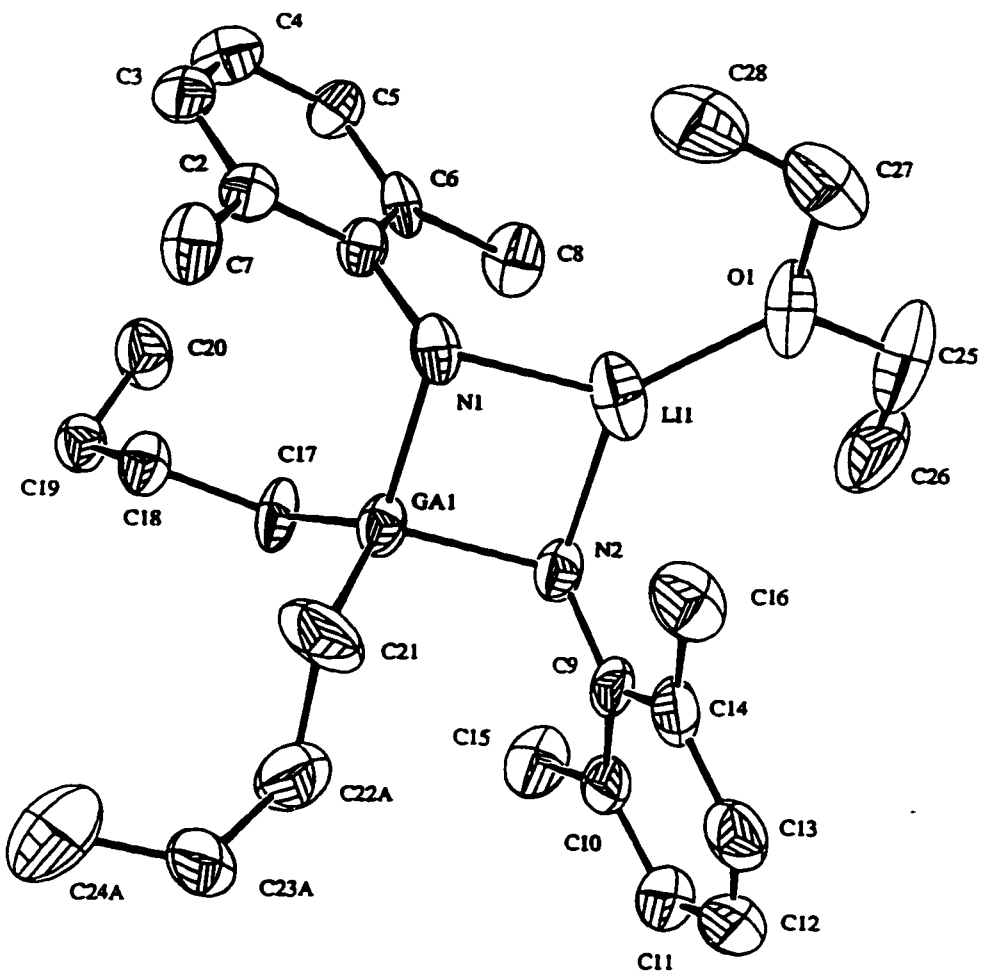

Figure 16: The single crystal XRD ORTEP diagram of $^{n}Bu_2Ga[NH(2,6\text{-}Me_2C_6H_3)]_2[Li(Et_2O)]$ **(11)** showing coordination of the lithium cation by the two amide ligands and supported by one diethylether molecule.

Table 8: Selected bond lengths and angles from the single crystal XRD of **11**.

Bond	Length in Å	Vertices	Angle in°
Ga1-N1	2.011(8)	N1-Ga1-N2	94.4(3)
Ga2-N2	2.006(7)	N1-Ga1-C17	111.2(4)
Ga1-C17	2.002(9)	N1-Ga1-C21	109.9(4)
Ga1-C21	1.985(1)	N2-Ga1-C17	106.3(3)
Ga1-Li1	2.782(2)	N2-Ga1-C21	112.0(5)
O1-Li1	1.977(2)	C17-Ga-C21	120.0(5)
N1-C1	1.425(1)	Ga1-N1-C1	115.9(5)
N1-Li1	2.027(2)	Ga1-N1-Li1	87.1(7)
N2-C9	1.388(1)	Ga1-N2-C9	120.1(6)
N2-Li1	2.06(2)	Ga1-N2-Li1	86.2(6)
		Ga1-Li1-N1	46.2(4)
		Ga1-Li1-N2	46.0(4)
		Ga1-Li1-O1	178.0(1)
		Ga1-C17-C18	114.2(6)
		O1-Li1-N1	135.4(1)
		O1-Li1-N2	132.4(1)

Gallium complexes containing primary amides have shown utility in exploring imido chemistry for gallium and preliminary thermal reactivity suggests that deeper investigation into their reactivities would yield fruitful results. The compounds **8-11** also demonstrate that the flexibility in the coordination environment around a metal centre and the use of amido ligands with different electronic and steric properties can tune their reactivity, giving these compounds a flexibility which will allow synthesis of novel systems.

Chapter 8: The siloxides and siloxo-amides

Reactivity of alkoxides and siloxides of the group III metals has been extremely well-explored, as Chapter 4 described. Given the ease of synthesis and thermal reactivity of these compounds, incorporation of the trimethylsiloxide group ($OSiMe_3$) in precursor materials for MPn extended solid synthesis is a natural extension of this work. Preparation of the lithium salt $LiOSiMe_3$, is simple and the resulting $LiOSiMe_3$ is easy to purify.[77] As well, this material can incorporate a coordinating base molecule, and thus has versatility similar to $LiN(SiMe_3$.

In order to assess the particular thermal behaviour of the siloxide group on gallium and indium, a series of these compounds were synthesised and a preliminary examination of their thermal behaviour was performed.

1. The siloxide compounds

$Ga(OSiMe)_3$ can be prepared and isolated by literature procedures.[78] It has been shown to be a monomer in the solid state by single crystal XRD and has a singlet in the ^1H NMR at 0.30 ppm.[78] Thermolysis of this compound in an NMR tube determined it to be remarkable stable, reacting only at 185°C over five days. This compound cleanly eliminates $(Me_3Si)_2O$, which has a characteristic signal at 0.11 ppm in the NMR. The

presence of this ether was also determined by MS and identified from a literature spectrum.[79] Interestingly enough, the ^{1}H NMR of the thermolysis products of $Ga(OSiMe)_3$ showed only the $(Me_3Si)_2O$ signal and no other. As well, the reaction mixture remained perfectly clear; there was not even a hint of precipitation of Ga_2O_3, the expected thermolysis product (Figure 17). One hypothesis is that the Ga_2O_3 was formed in microparticles which did not precipitate; this effect has been seen for GaAs in the literature.[12]

When $Ga(OSiMe_3)_3$ was stirred in hexane with an excess of pyridine, $Ga(OSiMe_3)_3$.py (**12**) resulted in good yield. This clear crystalline compound had an NMR similar to $Ga(OSiMe)_3$, with a singlet at 0.33 ppm and signals for pyridine shifted from those of free pyridine (8.73, 6.95, and 6.66 ppm). The shifting of these peaks and the fact that integration yields one pyridine for three siloxo groups determines the formulation of **12**, which was confirmed by elemental analysis.

The thermolysis of **12** at 190°C over 24 hr resulted in a several products, as shown by the plethora of singlets between 0.40 and 0.00 ppm and by the large number of pyridine environments seen in the spectrum. A peak at 0.11 ppm is obvious and indicates the presence of $(Me_3Si)_2O$. As with $Ga(OSiMe_3)_3$, there was no sign of precipitation of Ga_2O_3. Again, it may be soluble as microparticles (as above).

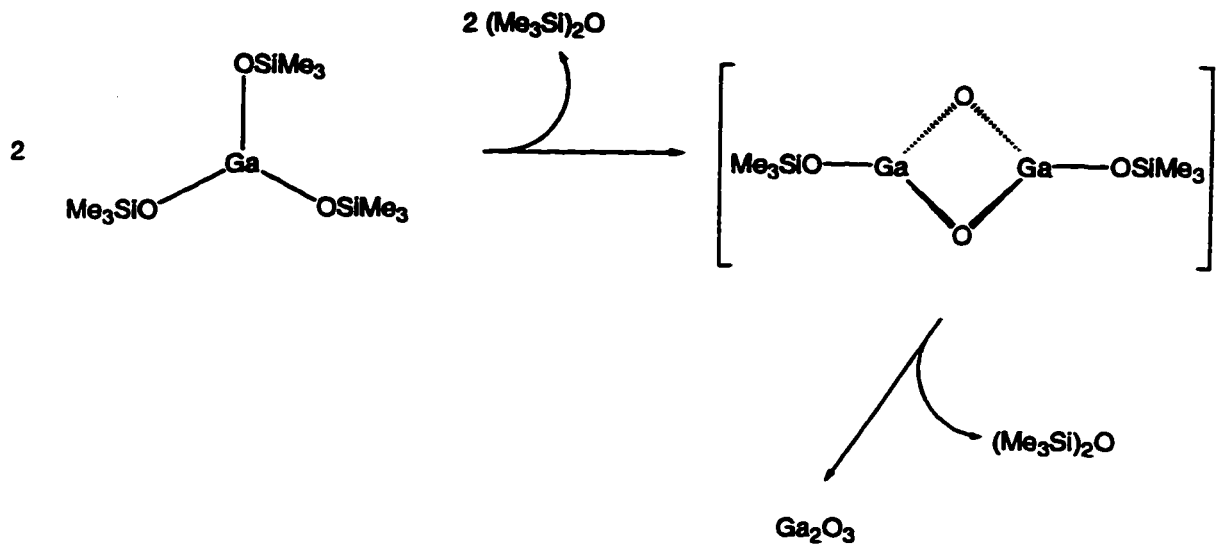

Figure 17: A proposed mechanism for elimination of bistrimethylsilyl ether from $Ga(OSiMe)_3$.

Similarly, when $InCl_3$ was stirred in diethylether with $LiOSiMe_3$ at 110°C in a sealed tube, followed by addition of pyridine and recrystallisation, $In(OSiMe_3)_3.py$ (**13**) could be isolated in decent yield. Pyridine was necessary as the material was too soluble to isolate without a coordinating base and not thermally stable enough for sublimation. The composition of **13** was determined to be similar to **12**.

Thermolysis of **13** also showed $(Me_3Si)_2O$ by ^1H NMR after heating this material at 120°C for 2 days, and the presence of bistrimethylsilyl ether was corroborated by MS. Similar to **12**, there were no additional ^1H NMR signals and no precipitation observed during this reaction. Nothing could be crystallised from a scale-up of this reaction, and characterisation of the crude reaction product indicated the presence of indium by XRF, and showed no IR nor ^1H NMR signals. Also, PXRD determined this material to be amorphous.

When $GaCl_3$ is stirred in hexane with two equivalents of $LiOSiMe_3$ followed by addition of excess pyridine and recrystallisation in toluene, $Ga(OSiMe_3)_2Cl.py$ (**14**) can be isolated after filtration. The composition of this material was determined by ^1H NMR and elemental analysis. The ^1H NMR showed a singlet for Me_3Si at 0.35 ppm and resonances for pyridinewhich were shifted from their free positions and integrated for one pyridine per two silyl groups.

This clear, crystalline material exhibited less thermal stability than **12**; evolution of $(Me_3Si)_2O$ at 140°C was detected by ^1H NMR from a sample heated in an NMR tube. The complex cleanly decomposed to an insoluble powdery material and bistrimethylsilyl

ether by 190°C. The integration of the NMR resonances showed clearly that all of the protons from the sample were present as the ether (by integration against the internal solvent standard) and the powdery material contained both gallium and chloride according to XRF spectroscopy. Also, a PXRD pattern showed the material to be amorphous, even after annealing at 400°C. Although the nature of the amorphous powder could not be determined, the reactivity of this compound again encourages the use of the siloxo group for elimination reactions.

The analogous indium compound $In(OSiMe_3)_2Cl.py$ (**15**) was synthesised by reaction of $InCl_3$ and $LiOSiMe_3$ in diethylether at 110°C and subsequent recrystallisation in pyridine. The formulation was determined through ^1H NMR and elemental analysis.

This material also undergoes thermal rearrangement and elimination of $(Me_3Si)_2O$ at a lower reaction temperature than $In(OSiMe_3)_3$ (**13**), showing the characteristic ^1H NMR peak for the ether after heating at 110°C for three days in a sealed NMR tube. Like **14**, this complex also produces a powder. XRF demonstrated the presence of indium and chloride in this material, without detecting any other elements. This material was amorphous according to PXRD, but as in the case of **14**, it shows promising reactivity for thermal eliminations.

The thermolyses of the siloxide compounds **12-15** demonstrates that these materials have appropriate thermal reactivity, in all cases cleanly eliminating bistrimethylsilyl ether at temperature which are accessible for thermolysis experiments. Since the elimination of $(Me_3Si)_2O$ is facile, clean and accessible at reasonably low temperatures, and since the

ligand provides steric bulk and a good handle for characterisation, it should be utilised in design of MPn extended solid precursors. The next section will detail some complexes which incorporate this ligand and describe there thermal behaviour.

2. The siloxo-amide compounds

The interaction of $GaN(SiMe_3)_2Cl_2$.thf (**1**) with $Li(OSiMe_3)$.thf takes one of two routes depending on the presence of coordinating solvents (Figure 18).

When the reaction was carried out in thf at room temperature, the compound $[Li(thf)_2][Ga(N(SiMe_3)_2)(OSiMe_3)_2Cl]$ (**16**) was produced. Assignment of this formula was based on spectroscopic data and satisfactory elemental analysis. The ^1H NMR shows two singlets of equal intensity (0.55 and 0.33 ppm) for the amido and siloxo groups respectively. The presence of two thf molecules per amido group is also apparent from this spectrum. As lithium commonly requires two additional coordinating base molecules in these LiCl-containing compounds, this was a good indication that the material was retaining LiCl. Subsequent attempts to remove the chloride anion by heating **16** in toluene (a high-boiling, non-coordinating solvent) or by reaction with silver salts often caused the decomposition of the complex, but never resulted in the clean loss of LiCl.

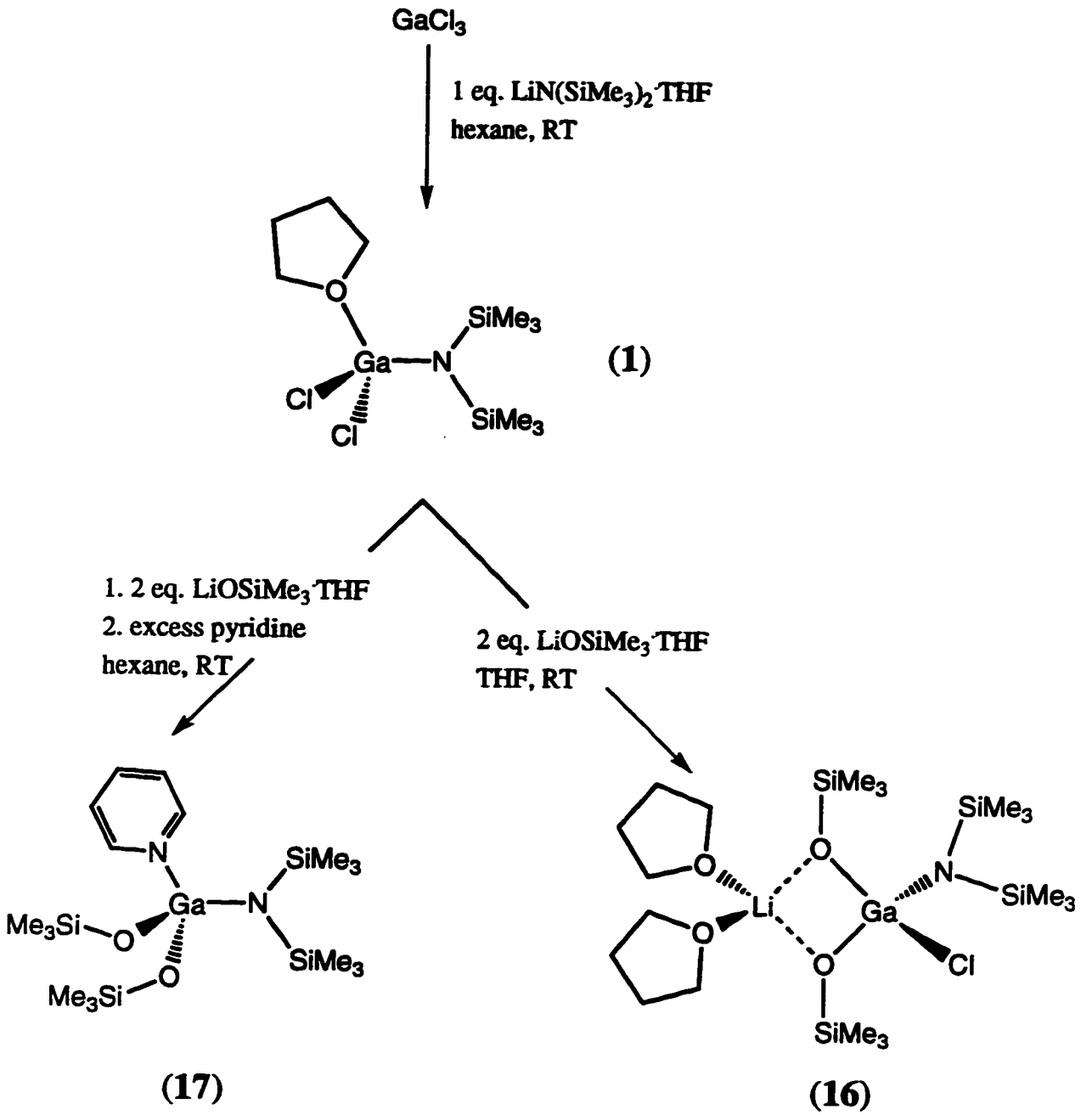

Figure 18: The solvent-dependent reaction pathways for $GaN(SiMe_3)_2Cl\cdot thf$ (1) and $LiOSiMe_3$.

Structural characterisation by single crystal XRD confirmed the molecular connectivity of **16** (Figure 19, , full crystal data in Appendix 4). The structure consists of a gallium centre in a pseudotetrahedral coordination sphere composed of a hexamethyldisilazido ligand (N1), two siloxo oxygens (O1, O2), and a chloride ligand (Cl1). A bridging interaction of the lithium cation with the lone pair of electrons on each of the siloxide oxygen atoms generates a molecular core which is made up of a planar Ga-O1-Li-O2 distorted square (O1-Ga1-O2 92.7°, Ga1-O2-Li1 88.1°, O1-Li1-O2 87.7°, Ga1-O1-Li1 91.4°). Additional selected bond distances and angles for **16** are given in Table 9.

Consistent with the spectroscopic data is the presence of two thf ligands completing the coordination of the Li cation. It is presumably the stabilising effect of excess thf that results in the formation of this bimetallic species.

Compound **16** was thermally stable up to 120°C when heated in a sealed NMR tube, after which point its thermal rearrangements result in a plethora of signals between 0.40 and 0.00 ppm. Thus, it appears that $[Li(thf)_2][Ga(N(SiMe_3)_2)(OSiMe_3)_2Cl]$ is a poor GaN precursor. However, among the products of this transformation are $(Me_3Si)_2O$ and $(Me_3Si)_2NH$ which could be identified by ^1H NMR, but attempts at scaling up this reaction and isolating a product were not effective.

A similar synthetic procedure using hexane as the solvent yielded an oily material from which a crystalline solid could be isolated upon addition of pyridine and recrystallisation in toluene. The assignment of the formula $Ga(N(SiMe_3)_2)(OSiMe_3)_2py$

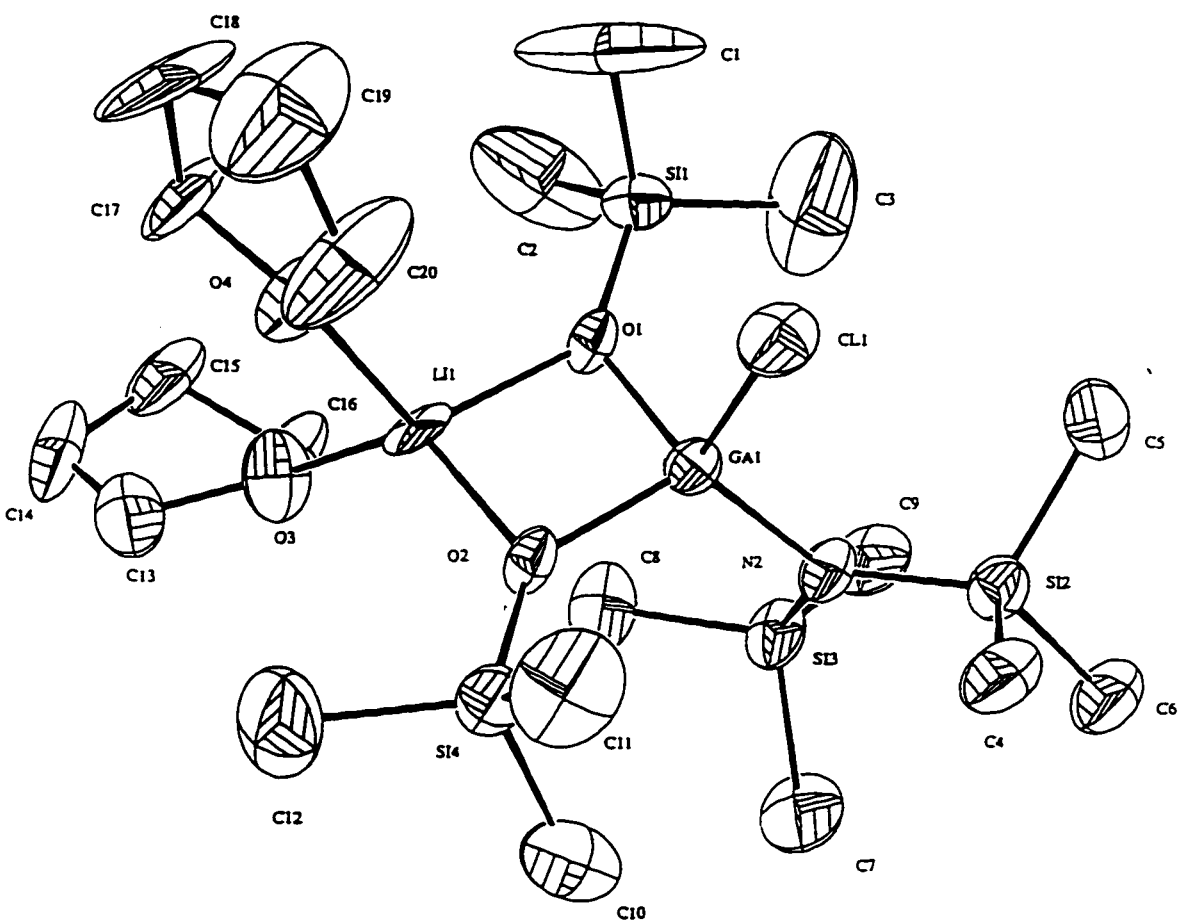

Figure 19: The single crystal XRD ORTEP diagram of $[Li(thf)_2][Ga(N(SiMe_3)_2)(OSiMe_3)_2Cl]$ (**16**) showing coordination of the lithium cation by the two siloxide ligands and supported by two thf molecules.

Table 9: Selected bond lengths and angles from the single crystal XRD of **16**.

Bond	Length in Å	Vertices	Angle in°
Ga1-Cl1	2.210(4)	Cl1-Ga1-O1	105.9(3)
Ga1-O1	1.849(10)	Cl1-Ga1-O2	103.9(3)
Ga1-O2	1.867(9)	Cl1-Ga1-N1	114.7(4)
Ga1-N1	1.888(11)	O1-Ga1-O2	92.7(4)
Ga1-Li1	2.68(3)	O1-Ga1-N1	116.7(5)
Si1-N1	1.724(12)	O2-Ga1-N1	120.0(5)
Si1-C1	1.880(16)	N1-Si1-C1	113.1(7)
Si1-C2	1.871(19)	N1-Si1-C2	112.6(7)
Si1-C3	1.869(19)	N1-Si1-C3	111.2(7)
Si2-N1	1.729(13)	N1-Si2-C4	112.0(7)
Si2-C4	1.841(19)	N1-Si2-C5	112.4(9)
Si2-C5	1.880(20)	N1-Si2-C6	111.0(8)
Si2-C6	1.891(21)	O1-Si3-C7	111.7(9)
Si3-O1	1.622(11)	O1-Si3-C8	110.4(8)
Si3-C7	1.845(24)	O1-Si3-C9	107.2(8)
Si3-C8	1.848(24)	O2-Si4-C10	110.9(11)
Si3-C9	1.854(25)	O2-Si4-C11	110.3(10)
Si4-O2	1.622(11)	O2-Si4-C12	111.8(10)
Si4-C10	1.82(3)	Ga1-O1-Si3	136.0(6)
Si4-C11	1.81(3)	Ga1-O1-Li1	91.4(9)
Si4-C12	1.81(3)	Si3-O1-Li1	132.4(10)
O1-Li1	1.90(3)	Ga1-O2-Si4	130.8(6)
O2-Li1	1.99(3)	Ga1-O2-Li1	88.1(8)
O3-C13	1.444(22)	Si4-O2-Li1	138.1(9)
O3-C16	1.425(22)	Ga1-N1-Si1	118.5(7)
O3-Li1	1.92(3)	Ga1-N1-Si2	117.0(6)
O4-C17	1.406(20)	Si1-N1-Si2	124.5(7)
O4-C20	1.42(3)	O1-Li1-O2	87.7(11)
O4-Li1	2.031(23)		

(**17**) for this complex was confirmed by elemental analysis and spectroscopic characterisation. The ^{1}H NMR again showed two singlets, now at 0.37 and 0.29 ppm, with the pyridine resonances shifted from their free positions and integrating to give one pyridine per amido group. Qualitative tests for lithium cations and chloride confirmed the absence of these ions. A monomeric, four coordinate structure, similar to that of the gallium centre in **16**, is suspected.

When **17** was heated to 155°C in a sealed NMR tube and the thermal rearrangement was monitored by ^{1}H NMR, loss of the two methyl singlets for the starting material, formation of free pyridine and growth of a new peak at 0.11 ppm, consistent with formation hexamethyldisiloxane, was observed. MS of the mother liquor from this NMR tube reaction confirmed the presence of $O(SiMe_3)_2$.[79]

When this reaction was reproduced under nitrogen in a Schlenk tube at 210°C, the grey solid which precipitated showed no noticeable change when subjected to strong mineral acids. The powder XRD pattern of the native material did not show any features. However, after annealing at only 350°C the onset of crystallinity is evident. Figure 20 shows the evolution of crystallinity of a sample of the solid upon annealing to the indicated temperatures.

Comparison of the diffraction patterns with the graphical representation for the hexagonal (wurtzite) phase for gallium nitride, also in Figure 20, shows there to be an excellent match with the experimental data.[70] The features of this spectrum are broad likely due to the low crystalline order of the material as might be anticipated

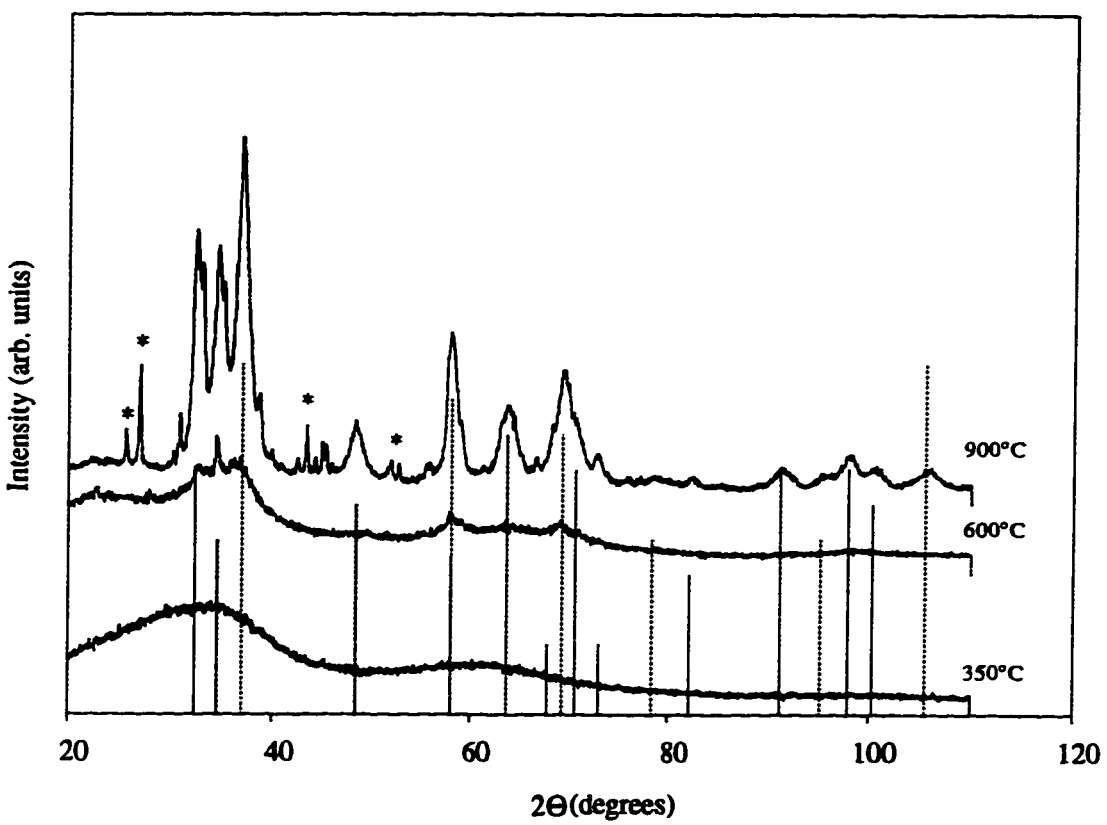

Figure 20: The PXRD of GaN from $Ga(N(SiMe_3)_2)(OSiMe_3)_2$ (**17**) showing improving crystallinity with annealing temperature. (the lines indicate the 2Θ literature values for hexagonal GaN) (* indicates a crystalline impurity)

for a refractory material which is produced in solution and subsequently undergoes little if any of the self-ordering that would occur at high temperatures. Table 10 shows the correspondence between the literature and experimental values for GaN.

Again, the intensity agreement between theory and experimental can be seen to be off, but the same trend is followed. The possible reasons for this were discussed in chapter 6.

In the case of indium, the number of equivalents of free base present in solution becomes crucial (Figure 21).

When the number of base molecules available from solution is at least two two, the result is $[Li(base)_2][In(N(SiMe_3)_2)(OSiMe_3)_2Cl]$. For instance, when $InCl_3thf_3$, $LiN(SiMe_3)_2$.thf and $LiOSiMe_3$.thf were mixed in sequence in hexane, and after filtration the result was a very soluble solid whose crude ^1H NMR showed thf resonances at 1.33 and 3.49 ppm. This compound is likely $[Li(thf)_2][In(N(SiMe_3)_2)(OSiMe_3)_2Cl]$, but isolation proved difficult, so excess pyridine was added and subsequent recrystallisation in toluene allowed the isolation of pure $[Li(py)_2][In(N(SiMe_3)_2)(OSiMe_3)_2Cl]$ (**18**), as characterised by elemental analysis and spectroscopic methods. The ^1H NMR of this compound indicated the presence of two equivalents of pyridine with resonances at 8.54, 6.94 and 6.67 ppm. As well, there were singlets at 0.53 and 0.23 ppm, for the amido and siloxo methyl groups respectively. Qualitative tests confirm the presence of lithium and chloride in the complex. The lithium chloride must have been present in the initial sample from hexane which could not be purified. The structure of this **18** is likely similar to **16**.

Table 10: The literature d-spacings and intensities for GaN as compared to those from a GaN sample resulting from thermolysis of **17**

GaN (literature)			GaN (experimental)	
d-spacing in Å	Intensity (%)	h k l	d-spacing in Å	Intensity (%)
2.76	70	1 0 0	2.76	56
2.59	50	0 0 2	2.58	47
2.43	100	1 0 1	2.41	63
1.88	60	1 0 2	1.89	21
1.59	90	1 1 0	1.60	36
1.46	80	1 0 3	1.48	18
1.38	20	2 0 0	1.38	10
1.36	80	1 1 2	1.36	2
1.33	70	2 0 1	1.33	3
1.30	20	0 0 4	1.30	3

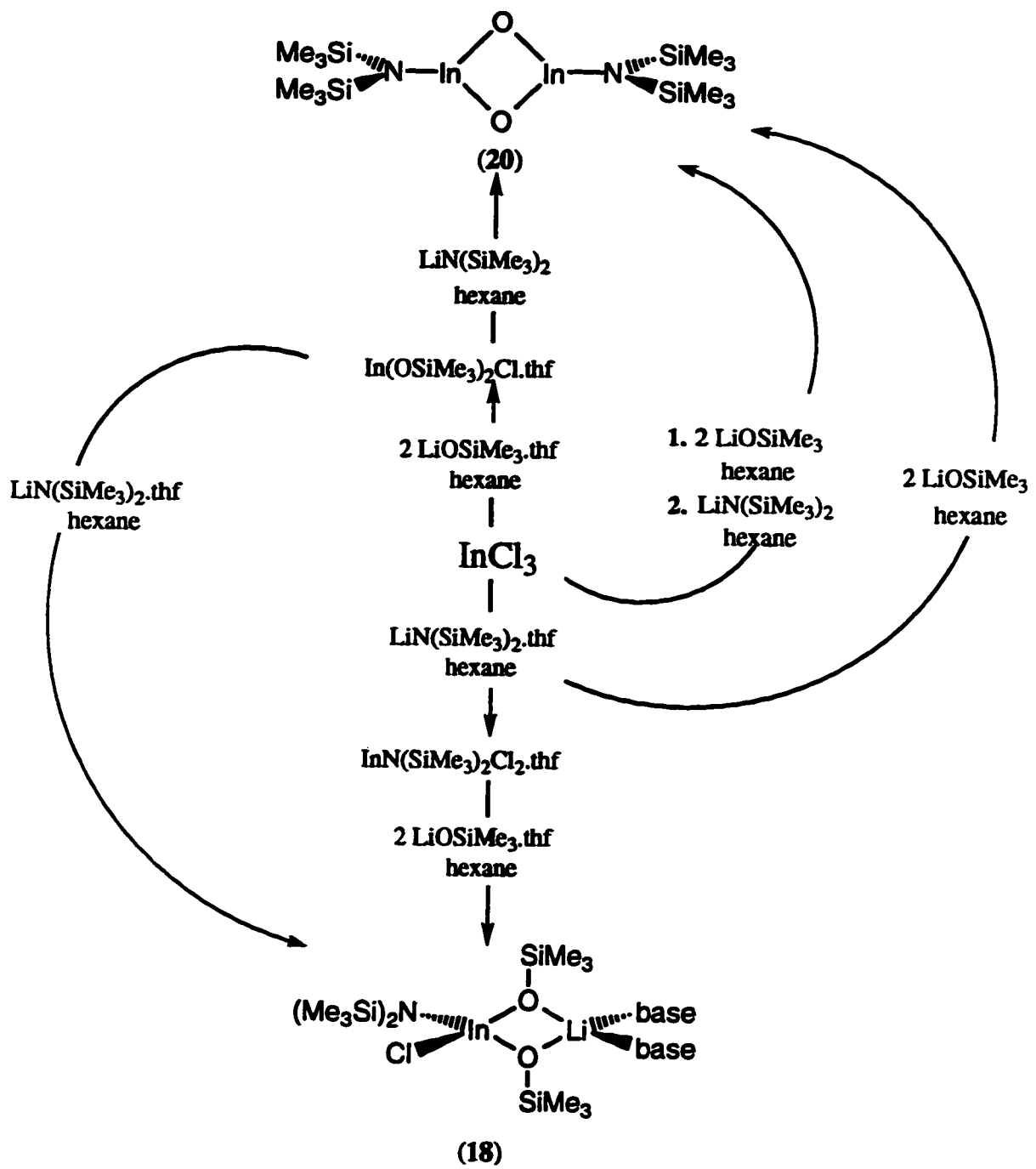

Figure 21: The solvent dependent reaction pathways for $InN(SiMe_3)_2Cl{\cdot}py$ (2) and $LiOSiMe_3$.

This material was resistant to thermolysis, showing no reactivity in a sealed NMR tube up to 230°C. As well, refluxing this material in toluene did not decompose it, nor aid in the elimination of LiCl from the first coordination sphere of the indium. Reaction with a variety of silver salts also did not aid in the removal of LiCl, but did cause decomposition of the compound.

When three equivalents of siloxo ligand was used in the synthesis described above, the complex $[Li(py)_2][In(N(SiMe_3)_2(OSiMe_3)_3]$ (**19**) was isolated in excellent yield by recrystallisation in toluene. The composition of this material is supported by elemental analysis and spectroscopic techniques. The ^1H NMR showed an integration of 2:3 for singlets due to the amido:siloxo groups at 0.50 and 0.32 ppm respectively. Pyridine resonances were also found, shifted from free pyridine and integrating to two equivalents per amido group. This suggests that the Li cation is coordinated to the ligand system of the indium complex, likely through the lone pairs on two of the siloxo groups, as the amido lone pair is inaccessible. The two pyridine molecules would then complete the coordination of the lithium. These structural features were confirmed using single crystal XRD (Figure 22).

Complex **19** crystallised in the monoclinic space group $P2_1/n$ with $Z = 4$. As shown in Figure 22 (, full crystal data in Appendix 5), the structure consists of a indium centre in a pseudotetrahedral coordination sphere composed of one amido ligand (In-N1 = 2.083(5)Å), and three siloxo In1-O1 = 2.059Å, In1-O2 = 2.060Å, In1-O3= 1.997Å). A bridging interaction of the lithium cation

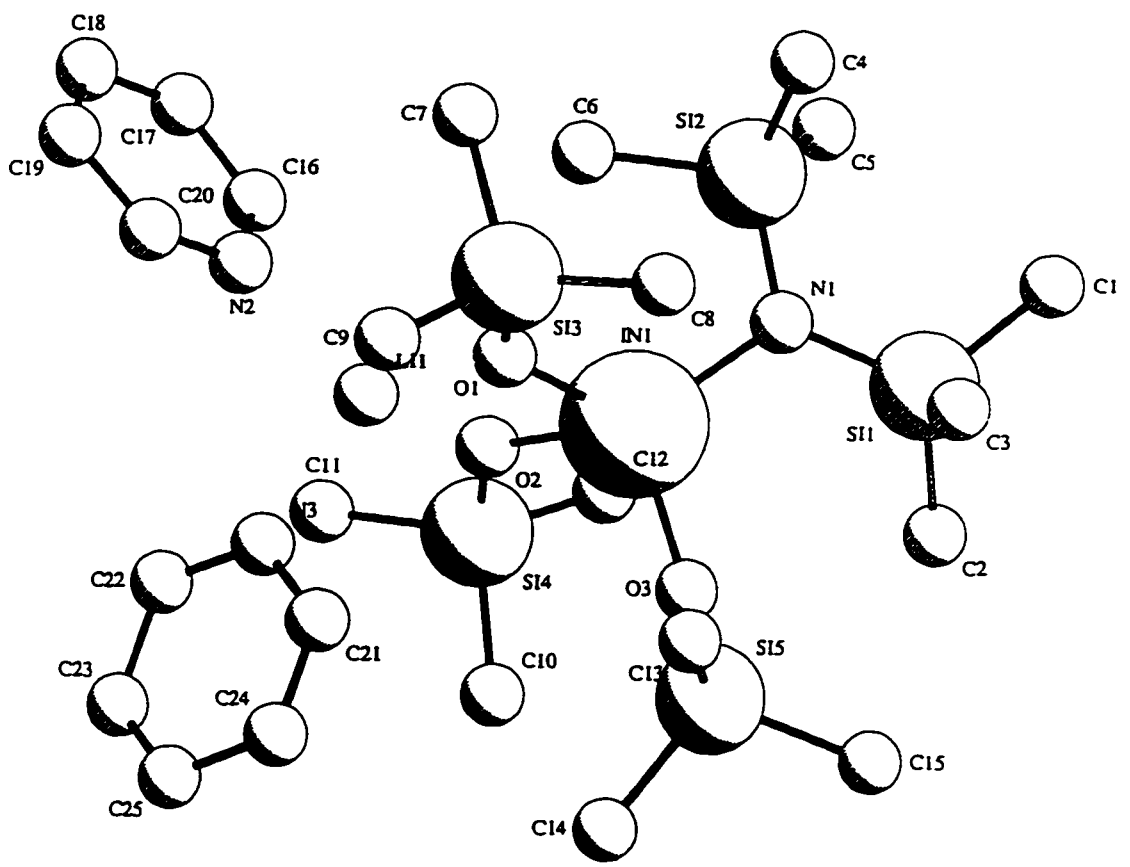

Figure 22: the single crystal XRD PLUTO diagram of $[Li(py)_2][In(N(SiMe_3)_2(OSiMe_3)_3]$ **(19)** showing coordination of the lithium cation by the two siloxide ligands and supported by two pyridine molecules.

with the lone pair of electrons on two of the siloxo oxygen atoms generates a molecular core which is made up of a In-O1-Li-O2 distorted square (O1-In1-O2 = 84.95°, In1-O2-Li1 = 92.0°, O1-Li1-O2 = 90.7°, In1-O1-Li1 = 91.9°). The sum of the core angles is 258.9°, showing a bend out of planarity. Additional selected bond distances and angles for **19** are given in Table 11. Consistent with the spectroscopic data is the presence of two pyridine ligands completing the distorted tetrahedral coordination of the Li cation.

When the presence of coordinating base was rigorously excluded, the reaction was surprising. $InCl_3$ reacted with $LiN(SiMe_3)_2$ and subsequently $LiOSiMe_3$ in hexane to give $[In(N(SiMe_3)_2)(\mu^2\text{-}O)]_x$ (**20**) after recrystallisation. This material is the result of $(Me_3Si)_2O$ elimination from a siloxo group rather than from the desired elimination from the amido group. Although a single crystal XRD for this compound was not accessible due to the crystal morphology of the compound, elemental analysis and spectroscopic characterisation of this compound both support its composition. Recrystallisation in hexane results in a fibrous white material with a single peak in the NMR at 0.34 ppm. This material will also retain one equivalent of toluene when recrystallised in this solvent, with no apparent effect on crystal morphology. Elemental analysis was satisfactory for the formulation of $[In(N(SiMe_3)_2)(\mu^2\text{-}O)]_x$ for the hexane-precipitated compound. The compound bearing one toluene could not be characterised by elemental analysis as the results showed a fluctuation in both the % weights for carbon and hydrogen. This fluctuation occurred in a range which suggested that the toluene was volatilising away during the weighing of the sample. A mass spectrum of **20** showed a peak at 290 m/z, which demonstrates the existence of the monomer. There were no peaks at appropriate

Table 11: Selected bond lengths and angles from the single crystal XRD of **19**.

Bond	Length in Å	Vertices	Angle in°
In1-O1	2.059(4)	O1-In1-O2	84.95(15)
In1-O2	2.060(3)	O1-In1-O3	110.19(18)
In1-O3	1.997(4)	O1-In1-N1	123.31(18)
In1-N1	2.083(5)	O1-In1-Li1	42.64(24)
Si1-N1	1.724(5)	O2-In1-O3	106.40(17)
Si1-C1	1.887(8)	O2-In1-N1	116.87(18)
Si1-C2	1.878(8)	O2-In1-Li1	42.50(24)
Si1-C3	1.873(8)	O3-In1-N1	111.63(19)
Si2-N1	1.723(5)	O3-In1-Li1	112.0(3)
Si2-C4	1.873(7)	N1-In1-Li1	135.8(3)
Si2-C5	1.878(8)	N1-Si1-C1	112.2(3)
Si2-C6	1.868(6)	N1-Si1-C2	110.7(3)
Si3-O1	1.626(4)	N1-Si1-C3	110.9(3)
Si3-C7	1.865(8)	N1-Si2-C4	111.2(3)
Si3-C8	1.855(7)	N1-Si2-C5	113.2(3)
Si3-C9	1.875(9)	N1-Si2-C6	110.2(3)
Si4-O2	1.621(4)	O1-Si3-C7	109.9(3)
Si4-C10	1.840(8)	O1-Si3-C8	110.1(3)
Si4-C11	1.856(7)	O1-Si3-C9	109.5(3)
Si4-C12	1.867(9)	O2-Si4-C10	109.9(3)
Si5-O3	1.598(5)	O2-Si4-C11	110.4(3)
Si5-C13	1.873(9)	O2-Si4-C12	109.8(3)
Si5-C14	1.850(8)	O3-Si5-C13	110.4(3)
Si5-C15	1.889(7)	O3-Si5-C14	111.7(3)
O1-Li1	1.957(11)	O3-Si5-C15	110.4(3)
O2-Li1	1.952(11)	In1-O1-Si3	135.89(24)
N2-C16	1.348(10)	In1-O1-Li1	91.9(3)
N2-C20	1.313(9)	Si3-O1-Li1	131.2(4)
N2-Li1	2.063(11)	In1-O2-Si4	128.67(22)
N3-C21	1.341(10)	In1-O2-Li1	92.0(3)
N3-C22	1.310(10)	Si4-O2-Li1	134.2(4)
N3-Li1	2.069(12)	In1-O3-Si5	154.9(3)
		In1-N1-Si1	115.8(3)
		In1-N1-Si2	116.7(3)
		Si1-N1-Si2	126.4(3)
		O1-Li1-O2	90.7(4)
		O1-Li1-N2	120.5(5)
		O1-Li1-N3	112.7(6)
		O2-Li1-N2	116.0(6)
		O2-Li1-N3	108.8(5)
		N2-Li1-N3	107.1(5)

weights to give a hint as to the extent of aggregation of this compound. In conjunction to this data, a ^{1}H NMR of this mother liquor of the reaction found a peak at 0.11 ppm, showing the generation of $(Me_3Si)_2O$ as a side-product of the reaction.

With the proven reactivity of the siloxide group and the promising thermolysis of compounds **16-20**, it is obvious that the siloxide ligand has a promising future for elimination reactions within this field. Such reactivity has utility for bond formation in group III-V chemistry, whether for MPn extended solid synthesis or to explore main-group multiple bonding.

Chapter 9: Conclusions

The thermal reactivity of compounds $GaN(SiMe_3)_2Cl_2$.thf (**1**) and $InN(SiMe_3)_2Cl_2$.py (**2**) resulted in no isolated MPn extended solid. Complex **1** could react by many routes under the conditions studied and thus did not produce GaN; while compound **2** was robust within the thermal window explored. Both compounds are suitable starting materials for other possible precursors, containing an existing metal-pnictide bond. As well, the silyl groups give good steric protection of the core.

The alkyl-pnictido compounds faired better as precursors. $Ga(^nBu)_2(N(SiMe_3)_2$.py (**3**) rearranged at 400°C to give amorphous GaN. $[Ga(^tBu)_2N(SiMe_3)_2]_2$ (**4**) did not rearrange so neatly, due to the reactivity of the ^tBu group. $Ga(^nBu)_2P(SiMe_3)_2$ (**5**) decomposed smoothly at 250°C to produce crystalline GaP with low impurities, and also showed an impressive resistance to reaction with air and water. Attempts to synthesise an phosphinido complex by dehalosilation of $Ga(^nBu)(Cl)P(SiMe_3)_2)]_2$ (**6**) led to many different products. Although there was evidence of trimethylsilylchloride elimination in an NMR thermolysis experiment, an phosphinido complex was not isolated.

The analogous indium compound $[(^nBu)_2InP(SiMe_3)_2]_2$ (**7**) did thermolyse to yield InP at 400°C, but In^0 was also evident. This material was crystalline at the reaction temperature, which suggests an unusual crystallisation mechanism may be operating. Among the characterised side-products of this reaction was isobutene, effectively demonstrating that β-hydrogen elimination was again responsible for this reduction. This same state of affairs was obvious for the meagerly

characterised compound $(^nBu)_3InP(SiMe_3)_3$, which demonstrated that at 110°C, **7** was formed and In^0 precipitated from the reaction mixture. Since In^0 is the first material produced, **7** and $(^nBu)_3InP(SiMe_3)_3$ are not a suitable precursors for InP.

The alkyl-amidos with primary amides showed mixed thermal reactivity as well. NMR data showed that $[Ga(^tBu)_2(NH^tBu)]_2$ (**8**) could form an imido complex $[^tBuGaN^tBu]_x$ at 120°C, but this material and its thf adduct $[^tBuGaN^tBu(thf)]_2$ were far too air-sensitive to fully charaterise. The ^{n}Bu analogue $[Ga(^nBu)_2(NH^tBu)]_2$ (**9**) showed no thermal reactivity in the window investigated, and NMR data showed the metal centre to be very congested, which may allow this materials its robust nature.

Changing the amido group did change the reactivity, as $Ga(^nBu)_2(NH(C_6H_3(Me)_2))(py)$ (**10**) demonstrated thermal reactivity at 170°C. Unfortunately, this material did not cleanly eliminate $H_2N(C_6H_3(Me)_2)$ to form the imide, it produced several different compounds according to NMR, none of which were isolated. This material could also be isolated as a lithium amide adduct $[Li(Et_2O)_2][Ga(^nBu)_2NH(C_6H_3(Me)_2)]$ (**11**).

The siloxide complex $Ga(OSiMe_3)_3.py$ (**12**) was also isolated and showed thermal reactivity to eliminate trimethylsilyl ether at 140°C, but this elimination was not clean. The analogous indium compound $In(OSiMe_3)_3.py$ (**13**) demonstrated better reactivity, cleanly eliminating $(Me_3Si)_2O$ in full. Unfortunately, while the products of this reaction were not isolated and characterisation by XRF determined the presence of indium, PXRD could not confirm that this amorphous material was indeed In_2O_3.

Siloxo-chloride compounds were also synthesised, and showed comparable thermal reactivity. $Ga(OSiMe_3)_2Cl.py$ (**14**) cleanly eliminated trimethylsilyl ether and the product was shown to contain gallium and chloride. Again, this amorphous material could not be characterised by XRD. The indium compound $In(OSiMe_3)_2Cl.py$ (**15**) showed analogous chemistry, also eliminating $(Me_3Si)_2O$ cleanly and producing an amorphous powder which contained both indium and chloride.

This siloxide thermal chemistry prompted the synthesis of several siloxo-amido complexes. When synthesis takes place in thf, the resulting complex maintains one equivalent of LiCl, which is stabilised by the basic solvent. The complex $[Li(thf)_2][Ga(N(SiMe_3)_2)(OSiMe_3)_2Cl]$ (**16**) does not thermolyse cleanly to GaN, and removal of the LiCl proved to be impractical. The more practical approach of performing the synthesis in non-coordinating hexane led to the synthesis of $Ga(N(SiMe_3)_2)(OSiMe_3)_2.py$ (**17**), which cleanly eliminates trimethylsilyl ether to produce amorphous GaN at 155°C.

The analogous indium chemistry shows a parallel situation. When too much coordinating base was present, the base-stabilised LiCl adduct $[Li(py)_2][In(N(SiMe_3)_2)(OSiMe_3)_2Cl]$ (**18**) was produced. When less than two equivalents of base per molecule were available in solution, $[In(N(SiMe_3)_2)(\mu^2\text{-}O)]_x$ (**20**) was made by trimethylsilyl elimination at the siloxo groups.

The successful elimination of the trimethylsilyl group, particularly as the robust and volatile ether $(Me_3Si)_2O$, demonstrates this group's utility as a attendant ligand for thermal production of MPn solid-state compounds. Also, its steric bulk, easy detection and inherent volatility offer many of the facets sought after in CVD precursors.

It can be seen from this thesis that the group $OSiMe_3$ allows elimination of the ligand environment surrounding the M-Pn core more effectively. When considering possible elimination mechanisms, it becomes apparant that a lone pair in the eliminating group could allow a centre around which elimination can take place. When the $OSiMe_3$ ligand is contrasted with an alkyl ligand (e.g ^nBu or ^tBu), the ability of this available lone pair is obvious. This lone pair could be a site to coordinate or "moor" a second molecule in the case of an intermolecular reaction. It could also provide a site to which a $SiMe_3$ moeity could transfer, providing an excellent leaving group (i.e. $(Me_3Si)_2O$). The lack of such a feature in the alkyl group denies it these possibilities and opens up this molecule to a more complicated thermal pathway.

Both alkyl-pnictido and siloxo-pnictido compounds are valuable possible precursors, as this work has demonstrated. Their ease of synthesis and tunability with a variety of ligands allow synthesis of precursors with specific properties, such as reaction temperature and volatility.

Chapter 10: Experimental

General Considerations: All manipulations were carried out in a Vacuum Atmospheres Company MO-20 dry box or on a vacuum line using standard schlenk techniques. Hexane, toluene, diethylether, and tetrahydrofuran (thf) were all dried under reflux with Na/K alloy and distilled using benzophenone as an indicator. Pyridine, $HN(SiMe_3)_2$, H_2N^tBu, and $H_2N(C_6H_3Me_2)$ were dried using CaH_2 under reflux and distilled. All corresponding lithium amide salts of these amines were synthesised by slow addition of the appropriate alkyllithium reagent at room temperature. $GaCl_3$ and $InCl_3$ were sublimed under vacuum at 30°C and 300°C, respectively. ^{t}BuLi, ^{t}BuMgCl and ^{n}BuLi were used as received from Aldrich Chemical Company. $InCl_3thf_3$, $LiOSiMe_3$,and $P(SiMe_3)_3$ were synthesised using literature procedures.[67, 70] All NMR spectra were run on a Gemini 200 MHz spectrometer with either deuterated benzene or deuterated pyridine as a solvent and internal standard (indicated per experimental). All infrared spectra were run on a Mattson 3000 FTIR spectrometer in a mineral oil mull between NaCl plates. All elemental analysis were run on a Perkin Elmer PE CHN 4000 elemental analyser weighed under air.

1. Amido-Chloro Compounds

Synthesis of $GaN(SiMe_3)_2Cl_2$.thf (1): Solid $LiN(SiMe_3)_2$.thf (1.4 g, 5.8 mmol) was added to a hexane solution of $GaCl_3$ (1.0 g, 5.7 mmol) at room temperature. The reaction was allowed to stir for 3 hr., after which a white solid was removed by filtration. Condensation of the solvent to the point of supersaturation and subsequent cooling to -30°C resulted in clear crystalline **1** (1.3 g, 60%). IR (cm^{-1}): 1452(s), 1368(s), 1256(s), 1144(w), 1032(m), 1004(m), 920(s), 892(s), 752(s), 724(m), 640(m). ^1H NMR (C_6D_6): 3.61 ppm (m, 4H, thf), 1.00 (m,4H, thf), 0.37 (s, 18H, Si*Me*$_3$). Elemental Analysis (Calc.: C = 32.19 %, H = 7.02 %, N = 3.75%; Exp.: C = 31.77%, H = 6.54%, N = 3.62%)

Synthesis of $InN(SiMe_3)_2Cl_2$.py (2): Solid $LiN(SiMe_3)_2$.thf (1.1 g, 4.5 mmol) was added to a diethylether suspension of $InCl_3$ (1.0 g, 4.5 mmol) at room temperature. The reaction was allowed to stir for 72 hr., after which a white solid was removed by filtration. Addition of 1 eq. of pyridine, evapouration of the solvent, extraction with hexane and cooling to -30°C gave white crystalline **2** (1.6 g, 85%). IR (cm^{-1}): 1612(s), 1524(m), 1435(s), 1360(m), 1235(w), 1203(m), 1190(m), 1154(m), 1094(s), 1065(s), 1012(s), 785(s), 707(s), 620(m). ^1H NMR (C_6D_6): 9.06 ppm (m, 2H, py), 6.67 (m, 1H, py), 6.52 (m, 2H, py), 0.38 (s, 18H, Si*Me*$_3$). Elemental Analysis (Calc.: C = 31.07%, H = 5.45%, N = 6.59%; Exp.: C = 31.64%, H = 5.30%, N = 7.01%)

2. Alkyl-Pnictido Compounds

Synthesis of $Ga(^nBu)_2(N(SiMe_3)_2)$.py (3): ^{n}BuLi (0.8 mL @ 2.5 M, 2.0 mmol) was added to a solution of 1 (0.36 g, 0.97 mmol) in hexane at room temperature. A white solid formed after a few minutes and the reaction was allowed to stir over night. The white solid was removed by filtration and excess pyridine was added. The solvents were removed under vacuum and the consequent solid was dissolved in toluene. This solution was left at -30°C for several days and clear, colourless crystals of **3** (.33 g, 81%) were collected. IR (cm^{-1}): 2871(s), 1606(m), 1459(s), 1376(m), 1243(s), 1068(m), 1041(m), 1014(w), 960(s), 881(s), 833(s), 754(m), 698(m), 669(m), 632(w). ^{1}H NMR (C_6D_6):): 8.34 ppm (m, 2H, py), 6.78 (m, 1H, py), 6.46 (m, 2H, py), 1.55 (m, 8H, butyl β and γ-CH_2), 1.10 (m, 6H, butyl CH_3), 0.85 (t, 4H, butyl α-CH_2), 0.33 (t, 18H, amido CH_3). Elemental Analysis (Calc.: C = 51.92%, H = 10.65%, N = 3.36%; Exp.: C = 51.50%, H = 10.06%, N = 3.79%)

Thermal Synthesis of GaN from 3: Compound **3** (0.5 g, 1.2 mmol) was placed in a Schlenk tube under a slight overpressure of nitrogen. The Schlenk tube was placed in a furnace preheated to 400°C for 15 min. The tube was then removed and allowed to reach room temperature. The resulting dark grey solid was washed with acetone and dried in air. The resulting material was ground and sealed in a quartz tube under vaccuum. The quartz tube was heated to 900°C overnight and allowed to cool to room temperature over an 8 hr. period. The solid was then ground to a fine powder and characterisation by PXRD and XRF confirmed the formulation GaN.

Synthesis of $[Ga(^tBu)_2N(SiMe_3)_2]_2$ (4): $GaN(SiMe_3)_2Cl_2$.thf (1.31 g, 3.5 mmol) was dissolved in diethylether and cooled to 0°C. A diethylether solution of ^tBuMgCl (3.5 mL @ 2.0 M, 7.0 mmol) was added dropwise by syringe over 5 min.; a white solid precipitated immediately. The solution was allowed to reach room temperature and stir for 3 hr. before a grey-white solid was removed by filtration. It was then evaporated to dryness and the resulting white residue was dissolved in hexane and allowed to recrystallise. Clear crystals of **4** resulted (0.91 g, 75%). IR: 2709(w), 1911(w), 1660(w), 1465(m), 1363(m), 1259(s), 1168(w), 1097(m), 1008(s), 975(s), 877(s), 817(s), 752(m), 673(m), 613(m). ^1H NMR (C_6D_6): 1.16 ppm (s, 18H, $C(CH_3)_3$), 0.17 (s, 18H, $NSiMe_3$). Elemental Analysis (Calc.: C = 48.83%, H = 10.54%, N = 4.07%; Exp.: C = 48.71%, H = 10.66%, N = 4.30%)

Synthesis of $[Ga(^nBu)_2P(SiMe_3)_2]_2$ (5): $^nBu_2GaCl$ (0.5 g, 2.3 mmol) was dissolved in diethylether and stirred. To this solution, $P(SiMe_3)_3$ (0.56 g, 2.2 mmol) was added dropwise. This yellow solution was stirred overnight and then evaporated to dryness. The resulting yellow solid was dissolved in approximately 5 mL of hexane to recrystallise. Clear cubic crystals of **5** was collected (0.59 g, 72%). IR: 2948(s), 1456(w), 1402(w), 1373(w), 1241(s), 1043(m), 836(s), 748(m), 688(m), 626(s), 464(m), 420(s). ^1H NMR (C_6D_6): 1.67 ppm (m, 4H, butyl β-CH_2), 1.58 (m, 4H, butyl γ-CH_2), 1.06 (t, 6H, butyl CH_3), 0.99 (m, 4H, butyl α-CH_2), 0.43 (t, 18H, phosphine CH_3). Elemental Analysis (Calc.: C = 46.54%, H = 10.04%, N = 0.00%; Exp.: C = 46.12%, H = 9.77%, N = 0.00%)

Thermal Synthesis of GaP from 5: Compound **5** (0.5 g, 1.4 mmol) was placed in a Schlenk tube under a slight overpressure of nitrogen. The Schlenk tube was placed in a furnace preheated to 400°C for 15 min. The tube was then removed and allowed to reach room temperature. The resulting dark grey solid was washed with acetone and dried in air and characterisation by PXRD and XRF confirmed the formulation GaP.

Synthesis of [Ga(^{n}Bu)(Cl)P(SiMe$_3$)$_2$)]$_2$ (6): ^{n}BuGaCl$_2$ (1.00 g, 5.1 mmol) was partially dissolved in diethylether and stirred. To this solution, P(SiMe$_3$)$_3$ (1.3 g, 5.2 mmol) was added dropwise. This homogeneous, colourless solution was stirred and heated in a sealed schlenk vessel to 110°C overnight. It was then evaporated to dryness and the resulting white solid was dissolved in approximately 5 mL of pyridine to recrystallise. White crystal filaments of **6** were collected (.73 g, 43%). IR: 1454(s), 1377(m), 1244(m), 845(s), 827(m), 750(w), 723(w), 698(w), 657(w), 629(m). ^{1}H NMR (C_6D_6): 1.84 ppm (m, 2H, butyl β-C*H*$_2$), 1.52 (m, 2H, butyl γ-C*H*$_2$), 1.14 (m, 2H, butyl α-C*H*$_2$), 0.98 (t, 3H, butyl C*H*$_3$), 0.48 (t, 18H, phosphine C*H*$_3$). Elemental Analysis (Calc.: C = 35.36%, H = 8.01%, N = 0.00%; Exp.: C = 34.97%, H = 7.54%, N = 0.10%)

Synthesis of [(^{n}Bu)$_2$InP(SiMe$_3$)$_2$]$_2$ (7): Bu$_2$InCl (0.50 g, 1.9 mmol) was dissolved in diethylether and stirred. To this solution, P(SiMe$_3$)$_3$ (0.47 g, 1.9 mmol) was added dropwise and this homogeneous, colourless solution was stirred overnight. It was then evaporated to dryness and the resulting white solid was dissolved in approximately 5 mL of toluene to recrystallise. White microcrystalline **7** was collected (0.45 g, 59%). IR: 1462(w), 1402(w), 1373(w), 1259(m), 1242(s), 1043(m), 837(s), 748 m 688(w), 627(m),

465(w), 420(m). ^{1}H NMR (C_6D_6): 1.88 ppm (m, 4H, butyl β-CH_2), 1.56 (m, 4H, butyl γ-CH_2), 1.20 (m, 4H, butyl α-CH_2), 1.05 (t, 6H, butyl CH_3), 0.41 (t, 18H, phosphine CH_3). Elemental Analysis (Calc.: C = 41.38%, H = 8.93%, N = 0.00%; Exp.: C = 41.85%, H = 9.28%, N = 0.00%)

Thermal Synthesis of InP and In^0 from 7: Compound **7** (0.5 g, 1.2 mmol) was placed in a Schlenk tube under a slight overpressure of nitrogen. The Schlenk tube was placed in a furnace preheated to 400°C for 15 min. The tube was then removed and allowed to reach room temperature. The resulting dark grey solid was washed with acetone and dried in air and characterisation by PXRD and XRF confirmed the formulation InP plus In metal.

3. Alkyl-amido Compounds with Primary Amides

Synthesis of $[Ga(^tBu)_2(NH^tBu)]_2$ (8): $GaCl_3$ (1.00 g, 5.7 mmol) was stirred in hexane with a pentane solution of ^tBuLi (6.6 mL @ 1.7 M, 5.8 mmol) for 5 hr. A white precipitate was filtered off and $LiNH^tBu$ 0.47 g, 5.8 mmol) was added. It was stirred for 48 hr. and was filtered to remove the formed precipitate. The solution was then evaporated to dryness and recrystallised in a thf/hexane solution. Clear crystals of **8** resulted (0.70 g, 49%). IR: 1461(s), 1375(m), 1193(m), 1176(m), 1016(m), 929(w), 908(w), 885(m), 808(s), 750(w), 723(w). ^1H NMR (C_6D_6): 2.12 ppm (br s, 1H, N*H*), 0.32 (s, 18H, $C(CH_3)_3$), 0.18 (s, 9H, $NC(CH_3)_3$). Elemental Analysis (Calc.: C = 56.28%, H = 11.02%, N = 5.47%; Exp.: C = 56.15%, H = 10.75%, N = 5.66%)

Synthesis of $[Ga(^nBu)_2(NH^tBu)]_2$ (9): $GaCl_3$ (1.00 g, 5.7 mmol) was stirred in hexane with a hexane solution of ^nBuLi (4.6 mL @ 2.5 M, 11.2 mmol) of for 5 hr. A white precipitate was removed and $LiNH^tBu$ (0.45 g, 5.7 mmol) was then added. The solution was stirred for 24 hr. and a white precipitate was again removed. The filtrate was then evaporated to dryness and recrystallised in a thf/hexane solution. A white crystalline **9** resulted (0.60 g, 36%). IR: 1461(s), 1373(s), 1205(m), 1068(m), 1045(m), 1020(m), 948(w), 914(w), 875(m), 754(w), 721(w). ^1H NMR (C_6D_6): 1.67 ppm (m, 4H, butyl β-CH_2), 1.52 (m, 4H, butyl γ-CH_2), 1.07 (m, 6H, butyl CH_3), 0.91 (s, 9H, $C(CH_3)_3$), 0.73 (m, 2H, butyl α-CH_2), 0.55 (m, 2H, butyl α-CH_2). Elemental Analysis (Calc.: C = 56.28%, H = 11.02%, N = 5.47%; Exp.: C = 55.62%, H = 10.51%, N = 5.17%)

Synthesis of $Ga(^nBu)_2(NH(C_6H_4(Me)_2))(py)$ (10): $GaCl_3$ (0.73 g, 4.1 mmol) in diethylether was stirred with a hexane solution of ^nBuLi (3.3 mL @ 2.5 M, 8.2 mmol) for 11 hr. The solution was then filtered to remove a white precipitate and $LiNH(Ph(Me)_2).thf$ (0.83 g, 4.2 mmol) was added. The solution was stirred for another 24 hr. and a white precipitate was again removed. The filtrate was then evaporated to dryness and excess pyridine was added. The solution was then evaporated, leaving an involatile oil **10** (0.78 g, 41%). IR: 3297(w), 1594(m), 1446(s), 1423(s), 1373(m), 1280(m), 1253(s), 1224(s), 1189(s), 1097(s), 1068(s), 1041(m), 1012(m), 836(s), 754(s), 698(s), 632(s). ^1H NMR (C_6D_6): 8.13 ppm (d, 2H, py), 7.15 (d, 1H, py), 6.90 (m, 2H, Ph *o-H*), 6.74 (m, 2H, py), 6.39 (m, 1H, Ph *p-H*), 3.09 (br s, 1H, N*H*), 2.36 (s, 6H, PhCH_3), 1.75 (m, 4H, butyl β-CH_2), 1.61 (m, 4H, butyl γ-CH_2), 1.04 (t, 6H, butyl CH_3), 0.77 (m, 4H, butyl α-CH_2) Elemental Analysis (Calc.: C = 65.82%, H = 8.68%, N = 7.31%; Exp: C = 65.65%, H = 8.75%, N = 7.46%)

Synthesis of $[Li(Et_2O)_2][Ga(^nBu)_2(NH(C_6H_4(Me)_2))_2]$ (11): $H_2N(Ph(Me)_2)$ (4.5 mL, 36 mmol) in hexane was cooled to -78°C and a hexane solution of ^nBuLi (28 mL @ 2.5 M, 70 mmol) was added by cannula. The solution was allowed to reach room temperature and a hexane solution of $GaCl_3$ (5.0 g, 30 mmol) was then added. This mixture was stirred for 17 hr., filtered, and evaporated to dryness. The residue was recrystallised from diethylether. Clear colourless crystals of **11** resulted (7.8 g, 38%). IR: 1592 (m), 1456 (s), 1376 (s), 1254 (m), 1224 (m), 1205 (m), 1096 (m), 909 (w), 824 (m), 756 (s), 680 (m). ^1H NMR (C_6D_6): 7.00 ppm (d, 4H, Ph *o-H*), 6.70 (m, 2H, Ph *p-H*), 2.79 (q, 8H, Et_2O), 2.63 (br s, 2H, N*H*), 2.22 (s, 12H, PhCH_3), 1.37 (m, 8H, butyl α and

β-CH_2), 0.89 (t, 6H, butyl CH_3), 0.58 (t, 6H, Et_2O), 0.53 (m, 4H, butyl α-CH_2).

Elemental Analysis (Calc.: C = 66.53%, H = 9.57%, N = 5.54%; Exp.: C = 66.15%, H = 9.75%, N = 5.46%)

4. Siloxo-Chloro Compounds

Synthesis of $Ga(OSiMe_3)_3.py$ (12): $GaCl_3$(0.50 g, 2.8 mmol) was dissolved in about 30 mL of hexane. To this clear solution, $LiOSiMe_3.thf$ (1.40, 8.3 mmol) was added and a white precipitate formed immediately. This solution was stirred overnight and then filtered. An excess of pyridine was added, the solution was evaporated to dryness, and the resulting white solid was recrystallised in toluene. Clear colourless crystals of **12** were isolated (.81, 69%). IR: 2952(s), 2925(s), 2854(s), 1596(m), 1442(m), 1376(w), 1245(s), 1070(m), 1004(m), 917(m), 835(s), 750(m), 701(w), 509(w). ^1H NMR (C_6D_6): 8.73 ppm (d, 2H, py), 6.95 (m, 1H, py), 6.66 (m, 2H, py), 0.33 (s, 27H, $OSiCH_3$). Elemental Analysis (Calc.: C = 40.38%, H = 7.75%, N = 3.77%; Exp.: C = 40.24%, H = 7.74%, N = 3.77%)

Synthesis of $In(OSiMe_3)_3.py$ (13): $InCl_3$ (1.0 g, 4.5 mmol) was partially dissolved in about 30 mL of diethylether. To this heterogeneous solution, $LiOSiMe_3$ (1.3 g, 13.5 mmol) was added and a white precipitate formed immediately. This solution was stirred overnight at 110°C and then filtered at room temperature. An excess of pyridine was added, the solution was evaporated to dryness, and the resulting white solid was recrystallised in thf. A white microcrystalline powder of **13** was isolated (0.91 g, 44%). IR: 2892(s), 1598(w), 1452(s), 1376(m), 1245(s), 1151(w), 1033(s), 933(s), 836(s), 750(s), 701(s), 676(w), 624(w). ^1H NMR (C_5D_5N): 8.71 ppm (d, 2H, py), 7.55 (m, 1H, py), 7.19 (m, 2H, py), 0.21 (s, 27H, $OSiCH_3$). Elemental Analysis (Calc.: C = 36.44%, H = 6.99%, N = 3.04%; Exp.: C = 37.23%, H = 7.21%, N = 3.01%)

Synthesis of $Ga(OSiMe_3)_2Cl.py$ (14): $GaCl_3$ (0.5 g, 2.8 mmol) was dissolved in about 30 mL of hexane. To this clear solution, $LiOSiMe_3$.thf (0.96 g, 5.7 mmol) was added and a white precipitate formed immediately. This solution was stirred overnight and then filtered. An excess of pyridine was added, the solution was evaporated to dryness, and the resulting white solid was recrystallised in toluene. Clear colourless crystals of **14** were isolated (0.6 g, 59%). IR: 2892(s), 1928(w), 1845(w), 1459(s), 1376(s), 1249(s), 1178(m), 1043(s), 902 (s), 844 (s), 752 (s), 684 (m), 632 (w), 509 (s), 441 (m). ^1H NMR (C_6D_6): 8.50 ppm (d, 2H, py), 6.92 (m, 1H, py), 6.66 (m, 2H, py), 0.35 (s, 18H, $OSiCH_3$). Elemental Analysis (Calc.: C = 36.43%, H = 6.39%, N = 3.86%; Exp.: C = 36.82%, H = 4.37%, N = 6.91%)

Synthesis of $In(OSiMe_3)_2Cl.py$ (15): $InCl_3$ (1.0 g, 4.5 mmol) was partially dissolved in about 30 mL of diethylether. To this heterogeneous solution, $LiOSiMe_3$ (0.85 g, 8.9 mmol) was added and a white precipitate formed immediately. This solution was stirred over night at 110°C and then filtered at room temperature. An excess of pyridine was added, the solution was evaporated to dryness, and the resulting white solid was recrystallised in pyridine. A white microcrystalline powder of **15** was isolated (1.1 g, 60%). IR: 2902(s), 1604(m), 1450(s), 1376(m), 1238(m), 1155(w), 1074(w), 1047(m), 971(m), 929(s), 833(s), 755(m), 694(m), 674(w), 632(w). ^1H NMR (C_5D_5N): 8.71 ppm (d, 2H, py), 7.55 (m, 1H, py), 7.19 (m, 2H, py), 0.35 (s, 18H, $OSiCH_3$). Elemental Analysis (Calc.: C = 32.40%, H = 5.69%, N = 3.44%; Exp.: C = 33.60%, H = 5.69%, N = 2.85%)

5. Siloxo-Amido Compounds

Synthesis of $[Li(thf)_2][Ga(N(SiMe_3)_2)(OSiMe_3)_2Cl]$ (16): A thf solution of $Li(OSiMe_3)$.thf (3.2 g, 19.0 mmol) was added to a -78°C thf solution of **1** (3.7 g, 9.9 mmol). After addition, the reaction mixture was allowed to reach room temperature and stirred for 17 hr. Evaporation of the solvent, extraction with hexane and cooling to -30°C gave white crystalline **16** (2.4g, 40%). IR (cm^{-1}): 1245(s), 1050(s), 975(s,br), 950(s,br), 905(s,br), 835(s), 750(s), 690(m), 605(w). ^1H NMR (C_6D_6): 3.48 ppm (m, 4H, thf), 1.33 (m, 4H, thf), 0.55 (s, 18H, NSi*Me*$_3$), 0.33 (s, 18H, OSi*Me*$_3$). Elemental Analysis (Calc.: C = 40.91%, H = 8.47%, N = 3.18%; Exp.: C = 40.73%, H = 7.96%, N = 2.89%)

Synthesis of $Ga(N(SiMe_3)_2)(OSiMe_3)_2$.py (17): A hexane solution of $LiN(SiMe_3)_2$.thf (1.6 g, 6.6 mmol) was added slowly to a hexane solution of $GaCl_3$ (1.2 g, 6.8 mmol) at room temperature. The reaction mixture was stirred for 22 hr. after which a white solid was removed by filtration. To this solution $Li(OSiMe_3)$.thf (2.3 g, 13.7 mmol) was added and the reaction mixture was stirred for another 14 hr. Following removal of a white solid, excess pyridine was added to the solution. Evaporation of the solvent, dissolution of the resulting solid in a minimal amount of toluene, and cooling to -30°C overnight resulted in clear, cubic crystals of **17** (2.5 g, 75%). IR (cm^{-1}): 1616(m), 1247(s), 1074(m), 1035(s), 989(s), 950(s), 910(s), 883(s), 838(s), 750(s), 694(m), 678(m), 647(m). 200 MHz ^1H NMR (C_6D_6): 8.52 ppm (m, 2H, py), 6.87 (m, 1H, py), 6.54 (m, 2H, py), 0.37 (s, 18H, NSi*Me*$_3$), 0.29 (s, 18H, OSi*Me*$_3$). Elemental Analysis (Calc.: C = 41.88%, H = 8.48%, N = 5.75%; Exp.: C = 42.47%, H = 8.78%, N = 5.58%)

Thermal Synthesis of GaN from 17: Compound **17** (0.5 g, 1.0 mmol) was placed in a Schlenk tube under a slight overpressure of nitrogen. The Schlenk tube was placed in a furnace preheated to 400°C for 15 min. The tube was then removed and allowed to reach room temperature. The resulting dark grey solid was washed with acetone and dried in air. The resulting material was ground and sealed in a quartz tube under vaccuum. The quartz tube was heated to 900°C overnight and allowed to cool to room temperature over an 8 hr. period. The solid was then ground to a fine powder and characterisation by PXRD and XRF confirmed the formulation GaN.

Synthesis of $[Li(py)_2][In(N(SiMe_3)_2)(OSiMe_3)_2Cl]$ (18): To a solution of $InCl_3(thf)_3$ (1.0 g, 2.3 mmol) in hexane, a hexane solution of $LiN(SiMe_3)_2$.thf (0.5 g, 2.1 mmol) was added at room temperature. This reaction mixture was stirred for 13 hr. with no observed precipitate forming. To this solution $Li(OSiMe_3)$.thf (0.8 g, 4.7 mmol) was added and the mixture was stirred for another 11 hr. A white solid was removed by filtration and an excess of pyridine was added to the solution. Evaporation of the solvent, dissolution of the resulting solid in a minimal amount of toluene, and cooling to -30°C overnight yielded clear cubic crystals of **18** (0.7 g, 48% yield). IR(cm^{-1}): 1594(m), 1259(s), 1245(s), 1151(m), 1093(m), 1035(m), 954(s), 916(s), 875(s), 835(m), 750(s), 701(s), 677(m), 619(s). ^1H NMR (C_6D_6): 8.54 ppm (m, 2H, py), 6.94 (m, 1H, py), 6.67 (m, 2H, py), 0.53 (s, 18H, NSi*Me*$_3$), 0.23 (s, 18H, OSi*Me*$_3$). Elemental Analysis (Calc C = 38.17%, H = 5.84%, N = 7.86%; Exp.: C = 37.59%, H = 6.18%, N = 7.73%)

Synthesis of $[Li(py)_2][In(N(SiMe_3)_2(OSiMe_3)_3]$ (19): $InCl_3thf_3$ (1.5 g,3.5 mmol) was dissolved in hexane and $Li(NSiMe_3)_2$.thf (0.9 g, 3.7 mmol) was added at room

temperature. This reaction was stirred for 5 hr. without precipitate forming. Subsequently, $Li(OSiMe_3)$.thf (1.78 g,10.5 mmol) was added and the solution was allowed to stir for another 20 hr. Following removal of a white precipitate, excess pyridine was added to the solution. Evaporation of the solvent, dissolution of the resulting solid in a minimal amount of toluene, and cooling to -30°C overnight yielded colourless crystals of **19** (2.2 g., 88%). IR: 1994(w), 1926(w), 1862(w), 1596(m), 1245(s), 1027(m), 956(s), 923(s), 875(s), 835(s), 748(s), 701(s), 674(m), 621(m). ^1H NMR (C_6D_6): 8.44 ppm (m, 4H, py), 6.96 (m, 2H, py), 6.64 (m, 4H, py), 0.50 (s, 18H, NSi*Me*$_3$), 0.32 ppm (s, 27H, OSi*Me*$_3$). Elemental Analysis (Calc.: C = 42.42%, H = 7.83%, N = 5.94%; Exp.: C = 42.39%, H = 7.56%, N = 5.68%)

Synthesis of $[In(N(SiMe_3)_2)(\mu^2\text{-}O)]_x$ (20): $Li(N(SiMe_3)_2$ (0.76 g, 4.5 mmol) was added to a solution of $InCl_3$ (1.0 g, 4.5 mmol) in hexane at room temperature. The solution was stirred for 24 hr., after which a white solid was removed by filtration and $Li(OSiMe_3)$ (0.88 g, 9.1 mmol) was added. The reaction was stirred for a further 24 hr. Following removal of a white solid by filtration, the solution was condensed to the point of supersaturation and cooling to -30°C yielded white microcrystalline **20** (0.71 g, 54%). IR 1597(m), 1460(s), 1442(s), 1377(s), 1246(s), 1180(w), 1077(w), 1041(m), 1001(w), 967(s), 928(s), 876(s), 840(s), 750(m), 725(w), 700(w), 640(w). ^1H NMR (C_6D_6): 0.34 ppm (s, 18H, Si*Me*$_3$). Elemental Analysis (Calc.: C = 24.75%, H = 6.23%, N = 4.81%; Exp.: C = 24.16%, H = 6.79%, N = 3.61%)

Appendix

1. Crystallographic Data for the single crystal XRD of $[^nBu_2GaP(SiMe_3)_2]_2$

EXPERIMENTAL DETAILS

A. Crystal Data

Empirical Formula	Ga2C28P2Si4H68
Formula Weight	718.57
Crystal Color, Habit	colourless, cube
Crystal Dimensions (mm)	0.400 x 0.400 x 0.400
Crystal System	triclinic
No. Reflections Used for Unit Cell Determination (2Θ range)	25 (6.1 - 17.9°)
Omega Scan Peak Width at Half-height	0.33
Lattice Parameters:	a = 11.179 (1) Å b = 20.462 (1) Å c = 9.712 (1) Å α = 94.93 (1)° β = 106.82 (1)° γ = 83.76 (1)° V= 2110.4 (8) Å^3
Space Group	P1-bar (#2)
Z value	2
D_{calc}	1.131 g/cm^3
F_{000}	768
μ(MoKa)	14.73 cm^{-1}

B. Intensity Measurements

Diffractometer	Rigaku AFC6S
Radiation	MoKa (X = 0.71069 Å)
Temperature	-148°C
Take-off Angle	6.0°
Detector Aperture	6.0 mm horizontal 6.0 mm vertical
Crystal to Detector Distance	40 cm
Scan Type	ω-2Θ
Scan Rate	4.0°/min (in omega) (3 rescans)
Scan Width	$(1.63 + 0.30 \tan\Theta)^{\circ}$
$2\Theta_{max}$	40.0°
No. of Reflections Measured	Total: 5248 Unique: 2540 (R_{int} = .064)
Corrections	Lorentz-polarization

C. Structure Solution and Refinement

Structure Solution	Patterson Method
Refinement	Full-matrix least-squares
Function minimized	$\Sigma w (\|Fo\| - \|Fc\|)$
Least-squares Weights	$4Fo^2/\sigma^2(Fo^2)$
p-factor	0.03
Anomalous Dispersion	All non-hydrogen atoms
No. Observations ($I>2.50\sigma(I)$)	2020
No. Variables	300
Reflection/Parameter Ratio	6.73
Residuals: R; R_w	0.044; 0.065
Goodness of Fit Indicator	3.34
Max Shift/Error in Final Cycle	0.21
Maximum Peak in Final Diff. Map	$0.61 e^-/Å^3$
Minimum peak in Final Diff. map	$-0.35 e^-/Å^3$

Positional parameters and B(eq)

	x	y	z	B(eq)
Ga(l)	0.9077(1)	0.24744(6)	0.2723(1)	1.91(7)
Ga(2)	0.5883(1)	0.24867(6)	0.2538(1)	1.86(7)
P(1)	0.7435(3)	0.3298(1)	0.3176(3)	1.8(1)
P(2)	0.7522(3)	0.1661(1)	0.2117(3)	1.9(1)
S1(1)	0.7327(3)	0.1192(2)	-0.0118(3)	2.4(2)
S1(2)	0.7781(3)	0.0828(2)	0.3566(3)	2.2(2)
S1(3)	0.6716(3)	0.4139(1)	0.1714(3)	2.5(2)
S1(4)	0.7993(3)	0.3748(2)	0.5460(3)	2.5(2)
C(1)	0.449(1)	0.2669(5)	0.073(1)	1.8(2)
C(2)	0.373(1)	0.2045(5)	0.037(1)	2.7(3)
C(3)	0.889(1)	0.0875(5)	-0.029(1)	3.1(6)
C(4)	0.630(1)	0.051015)	-0.054(1)	3.6(6)
C(5)	0.664(1)	0.1823(6)	-0.144(1)	3.9(6)
C(6)	0.890(1)	0.0148(4)	0.316(1)	2.4(5)
C(7)	0.624(1)	0.0505(5)	0.332(1)	3.6(6)
C(8)	1.264(1)	0.0864(6)	0.329(1)	4.3(3)
C(11)	0.956(1)	0.4055(6)	0.583(1)	3.6(6)
C(12)	0.809(1)	0.3096(6)	0.671(1)	3.8(6)
C(13)	0.687(1)	0.4440(6)	0.576(1)	3.6(6)
C(14)	0.778(1)	0.4796(5)	0.219(1)	3.9(6)
C(15)	0.515(1)	0.4455(5)	0.188(1)	3.1(6)
C(16)	0.527(1)	0.2335(5)	0.420(1)	1.9(5)
C(17)	0.449(1)	0.2960(5)	0.456(1)	2.0(5)
C(18)	0.405(1)	0.2934(5)	0.590(1)	2.8(3)
C(19)	0.333(1)	0.3553(5)	0.627(1)	4.1(6)
C(20)	0.263(1)	0.2123(6)	-0.101(1)	4.0(7)
C(21)	1.047(1)	0.2275(6)	0.450(1)	2.9(6)
C(22)	0.956(1)	0.2770(6)	0.108(1)	3.0(6)
C(23)	1.039(1)	0.3351(5)	0.163(1)	3.5(6)
C(24)	1.057(1)	0.3728(7)	0.049(1)	6.0(8)
C(25)	1.140(1)	0.4294(7)	0.11611)	6.2(9)
C(26)	0.835(1)	0.1138(5)	0.548(1)	2.6(5)
C(27)	0.656(1)	0.3832(6)	-0.02011)	3.8(6)
C(28)	0.187(1)	0.1532(8)	-0.137(1)	6.3(9)
C(29)	1.181(1)	0.1526(5)	0.324(1)	2.9(3)
C(30)	1.126(1)	0.1622(6)	0.447(1)	3.6(6)
H(1)	0.9274	0.0531	0.0382	3.7
H(2)	0.8857	0.0685	-0.1233	3.7
H(3)	0.9460	0.1213	-0.0070	3.7
H(4)	0.5503	.0668	-0.0451	4.2
H(5)	0.6257	0.0326	-0.1467	4.2

	x	y	z	B(eq)
H(6)	0.6666	0.0181	0.0153	4.2
H(7)	0.7155	0.2194	-0.1251	4.9
H(8)	0.6561	0.1655	-0.2402	4.9
H(9)	0.5804	0.1995	-0.1388	4.9
H(10)	0.8010	-0.0209	0.3782	2.9
H(ll)	0.8588	-0.0034	0.2180	2.9
H(12)	0.9711	0.0292	0.3268	2.8
H(13)	0.5666	0.0848	0.3543	3.8
H(14)	0.5918	0.0345	0.2348	3.8
H(15)	0.6336	0.0157	0.3941	3.8
H(16)	1.2124	0.0523	0.3275	5.7
H(17)	1.2969	0.0808	0.2499	5.7
H(18)	1.3292	0.0872	0.4167	5.7
H(19)	1.0187	0.3701	0.5671	4.0
H(20)	0.9568	0.4393	0.5206	4.0
H(zi)	0.9876	0.4222	0.6804	4.0
H(22)	0.7206	0.2937	0.6542	4.9
H(23)	0.8594	0.2716	0.6615	4.9
H(24)	0.8278	0.3254	0.7713	4.9
H(25)	0.7103	0.4~20	0.6741	4.5
H(26)	0.6816	0.4794	0.5148	4.5
H(27)	0.6037	0.4301	0.5564	4.5
H(28)	0.8621	0.4644	0.2083	5.0
H(29)	0.7492	0.5165	0.1579	5.0
H(30)	0.7923	0.4970	0.3168	5.0
H(31)	0.5170	0.4616	0.2861	3.5
H(32)	0.4745	0.4793	0.1260	3.5
H(33)	0.4574	0.4099	0.1664	3.5
H(34)	0.4786	0.1968	0.4003	2.5
H(35)	0.5968	0.2255	0.5042	2.5
H(36)	0.4902	0.3355	0.4621	2.5
H(37)	0.3700	0.3032	0.3740	2.5
H(38)	0.3615	0.2533	0.5826	3.1
H(39)	0.4849	0.2826	0.6712	3.1
H(40)	0.3851	0.3900	0.6339	5.9
H(41)	012617	0.3608	0.5450	5.9
H(ez)	0.3119	0.3518	0.7094	5.9
H(43)	0.2004	0.2489	-0.0888	4.9
H(44)	0.2855	0.2214	-0.1852	4.9
H(45)	1.1051	0.2649	0.4662	3.2
H(46)	1.0148	0.234~	0.5328	3.2
HI47)	0.9926	0.2411	0.0622	3.4
H(48)	0.8787	0.2937	0.0365	3.4

	x	y	z	B(eq)
H(49)	1.0152	0.3624	0.2360	4.6
H(50)	1.1271	0.3145	0.2158	4.6
H(51)	1.0873	0.3467	-0.0236	8.4
H(52)	0.9722	0.3930	-0.0072	8.4
H(53)	1.2222	0.4101	0.1656	6.3
H(54)	1.1509	0.4561	0.0436	6.3
H(55)	1.1071	014565	0.1814	6.3
H(56)	0.8466	0.0799	0.6131	3.0
H(57)	0.9167	0.1317	0.5669	3.0
H(58)	0.7795	0.1489	0.5722	3.0
H(59)	0.6013	0.3474	-0.0451	3.6
H(60)	016192	0.4169	-0.0843	3.6
H(61)	0.7347	0.3665	-0.0331	3.6
H(62)	0.1644	0.1402	-0.0560	8.1
H(63)	0.1212	0.1524	-0.2192	8.1
H(64)	0.2488	0.1129	-0.1533	8.1
H(65)	1.2326	0.1882	0.3238	4.3
H(66)	1.1181	0.1534	0.2334	4.3
H(67)	1.1913	0.1604	0.5381	4.6
H(68)	1.0708	0.1300	0.4444	4.6

Thermal parameters (U values)

	U11	U22	U33	U12	U13	U23
Ga(l)	0.025(1)	0.0252(9)	0.0237(7)	-0.0009(7)	0.0094(8)	0.0004(6)
Ga(2)	0.023(1)	0.0272(9)	0.0209(7)	-0.0028(7)	0.0064(7)	0.0003(6)
P(l)	0.024(2)	0.024(2)	0.020(2)	-0.002(2)	0.008(2)	-0.003(1)
P(2)	0.029(3)	0.022(2)	0.020(2)	-0.004(2)	0.007(2)	0.000(1)
Si(l)	0.036(3)	0.033(2)	0.020(2)	-0.002(2)	0.008(2)	-0.003(1)
Si(2)	0.032(3)	0.030(2)	0.023(2)	-0.004(2)	0.008(2)	0.004(1)
Si(3)	0.040(3)	0.022(2)	0.037(2)	0.008(2)	0.020(2)	0.008(2)
Si(4)	0.036(3)	0.033(2)	0.028(2)	-0.007(2)	0.012(2)	-0.009(2)
C(1)	0.023(3)					
C(2)	0.035(3)					
C(3)	0.03(1)	0.049(9)	0.037(7)	0.004(7)	0.021(7)	-0.007(6)
C(4)	0.05(1)	0.041(9)	0.042(7)	0.004(8)	0.020(7)	-0.017(6)
C(5)	0.07(1)	0.07(1)	0.016(6)	0.001(8)	0.016(7)	-0.009(6)
C(6)	0.05(1)	0.005(6)	0.036(6)	0.014(6)	0.013(7)	-0.001(5)
C(7)	0.05(1)	0.042(9)	0.045(7)	-0.006(8)	0.014(8)	0.017(6)
C(8)	0.055(4)					
C(11)	0.05(1)	0.043(9)	0.046(7)	-0.014(8)	0.013(7)	-0.012(6)
C(12)	0.05(1)	0.07(1)	0.018(6)	-0.007(8)	0.005(7)	-0.003(6)
C(13)	0.04(1)	0.06(1)	0.049(7)	-0.012(8)	0.024(8)	-0.023(6)
C(14)	0.05(1)	0.039(9)	0.069(8)	-0.017(8)	0.031(8)	-0.001(7)
C(15)	0.04(1)	0.020(7)	0.058(8)	0.015(7)	0.020(8)	0.005(6)
C(16)	0.014(8)	0.020(7)	0.039(7)	0.002(6)	0.009(7)	0.005(5)
C(17)	0.029(9)	0.018(7)	0.033(6)	-0.004(7)	0.009(7)	0.005(5)
C(18)	0.036(3)					
C(19)	0.06(1)	0.025(8)	8.868(8)	0.025(7)	0.036(8)	-0.009(6)
C(20)	0.05(1)	0.05(1)	0.051(8)	-0.003(8)	0.01718)	-0.002(7)
C(21)	0.026(9)	0.06(1)	0.032(7)	-0.012(8)	0.016(7)	0.004(6)
C(22)	0.04(1)	0.041(9)	0.036(7)	0.002(8)	0.020(7)	-0.004(6)
C(23)	0.07(1)	0.021(8)	0.059(8)	0.015(8)	0.044(9)	0.008(7)
0(24)	0.10(1)	0.08(1)	0.052(9)	-0.02(1)	0.03(1)	-0.002(8)
C(25)	0.07(1)	0.08(1)	0.10(1)	-0.02(1)	0.04(1)	-0.00(1)
C(26)	0.033(9)	0.038(8)	0.025(6)	0.008(7)	8.005(7)	0.006(5)
C(27)	0.06(1)	0.054(9)	0.031(7)	0.012(8)	0.017(7)	0.013(6)
C(28)	0.06(1)	0.13(2)	0.044(8)	-0.06(1)	-0.006(8)	-0.011(9)
C(29)	0.037(3)					
C(30)	0.04(1)	0.040(9)	0.52(8)	0.015(8)	0.020(8)	0.012(6)

2. Crystallographic Data for the single crystal XRD of $^tBu_2Ga(\mu\text{-}N(H)^tBu)]_2$

EXPERIMENTAL DETAILS

A. Crystal Data

Empirical Formula	Ga2N2C24H56
Formula Weight	512.15
Crystal Color, Habit	colourless, cube
Crystal Dimensions (mm)	0.20 x 0.20 x 0.20
Crystal System	triclinic
No. Reflections Used for Unit Cell Determination (2Θ range)	24 (40.0 - 50.0°)
Lattice Parameters:	
	a = 10.265(5) Å
	b = 15.752(6) Å
	c = 8.9424(4) Å
	α = 90.32(2)°
	β = 105.61(3)°
	γ = 88.24(4)°
	V= 1390.5(9) Å^3
Space Group	P1
Z value	2
D_{calc}	1.223 g/cm^3
F_{000}	552.93
μ(MoKa)	19.4 cm^{-1}

B. Intensity Measurements

Diffractometer	Rigaku AFC6S
Radiation	MoKa (X = 0.71069 Å)
Temperature	-148°C
Take-off Angle	6.0°
Detector Aperture	6.0 mm horizontal 6.0 mm vertical
Crystal to Detector Distance	40 cm
Scan Type	ω-2Θ
Scan Rate	4.0°/min (in omega) (3 rescans)
Scan Width	$(1.63 + 0.30 \tan\Theta)^{\circ}$
$2\Theta_{max}$	49.8°
No. of Reflections Measured	Total: 4806 Unique: 4507 (R_{int} = .026)
Corrections	none

C. Structure Solution and Refinement

Structure Solution	Patterson Method
Refinement	Full-matrix least-squares
Function minimized	$\Sigma w (\|Fo\| - \|Fc\|)$
Least-squares Weights	$4Fo^2/\sigma^2(Fo^2)$
p-factor	0.03
Anomalous Dispersion	All non-hydrogen atoms
No. Observations ($I>2.50\sigma(I)$)	2020
No. Variables	300
Reflection/Parameter Ratio	6.73
Residuals: R; R_w	0.035; 0.040
Goodness of Fit Indicator	2.41
Max Shift/Error in Final Cycle	0.219
Maximum Peak in Final Diff. Map	$0.920 e^-/Å^3$
Minimum peak in Final Diff. map	$-1.170 e^-/Å^3$

Positional parameters and B(eq)

	X	Y	Z	B(eq)
Ga1	0.87602(4)	0.940942(23)	0.45652(4)	1.522(17)
Ga2	0.63764(4)	0.450787~23)	1.06141(4)	1.388(16)
N1	1.0840(3)	0.93287(17)	0.4962(3)	1.73(13)
N2	0.4611(3)	0.47323(17)	1~1254(3)	1.46(12)
C1	0~7522(4)	0.93119(24)	0.2332(4)	2.39(17)
C2	0.7715(4)	1.0019(3)	0.1265(4)	3.13(18)
C3	0.6039(4)	0.9376(3)	0.2429(5)	3.57(21)
C4	0.7672(4)	0.8455(3)	0.1551(4)	3.12(18)
C5	0.8241(4)	0.86559(22)	0.6172(4)	2.13(16)
C6	0.6918(4)	0.8938(3)	0.6550(5)	2.99(19)
C7	0.8015(5)	0.7767(3)	0.5470(5)	3.29(20)
C8	0.9348(4)	0.85705(25)	0.7707(4)	2.75(18)
C9	1.1613(4)	0.87433(22)	0.4138(4)	2.09(16)
C10	1.1342(4)	0.90296(23)	0.2447(4)	2.51(17)
C11	1.3131(4)	0.8780(3)	0.4940(5)	2.87(19)
C12	1.1169(4)	0.78349(23)	0.4210(4)	2.73(18)
C13	0.6800(4)	0.33400(22)	0.9799(4)	2.07(15)
C14	0.8229(4)	0.3360(3)	0.9543(5)	2.88(18)
C15	0.6838(4)	0.25985(24)	1.0909(5)	2.96(18)
C16	0.5817(4)	0.31163(24)	0.8217(4)	2.81(17)
C17	0.7934(31	0.49773(23)	1.2343(4)	1.92(15)
C18	0.7496(41	0.57149(24)	1.3226(4)	2.40(16)
C19	0.9157(41	0.5262(3)	1.1818(4)	2.80(18)
C20	0.8463(4)	0.4251(3)	1.3512(4)	2.79(17)
C21	0.3919(4)	0.41104(22)	1.2030(4)	1.83(15)
C22	0.4917(4)	0.37618(24)	1.3509(4)	2.47(17)
C23	0.3402(4)	0.33887(23)	1.0914(4)	2.38(17)
C24	0.2743(4)	0.45573(25)	1.2476(4)	2.37(17)
NH1	1.101(4)	0.9084(22)	0.602(4)	3.2(9)
NH2	0.492(4)	0.5116(211	1.203(4)	2.9(8)
H2A	0.753(4)	1.0583(22)	0.163(4)	3.3(9)
H2B	0.712(4)	1.0008(25)	0.025(5)	4.4(1)
H2C	0.856(4)	1.0001(22)	0.101(4)	3.3(9)
H3A	0.544(4)	0.9367(24)	0.135(4)	4.1(10)
H3B	0.577(4)	0.888(3)	0.288(5)	5.3(111
H3C	0.591(4)	0.9997(24)	0.267(4)	4.2(10)
H4A	0.706(4)	0.8454(22)	0.056(4)	3.3(91
H4B	0.849(4)	0.8377(22)	0.131(4)	3.6(9)
H4C	0.753(4)	0.7957(23)	0.215(4)	4.4(10)
H6A	0.615(4)	0.907(3)	0.558(5)	5.1(11)
H6B	0.658(4)	0.8531(22)	0.709(4)	3.3(9)

	X	Y	Z	B(eq)
H6C	0.697(4)	0.9505(23)	0.709(4)	3.7(9)
H7A	0.732(3)	0.7783(21)	0.460(4)	2.8(8)
H7B	0.885(4)	0.7517(22)	0.518(4)	3.4(9)
H7C	0.782(4)	0.7367(22)	0.617(4)	3.2(9)
H8A	0.909(3)	0.8209(21)	0.837(4)	2.7(8)
H8B	0.950(4)	0.9139(21)	0.829(4)	3.0(8)
H8C	1.017(4)	0.8320(21)	0.754(4)	2.9
H10A	1.051(4)	0.8966(22)	0.192(4)	3.5(9)
H10B	1.154(3)	0.9665(20)	0.239(4)	2.3
H10C	1.182(4)	0.8654(25)	0.190(4)	4.6(10)
H11A	1.326(3)	0.8565(19)	0.603(4)	1.7(7)
H11B	1.346(4)	0.9389(22)	0.490(4)	3.3(9)
H11C	1.364(4)	0.8378(21)	0.445(4)	2.8(8)
H12A	1.120(4)	0.7648(24)	0.529(4)	4.4(10)
H12B	1.176(41	0.7396(23)	0.373(4)	4.0(10)
H12C	1.024(3j	0.7767(21)	0.365(4)	2.8(8)
H14A	0.848(4)	0.2772(21)	0.910(4)	2.9(8)
H14B	0.824(4)	0.3804(23)	0.872(4)	3.7(9)
H14C	0.890(4)	0.3476(24)	1.054(4)	4.5(10)
H15A	0.750(3)	0.2725(21)	1.201(4)	2.5(8)
H15B	0.711(4)	0.2057(25)	1.049(5)	4.8(10)
H15C	0.608(4)	0.2488(22)	1.110(4)	3.5(9)
H16A	0.585(4)	0.3590(22)	0.735(4)	3.6(9)
H16B	0.612(4)	0.2575(22)	0.782(4)	3.0(8)
H16C	0.491(4)	0.3016(21)	0.832(4)	2.9(8)
H18A	0.678(3)	0.5586(19)	1.370(3)	1.7(7)
H18B	0.721(3)	0.6202(20)	1.259(4)	2.5(8)
H18C	0.828(4)	0.5932(22)	1.409(4)	3.6(9)
H19A	0.991(3)	0.5439(21)	1.274(4)	2.7(8)
H19B	0.902(4)	0.5771(22)	1.116(4)	3.2(9)
H19C	0.955(4)	0.4822(21)	1.116(4)	2.8(8)
H20A	0.786(3)	0.4029(21)	1.396(4)	2.5(8)
H20B	0.917(4)	0.4497(21)	1.443(4)	3.0(8)
H20C	0.884(4)	0.3753(23)	1.296(4)	4.0(10)
H22A	0.442(4)	0.3350(21)	1.403(4)	2.9(8)
H22B	0.561(3)	0.3450(19)	1.328(4)	1.9(7)
H22C	0.524(3)	0.4244(21)	1.425(4)	2.8(8)
H23A	0.271(3)	0.3615(21)	1.000(4)	2.6(8)
H23B	0.291(4)	0.2970(25)	1.136(5)	4.8(10)
H23C	0.409(4)	0.310(3)	1.061(5)	4.9(10)
H24A	0.215(3)	0.4781(20)	1.162(4)	2.3(8)
H24B	0.305(4)	0.5057(22)	1.320(4)	3.4(9)
H24C	0.229(4)	0.4135(22)	1.301(4)	2.9(8)

Thermal parameters (U values)

	U11	U22	U33	U12	U13	U23
Ga1	1.625(22)	2.317(20)	1.864(19)	-0.249(17)	0.492(17)	-0.051(16)
Ga2	1.279(21)	2.353(20)	1.561(18)	0.071(16)	0.256(16)	0.019(15)
N1	1.86(17)	2.57(16)	2.31(15)	0.05(13)	0.87(13)	-0.10(12)
N2	1.44(16)	2.61(15)	1.49(14)	-0,08(13)	0.36(12)	0.30(12)
C1	2.77(23)	3.92(23)	2.14(19)	-0.73(18)	0.18(17)	-0.26(16)
C2	3.6(3)	4.9(3)	2.72(21)	-0,66(21)	-0.51(19)	0.30(18)
C3	2.29(24)	6.5(3)	4.1(3)	-0,78(22)	-0.28(20)	-0.46(22)
C4	4.1(3)	4.6(3)	2.88(22)	-1.34(21)	0.33(20)	-0.84(19)
C5	2.38(22)	3.09(20)	2.92(20)	-0,51(17)	1.20(17)	0.29(16)
C6	3.08(25)	4.8(3)	3.82(23)	-0.86(20)	1.42(20)	0.78(19)
C7	4.9(3)	3.74(24)	4.22(25)	-1.82(21)	1.70(22)	0.12(19)
C8	3.06(24)	3.92(23)	3.55(23)	-0,07(19)	0.99(19)	1.15(18)
C9	2.54(22)	2.99(20)	2.53(19)	0.44(17)	0.95(17)	-0.16(16)
C10	3.66(25)	3.31(22)	2.96(21)	0.10(18)	1.60(19)	-0.03(17)
C11	2.35(23)	4.35(24)	4.25(24)	0.91(19)	1.09(19)	-0.04(19)
C12	4.3(3)	2.94(21)	3.35(22)	0.61(19)	1.43(20)	-0.15(17)
C13	2.44(22)	2.66(19)	2.65(19)	0.51(16)	0.58(17)	-0.21(15)
C14	3.11(25)	4.09(24)	3,86(23)	0.69(19)	1.20(20)	-0.47(19)
C15	3.8(3)	2.98(22)	4,34(24)	0.74(19)	0.87(21)	0.35(18)
C16	3.42(25)	3.49(22)	3.40(22)	0.42(19)	0.40(19)	-0.89(18)
C17	1.40(20)	3.57(21)	2.10(18)	-0.18(16)	0.04(15)	-0.15(15)
C18	2.24(22)	3.98(22)	2.61(20)	-0.37(18)	0.12(17)	-0.52(17)
C19	1.70(22)	5.4(3)	3.14(22)	-0.63(19)	-0.02(18)	-0,30(19)
C20	2.27(23)	4.64(25)	3.05(22)	-0.41(19)	-0.40(18)	0.43(18)
C21	2.01(21)	3.10(20)	1.96(18)	-0.29(16)	0.69(16)	0.41(15)
C22	2.99(24)	3.60(22)	2.67(20)	-0.34(18)	0.52(18)	0.83(17)
C23	2,57(23)	3.49(21)	2.98(21)	-0.79(18)	0.68(18)	0.35(17)
C24	2.44(22)	4.50(23)	2.31(19)	-0.25(18)	1.06(17)	0.49(17)

3. Crystallographic Data for the single crystal XRD of $^{n}Bu_2Ga[NH(2,6\text{-}Me_2C_6H_3)]_2[Li(Et_2O)]$

EXPERIMENTAL DETAILS

A. Crystal Data

Empirical Formula	GaON2C28H48Li
Formula Weight	505.35
Crystal Color, Habit	colourless, cube
Crystal Dimensions (mm)	0.200 x 0.200 x 0.200
Crystal System	monoclinic
No. Reflections Used for Unit Cell Determination (2Θ range)	25 (40 - 50°)
Lattice Parameters:	a = 8.6663(22) Å b = 22.305(3) Å c = 15.570 (3) Å β = 103.471 (17)°
Space Group	P 21/n
Z value	4
D_{calc}	1.147 g/cm^3
F_{000}	1089.11
μ(MoKa)	9.6 cm^{-1}

B. Intensity Measurements

Diffractometer	Rigaku AFC6S
Radiation	MoKa (X = 0.71069 Å)
Temperature	-148°C
Take-off Angle	6.0°
Detector Aperture	6.0 mm horizontal 6.0 mm vertical
Crystal to Detector Distance	40 cm
Scan Type	ω-2Θ
Scan Rate	4.0°/min (in omega) (3 rescans)
Scan Width	$(1.63 + 0.30 \tan\Theta)^{\circ}$
No. of Reflections Measured	Total: 5471 Unique: 5115
Corrections	none

C. Structure Solution and Refinement

Structure Solution	Patterson Method
Refinement	Full-matrix least-squares
Function minimized	$\Sigma w (\|Fo\| - \|Fc\|)$
Least-squares Weights	$4Fo^2/\sigma^2(Fo^2)$
Anomalous Dispersion	All non-hydrogen atoms
No. Observations ($I>2.50\sigma(I)$)	3518
No. Variables	326
Reflection/Parameter Ratio	6.73
Residuals: R; R_w	0.120; 0.050
Goodness of Fit Indicator	9.05
Maximum Peak in Final Diff. Map	$0.820 e^-/Å^3$
Minimum peak in Final Diff. map	$-0.780 e^-/Å^3$

Positional parameters and B(eq)

	x	y	z	B(eq)
Ga1	0.80463(13)	0.11109(4)	0.21246(7)	2.84(4)
O1	0.5338(8)	0.2873(3)	0.2676(6)	4.6(4)
N1	0.8032(9)	0.1569(3)	0.3235(5)	2.7(3)
N2	0.6423(9)	0.1637(3)	0.1348(5)	3.0(3)
C1	0.7703(10)	0.1226(4)	0.3945(6)	2.4(3)
C2	0.8943(10)	0.0976(4)	0.4601(6)	2.6(31
C3	0.8588(11)	0.0651(4)	0.5286(6)	3.1(4)
C4	0.7032(12)	0.0550(5)	0.5343(6)	3.7(5)
C5	0.5818(11)	0.0800(4)	0.4698(6)	3.0(4)
C6	0.6115(10)	0.1120(3)	0.3978(6)	2.6(41
C7	1.0647(11)	0.1052(4)	0.4552(7)	3.4(4)
C8	0.4754(11)	0.1376(5)	0.3278(8)	3.8(5)
C9	0.6687(11)	0.1856(4)	0.0560(6)	2.9(4)
C10	0.5988(11)	0.1582(4)	-0.0264(6)	3.2(4)
C11	0.6245(13)	0.1833(5)	-0.1040(7)	4.1(5)
C12	0.7196(15)	0.2332(6)	-0.1015(8)	4.7(5)
C13	0.7924(12)	0.2583(5)	-0.0232(8)	4.0(5)
C14	0.7677(12)	0.2354(4)	0.0560(7)	3.3(4)
C15	0.5021(14)	0.1021(5)	-0.0275(7)	4.4(5)
C16	0.8440(14)	0.2664(5)	0.1414(8)	4.5(5)
C17	0.7033(12)	0.0305(4)	0.2129(7)	3.5(4)
C18	0.7993(11)	-0.0136(4)	0.2797(6)	3.0(4)
C19	0.7133(11)	-0.0718(4)	0.2884(6)	3.0(4)
C20	0.5650(14)	-0.0625(5)	0.3230(8)	4.4(5)
C21	1.0160(15)	0.1181(7)	0.1845(9)	5.6(7)
C22A	0.997(3)	0.0842(15)	0.0918(17)	6.2(14)
C22B	1.123(5)	0.0738(23)	0.175(4)	14.7(36)
C23A	1.157(4)	0.0681(10)	0.0781(18)	6.0(15)
C23B	1.085(4)	0.0225(15)	0.1167.(22)	7.4(17)
C24A	1.234(4)	0.0170(14)	0.1248(17)	6.6(14)
C24B	1.184(4)	-0.0268(24)	0.1226(24)	10.6(26)
C25	0.4179(16)	0.3193(6)	0.2053(11)	6.5(7)
C26	0.3460(21)	0.2833(7)	0.1323(9)	7.2(8)
C27	0.5751(15)	0.3222(5)	0.3488(10)	5.3(6)
C28	0.6840(16)	0.2870(6)	0.4186(9)	5.7(6)
Li1	0.6459(21)	0.2134(7)	0.2470(15)	4.2(9)
H1	0.916	0.181	0.341	3.5
H2	0.531	0.139	0.124	3.8
H3	0.956	0.047	0.583	4.1
H4	0.674	0.028	0.589	4.3
H5	0.456	0.070	0.471	3.5

	x	y	z	B(eq)
H7C	1.075	0.132	0.397	4.2
H7A	1.136	0.129	0.514	4.2
H7B	1.123	0.063	0.450	4.2
H8C	0.519	0.163	0.280	3.5
H8A	0.401	0.101	0.294	3.5
H8B	0.399	0.167	0.357	3.5
H11	0.569	0.161	-0.170	4.7
H12	0.725	0.254	-0.166	5.9
H13	0.879	0.296	-0.023	4.6
H17A	0.682	0.011	0.146	3.6
H17B	0.584	0.036	0.227	3.6
H18A	0.834	0.009	0.346	3.4
H18B	0.915	-0.023	0.263	3.4
H19A	0.684	-0.094	0.226	4.0
H19B	0.796	-0.102	0.336	4.0
H20C	0.506	-0.105	0.330	5.0
H20A	0.595	-0.042	0.391	5.0
H20B	0.483	-0.034	0.281	5.0
H25A	0.467	0.358	0.176	7.0
H25B	0.320	0.337	0.232	7.0
H26C	0.256	0.307	0.084	6.4
H26A	0.435	0.266	0.101	6.4
H26B	0.288	0.245	0.156	6.4
H27A	0.469	0.333	0.374	6.7
H27B	0.633	0.364	0.341	6.7
H28C	0.717	0.310	0.481	5.4
H28A	0.627	0.244	0.430	5.4
H28B	0.791	0.275	0.397	5.4
H22AA	0.936	0.111	0.038	7.3
H22AB	0.930	0.042	0.093	6.6
H23AA	1.145	0.062	0.008	7.3
H23AB	1.232	0.106	0.100	7.3
H24AC	1.352	0.009	0.108	6.6
H24AA	1.225	0.019	0.195	6.6
H24AB	1.167	-0.025	0.103	6.6
H22BA	1.223	0.093	0.168	12.9
H22BB	1.158	0.051	0.246	12.9
H23BA	1.078	0.040	0.051	9.4
H23BB	0.971	0.005	0.120	9.4
H24BC	1.135	-0.059	0.069	8.7
H24BA	1.300	-0.014	0.116	8.7
H24BB	1.193	-0.049	0.185	8.7
H21A	1.107	0.097	0.236	6.7

	x	y	z	B(eq)
H21B	1.048	0.165	0.179	6.7
H15C	0.496	0.090	0.039	4.8
H15A	0.382	0.109	-0.067	4.8
H15B	0.555	0.065	-0.056	4.8
H16C	0.813	0.243	0.196	5.3
H16A	0.972	0.266	0.151	5.3
H16B	0.804	0.312	0.140	5.3

Thermal parameters (U values)

	U11	U22	U33	U12	U13	U33
Ga1	4.38(6)	2.21(5)	3.76(5)	-0.03(4)	0.06(4)	0.21(4)
O1	4.3(4)	3.1(4)	9.4(6)	0.4(3)	0.1(4)	1.6(4)
N1	3.3(4)	1.7(3)	4.9(5)	-0.5(3)	0.2(3)	-0.5(3)
N2	4.5(5)	2.7(4)	3.9(4)	-0.1(3)	0.3(3)	0.6(3)
C1	2.9(4)	2.7(4)	3.3(4)	-0.3(3)	0.5(3)	0.1(3)
C2	3.5(5)	2.9(4)	3.2(4)	-0.5(4)	-0.1(4)	-0.5(4)
C3	4.2(5)	3.8(5)	3.1(5)	-0.3(4)	-0.6(4)	-0.8(4)
C4	4.4(6)	5.8(6)	3.6(5)	-0.3(5)	0.5(4)	0.3(5)
C5	3.8(5)	3.8(5)	3.8(5)	-0.6(4)	0.9(4)	0.8(4)
C6	3.8(5)	0.6(3)	5.3(5)	-0.5(3)	0.9(4)	-0.4(3)
C7	2.7(5)	4.0(5)	5.4(6)	-0.2(4)	-0.7(4)	0.4(5)
C8	2.4(5)	5.2(6)	6.8(7)	0.1(4)	1.0(4)	0.9(5)
C9	3.6(5)	3.5(5)	3.9(5)	1.3(4)	0.6(4)	1.1(4)
C10	3.9(5)	4.2(5)	3.6(5)	1.3(4)	-0.1(4)	0.4(4)
C11	5.5(6)	5.4(6)	4.6(6)	1.4(5)	1.3(5)	0.8(5)
C12	6.5(7)	6.5(7)	5.7(7)	2.7(6)	3.1(6)	1.3(6)
C13	4.2(6)	4.5(6)	7.2(7)	0.9(5)	2.8(5)	0.4(5)
C14	4.3(5)	2.7(5)	5.6(6)	1.0(4)	1.5(5)	0.8(4)
C15	6.6(7)	4.8(6)	4.1(6)	-0.3(5)	-1.2(5)	-0.4(5)
C16	6.2(7)	3.6(6)	7.7(8)	-1.3(5)	2.5(6)	-1.1(5)
C17	5.1(6)	2.1(4)	5.2(6)	-0.2(4)	-0.7(5)	0.8(4)
C18	4.2(5)	2.5(4)	4.2(5)	0.0(4)	-0.2(4)	-0.1(4)
C19	4.1(5).	3.0(5)	4.1(5)	0.4(4)	0.1(4)	0.0(4)
C20	6.2(7)	3.8(6)	7.3(8)	0.7(5)	2.4(6)	0.8(5)
C21	5.7(7)	8.8(10)	7.5(9)	2.5(7)	2.8(6)	-1.0(7)
C22A	7.0(17)	11.8(25)	5.5(15)	3.1(17)	2.8(13)	2.3(16)
C22B	9.8(28)	19.2(46)	29.8(66)	-4.2(29)	10.4(37)	-18.1(48)
C23A	13.6(26)	2.9(11)	8.2(18)	1.4(13)	6.5(18)	1.3(11)
C23B	7.8(20)	9.5(23)	10.2(23)	-2.6(17)	0.8(17)	-5.3(19)
C24A	8.6(20)	8.8(21)	5.4(15)	-0.7(16)	-2.5(14)	0.7(14)
C24B	7.3(21)	23.5(53)	8.3(24)	2.3(27)	-0.4(18)	-4.9(29)
C25	6.6(8)	5.9(8)	10.8(12)	0.4(7)	-0.7(8)	4.1(8)
C26	13.3(14)	6.9(9)	5.1(8)	0.7(9)	-2.0(8)	1.5(7)
C27	6.7(8)	4.2(6)	10.8(11)	-1.3(6)	5.2(8)	-1.5(7)
C28	6.6(8)	7.9(9)	7.1(8)	-1.5(7)	1.1(7)	-2.9(7)
Li1	4.3(9)	2.6(8)	9.3(14)	0.8(7)	1.6(9)	0.4(9)

4. Crystallographic Data for the single crystal XRD of $[Li(thf)_2][Ga(N(SiMe_3)_2)(OSiMe_3)_2Cl]_2$

EXPERIMENTAL DETAILS

A. Crystal Data

Empirical Formula	GaSi4ClNC20H52Li
Formula Weight	595.08
Crystal Color, Habit	colourless, cube
Crystal Dimensions (mm)	0.400 x 0.200 x 0.300
Crystal System	monoclinic
No. Reflections Used for Unit Cell Determination (2Θ range)	25 (40 - 50°)
Lattice Parameters:	
	a = 16.719(7) Å
	b = 15.458(7) Å
	c = 26.490(4) Å
Space Group	C 2/c
Z value	8
D_{calc}	1.156 g/cm^3
F_{000}	2549.62
μ(MoKa)	10.60 cm^{-1}

B. Intensity Measurements

Diffractometer	Rigaku AFC6S
Radiation	MoKa (X = 0.71069 Å)
Temperature	-148°C
Take-off Angle	6.0°
Detector Aperture	6.0 mm horizontal 6.0 mm vertical
Crystal to Detector Distance	40 cm
Scan Type	ω-2Θ
Scan Rate	4.0°/min (in omega) (3 rescans)
Scan Width	$(1.63 + 0.30 \tan\Theta)^{\circ}$
$2\Theta_{max}$	40.0°
No. of Reflections Measured	Total: 6012 Unique: 5789

C. Structure Solution and Refinement

Structure Solution	Patterson Method
Refinement	Full-matrix least-squares
Function minimized	$\Sigma w (\|Fo\| - \|Fc\|)$
Least-squares Weights	$4Fo^2/\sigma^2(Fo^2)$
Anomalous Dispersion	All non-hydrogen atoms
No. Observations ($I>2.50\sigma(I)$)	3974
No. Variables	290
Residuals: R; R_w	.144, .078
Goodness of Fit Indicator	.078
Maximum Peak in Final Diff. Map	-1.540 $e^-/Å^3$
Minimum peak in Final Diff. map	0.940 $e^-/Å^3$

Positional parameters and B(eq)

	X	Y	Z	B(eq)
Ga1	0.78128(9)	0.49020(10)	0.11807(5)	2.36(6)
Si2	0.8529(3)	0.5994(3)	0.03260(15)	3.18(17)
Si1	0.6113(3)	0.5453(3)	0.15641(16)	3.42(17)
Cl1	0.8434(3)	0.5816(3)	0.17062(14)	3.91(16)
Si3	0.7293(3)	0.4587(3)	0.00632(15)	3.71(19)
Si4	0.8968(3)	0.3253(3)	0.13547(17)	3.59(18)
O2	0.8150(5)	0.3811(6)	0.1382(3)	2.7(4)
O1	0.6808(5)	0.4757(6)	0.1447(3)	2.7(4)
N2	0.7890(7)	0.5175(8)	0.0492(4)	2.8(5)
03	0.6527(7)	0.2601(8)	0.1603(5)	4.5(5)
04	0.7329(7)	0.3621(9)	0.2469(4)	4.6(6)
C4	0.9580(10)	0.5753(12)	0.0554(6)	4.2(7)
C5	0.8228(12)	0.7071(11)	0.0580(7)	4.6(8)
C6	0.8574(11)	0.6140(13)	-0.0377(6)	4.6(8)
C7	0.7890(15)	0.4055(14)	-0.0437(6)	6.0(11)
C16	0.5753(11)	0.2598(13)	0.1353(6)	4.7(8)
C8	0.6758(13)	0.3705(13)	0.0374(7)	5.2(9)
C9	0.6517(13)	0.5304(14)	-0.0269(6)	5.2(9)
C13	0.6616(12)	0.1760(12)	0.1839(7)	4.8(8)
C10	0.9187(13)	0.3023(14)	0.0692(9)	5.9(10)
C14	0.5768(13)	0.1450(14)	0.1929(7)	5.7(9)
C11	0.9836(12)	0.3838(18)	0.1644(9)	6.8(12)
C15	0.5236(13)	0.2171(15)	0.1751(6)	5.5(10)
C20	0.7984(14)	0.4082(22)	0.2709(7)	8.5(16)
C17	0.6777(14)	0.3366(14)	0.2839(6)	5.8(10)
C3	0.612(3)	0.636(3)	0.1124(21)	19.8(36)
C12	0.8801(15)	0.2208(18)	0.1675(12)	9.2(16)
C19	0.7749(20)	0.4283(24)	0.3214(10)	10.5(19)
C1	0.6242(21)	0.588(3)	0.2203(11)	13.6(23)
C18	0.7066(17)	0.3783(21)	0.3320(7)	8.9(15)
C2	0.5139(15)	0.4935(20)	0.1528(16)	11.2(23)
Li1	0.7175(15)	0.3611(17)	0.1700(7)	3.1(9)
H1C	0.683	0.623	0.224	12.1
H1A	0.578	0.636	0.227	12.1
H1B	0.623	0.539	0.248	12.1
H2C	0.511	0.437	0.180	10.3
H2A	0.465	0.537	0.164	10.3
H2B	0.497	0.468	0.116	10.3
H3C	0.603	0.614	0.074	19.3
H3A	0.563	0.681	0.121	19.3
H3B	0.668	0.671	0.117	19.3

	X	Y	Z	B(eq)
H4C	0.976	0.513	0.042	4.6
H4A	0.998	0.624	0.043	4.6
H4B	0.961	0.573	0.097	4.6
H5C	0.819	0.705	0.099	5.3
H5A	0.865	0.757	0.049	5.3
H5B	0.764	0.726	0.042	5.3
H6C	0.798	0.629	-0.055	5.3
H6A	0.897	0.667	-0.047	5.3
H6B	0.878	0.555	-0.056	5.3
H7C	0.824	0.453	-0.065	6.1
H7A	0.832	0.358	-0.028	6.1
H7B	0.750	0.371	-0.072	6.1
H8C	0.717	0.328	0.058	5.6
H8A	0.635	0.398	0.065	5.6
H8B	0.640	0.333	0.010	5.6
H9C	0.616	0.564	-0.001	5.8
H9A	0.683	0.580	-0.050	5.8
H9B	0.614	0.494	-0.053	5.8
H10C	0.869	0.268	0.050	6.4
H10A	0.929	0.362	0.048	6.4
H10B	0.972	0.262	0.067	6.4
H11C	0.992	0.444	0.145	7.0
H11A	0.975	0.395	0.204	7.0
H11B	1.037	0.343	0.161	7.0
H12C	0.867	0.231	0.206	8.7
H12A	0.830	0.187	0.148	8.7
H12B	0.933	0.181	0.165	8.7
H13A	0.693	0.131	0.160	5.4
H13B	0.696	0.182	0.220	5.4
H14A	0.569	0.131	0.233	5.8
H14B	0.563	0.087	0.171	5.8
H15A	0.466	0.192	0.160	5.6
H15B	0.510	0.261	0.206	5.6
H16A	0.555	0.325	0.125	5.3
H16B	0.574	0.222	0.100	5.3
H17A	0.616	0.357	0.272	6.6
H17B	0.676	0.266	0.288	6.6
H1BA	0.718	0.332	0.361	9.4
H18B	0.658	0.423	0.345	9.4
H19A	0.827	0.413	0.347	10.1
H19B	0.766	0.498	0.323	10.1
H20A	0.812	0.467	0.248	8.4
H20B	0.854	0.369	0.270	8.4

Thermal parameters (U values)

	U11	U22	U33	U12	U13	U23
Ga1	3.16(8)	3.44(8)	2.38(7)	-0.10(6)	0.04(6)	0.08(6)
Si2	4.76(25)	4.16(23)	3.17(20)	-0.15(19)	0.42(17)	0.48(17)
Si1	4.11(24)	4.72(25)	4.21(23)	0.70(19)	0.64(18)	-0.62(19)
Cl1	5.53(24)	5.65(24)	3.67(19)	-1.82(19)	0.15(17)	-1.48(17)
Si3	6.6(3)	5.3(3)	2.18(19)	-1.35(23)	-0.23(18)	0.22(18)
Si4	3.69(24)	5.3(3)	4.72(25)	0.97(20)	0.54(19)	1.19(21)
02	3.2(5)	4.3(5)	2.8(5)	0.0(4)	0.3(4)	1.4(4)
O1	3.5(5)	4.2(5)	2.7(5)	-0.2(4)	0.3(4)	1.2(4)
N2	3.9(7)	4.3(7)	2.4(5)	-0.5(5)	0.2(5)	0.7(5)
O3	4.7(7)	5.3(7)	6.9(8)	-2.1(6)	-1.4(6)	1.3(6)
O4	5.0(7)	9.0(9)	3.7(6)	-2.0(6)	0.2(5)	0.4(6)
C4	5.2(10)	6.9(12)	3.9(9)	-1.0(9)	1.1(7)	-0.4(8)
C5	7.5(13)	4.2(9)	5.9(11)	-0.7(9)	0.7(9)	0.5(8)
C6	6.4(11)	6.9(12)	4.1(9)	-1.3(9)	1.2(8)	0.1(8)
C7	12.5(19)	7.7(14)	2.7(8)	1.0(13)	1.4(10)	-1.4(9)
C16	6.9(12)	8.3(13)	2.6(8)	-2.4(10)	0.5(7)	0.7(8)
C8	8.7(14)	6.6(12)	4.5(9)	-3.0(11)	-1.3(9)	0.4(9)
C9	8.7(14)	8.9(14)	2.3(8)	0.2(11)	-0.2(8)	-0.4(8)
C13	7.6(13)	4.9(10)	5.8(11)	-0.6(9)	-0.4(9)	0.7(9)
C10	6.5(13)	6.5(13)	9.6(6)	0.7(10)	0.4(11)	-1.8(12)
C14	9.7(15)	7.8(14)	4.0(9)	-3.3(12)	-0.5(9)	2.7(9)
C11	4.7(12)	12.2(20)	8.8(16)	0.3(12)	-1.8(10)	1.8(15)
C15	8.8(14)	9.8(16)	2.5(8)	-1.9(12)	1.3(8)	0.2(9)
C20	8.5(16)	20.5(31)	3.2(10)	-5.9(19)	-0.7(10)	0.5(14)
C17	10.9(16)	8.9(15)	2.3(8)	-3.3(13)	3.0(9)	-0.1(9)
C3	21.0(40)	15.9(33)	40.0(70)	15.0(32)	21.6(46)	18.8(42)
C12	8.5(17)	10.1(20)	17.0(28)	4.8(15)	5.2(18)	7.6(20)
C19	14.7(27)	17.3(32)	7.8(17)	-7.5(25)	0.2(17)	-2.0(19)
C1	15.9(29)	26.4(45)	9.1(20)	11.3(30)	-1.2(19)	-11.2(26)
C18	14.3(23)	17.1(27)	3.0(10)	-3.6(20)	4.6(12)	-4.4(14)
C2	5.2(15)	10.4(22)	27.1(45)	-0.1(14)	1.2(20)	-6.6(26)
Li1	5.7(15)	5.5(15)	0.6(9)	-0.5(12)	1.1(9)	-0.6(9)

5. Crystallographic Data for the single crystal XRD of $[Li(py)_2][In(N(SiMe_3)_2(OSiMe_3)_3]$

EXPERIMENTAL DETAILS

A. Crystal Data $[Li(py)_2][In(N(SiMe_3)_2(OSiMe_3)_3]$

Empirical Formula	InSi5O3N3C25LiH55
Formula Weight	697.84
Crystal Color, Habit	colourless, cube
Crystal Dimensions (mm)	0.400 x 0.400 x 0.400
Crystal System	monoclinic
No. Reflections Used for Unit Cell Determination (2Θ range)	25 (40 - 50°)
Lattice Parameters:	a = 10.624(3) Å b = 17.778(4) Å c = 11.462(4)) Å β = 116.317(21)°
Space Group	P 21
Z value	2
D_{calc}	1.425 g/cm^3
F_{000}	843.88
μ(MoKa)	7.90 cm^{-1}

B. Intensity Measurements

Diffractometer	Rigaku AFC6S
Radiation	MoKa (X = 0.71069 Å)
Temperature	-148°C
Take-off Angle	6.0°
Detector Aperture	6.0 mm horizontal 6.0 mm vertical
Crystal to Detector Distance	40 cm
Scan Type	ω-2Θ
Scan Rate	4.0°/min (in omega) (3 rescans)
Scan Width	$(1.63 + 0.30 \tan\Theta)^{\circ}$
$2\Theta_{max}$	40.0°
No. of Reflections Measured	Total: 3740 Unique:3541

C. Structure Solution and Refinement

Structure Solution	Patterson Method
Refinement	Full-matrix least-squares
Function minimized	$\Sigma w (\|Fo\| - \|Fc\|)$
Least-squares Weights	$4Fo^2/\sigma^2(Fo^2)$
Anomalous Dispersion	All non-hydrogen atoms
No. Observations ($I>2.50\sigma(I)$)	3495
No. Variables	343
Residuals: R; R_w	0.039, 0.053
Goodness of Fit Indicator	2.89
Max Shift/Error in Final Cycle	0.21
Maximum Peak in Final Diff. Map	$1.94e^-/Å^3$
Minimum peak in Final Diff. map	$-1.090e^-/Å^3$

Positional parameters and B(eq)

	x	y	z	B(eq)
In1	0.80518(3)	0.21670	0.19091(3)	1.905(14)
Si1	0.76270(19)	0.30597(10)	-0.06956(15)	2.60(8)
Si2	0.97319(17)	0.36984(10)	0.19481(16)	2.34(7)
Si3	1.10962(17)	0.11684(10)	0.34785(17)	2.58(7)
Si4	0.59692(16)	0.27127(10)	0.32204(15)	2.25(7)
Si5	0.59903(18)	0.07267(10)	-0.01451(16)	2.56(7)
01	0.9627(4)	0.15396(25)	0.3310(4)	2.40(18)
02	0.7460(4)	0.23974(22)	0.3357(3)	1.94(16)
03	0.6576(5)	0.1491(3)	0.0645(4)	2.98(21)
N1	0.8429(5)	0.3086(3)	0.0982(5)	2.48(23)
N2	1.0155(5)	0.2158(4)	0.6384(4)	2.71(22)
N3	0.7898(6)	0.0784(3)	0.4861(5)	2.93(23)
C1	0.8019(10)	0.3925(5)	-0.1430(7)	4.3(4)
C2	0.5667(8)	0.3018(5)	-0.1338(7)	3.9(3)
C3	0.8236(8)	0.2227(5)	-0.1308(6)	3.4(3)
C4	1.1389(7)	0.3539(5)	0.1784(7)	3.7(4)
C5	0.9212(8)	0.4714(4)	0.1597(8)	3.9(4)
C6	1.0128(7)	0.3568(4)	0.3695(6)	3.1(3)
C7	1.2604(7)	0.1755(6)	0.4601(7)	4.1(4)
C8	1.1112(7)	0.1089(5)	0.1872(7)	3.7(3)
C9	1.1300(9)	0.0210(6)	0.4223(10)	5.3(5)
C10	0.4575(7)	0.2021(6)	0.2357(7)	4.4(4)
C11	0.6069(8)	0.2868(6)	0.4853(7)	4.6(4)
C12	0.553(10)	0.3617(6)	0.2295(11)	6.2(6)
C13	0.7474(9)	0-0073(5)	0.0118(9)	5.0(4)
C14	0.4770(9)	0.0242(5)	0.0360(7)	4.4(4)
C15	0.4948(8)	0.0928(5)	-0.1941(6)	3.9(4)
C16	1.0166(7)	0.2901(4)	0.6627(7)	3.2(3)
C17	1.1073(8)	0.3227(5)	0.7772(8)	4.3(4)
C18	1.2009(8)	0.2780(6)	0.8770(8)	4.9(4)
C19	1.1970(8)	0.2022(6)	0.8545(7)	5.2(4)
C20	1.1051(8)	0.1739(5)	0.7330(7)	3.9(3)
C21	0.7481(9)	0.0254(5)	0.3933(7)	4.3(4)
C22	0.7428(10)	0.0736(5)	0.5740(9)	4.8(5)
C23	0.6412(12)	0.0179(7)	0.5642(13)	7.7(8)
C24	0.6597(11)	-0.0321(6)	0.3825(9)	6.4(5)
C25	0.6058(11)	-0.0356(8)	0.4741(14)	8.2(7)
Li1	0.8884(10)	0.1720(6)	0.4573(9)	2.6(4)
H1C	0.916	0.397	-0.107	5.1
H1A	0.754	0.387	-0.248	5.1
H1B	0.763	0.442	-0.115	5.1

	x	y	z	B(eq)
H2C	0.529	0.349	-0.102	4.6
H2A	0.518	0.302	-0.242	4.6
H2B	0.536	0.250	-0.104	4.6
H3C	0.802	0.171	-0.091	4.5
H3A	0.769	0.220	-0.236	4.5
H3B	0.935	0.227	-0.101	4.5
H4C	1.170	0.295	0.197	4.6
H4A	1.120	0.367	0.079	4.6
H4B	1.222	0.389	0.244	4.6
H5C	0.897	0.483	0.059	4.5
H5A	0.831	0.482	0.176	4.5
H5B	1.008	0.507	0.223	4.5
H6C	0.919	0.366	0.382	4.0
H6A	1.051	0.300	0.400	4.0
H6B	1.093	0.396	0.430	4.0
H7C	1.260	0.180	0.553	4.7
H7A	1.358	0.150	0.471	4.7
H7B	1.253	0.231	0.418	4.7
H8C	1.100	0.164	0.143	4.9
H8A	1.208	0.084	0.197	4.9
H8B	1.023	0.074	0.122	4.9
H9C	1.040	-0.014	0.359	5.9
H9A	1.224	-0.004	0.434	5.9
H9B	1.126	0.026	0.515	5.9
H10C	0.450	0.192	0.139	5.0
H10A	0.479	0.150	0.288	5.0
H108	0.357	0.224	0.224	5.0
H11C	0.630	0.236	0.541	5.9
H11A	0.688	0.329	0.539	5.9
H11B	0.507	0.309	0.477	5.9
H12C	0.638	0.402	0.283	7.2
H12A	0.548	0.353	0.135	7.2
H12B	0.457	0.384	0.223	7.2
H13C	0.819	0.034	-0.018	5.2
H13A	0.801	-0.008	0.113	5.2
H13B	0.706	-0.043	-0.047	5.2
H14C	0.528	0.011	0.139	5.2
H14A	0.387	0.061	0.018	5.2
H14B	0.437	-0.027	-0.019	5.2
H15C	0.411	0.131	-0.211	4.3
H15A	0.564	0.119	-0.231	4.3
H15B	0.454	0.042	-0.248	4.3
H16	0.943	0.326	0.587	4.1

	x	y	z	B(eq)
H17	1.104	0.383	0.790	5.5
H18	1.276	0.302	0.971	5.5
H19	1.270	0.166	0.930	5.7
H20	1.105	0.112	0.717	4.6
H21	0.786	0.030	0.320	4.8
H22	0.776	0.115	0.653	6.0
H23	0.599	0.019	0.633	9.4
H24	0.635	-0.076	0.306	6.1
H25	0.533	-0.079	0.473	7.6

Thermal parameters (U values)

	U11	U22	U33	U12	U13	U23
In1	2.549(15)	2.189(16)	2.637(15)	-0.141(16)	1.274(13)	-0.125(16)
Si1	4.57(10)	2.76(9)	2.62(8)	-0.17(8)	1.65(7)	0.25(7)
Si2	3.14(8)	2.37(8)	3.74(8)	-0.57(7)	1.85(7)	-0.39(7)
Si3	2.54(8)	3.10(9)	4.22(9)	0.62(7)	1.54(7)	0.34(8)
Si4	2.55(7)	3.14(9)	3.02(7)	0.55(7)	1.39(6)	0.30(7)
Si5	3.40(8)	2.46(9)	2.87(8)	-0.51(7)	0.50(7)	-0.45(61
01	2.71(20)	3.42(24)	3.12(20)	0.73(18)	1.41(17)	0.89(18)
02	2.42(18)	2.87(22)	2.40(17)	0.02(15)	1.35(15)	-0.15(14)
03	4.41(25)	3.07(25)	3.26(221	-1.01(20)	1.16(20)	-1.13(18)
N1	3.6(3)	3.3(3)	3.01(24)	0.02(22)	1.88(21)	0.01(21)
N2	3.40(22)	3.8(3)	2.74(21)	0.3(3)	1.02(18)	0.5(3)
N3	3.8(3)	3.5(3)	3.6(3)	0.19(24)	1.38(23)	0.54(23)
C1	8.3(6)	3.9(4)	3.5(4)	-0.6(4)	2.0(4)	0.9(3)
C2	5.0(4)	4.5(4)	4.4(4)	0.7(4)	1.2(3)	0.4(3)
C3	6.9(4)	3.1(4)	3.6(3)	0.0(4)	2.8(3)	-0.2(3)
C4	3.6(3)	5.1(5)	6.3(4)	-0.6(3)	3.1(3)	-0.4(4)
C5	5.2(4)	2.6(4)	5.8(4)	-0.1(3)	1.4(4)	-0.5(3)
C6	4.1(3)	4.2(4)	3.2(3)	-1.4(3)	1.5(3)	-0.9(3)
C7	3.1(3)	7.5(6)	4.6(4)	0.1(4)	1.4(3)	-0.1(4)
C8	4.1(3)	5.6(5)	5.6(4)	-0.1(3)	3.1(3)	-1.4(4)
C9	6.0(5)	5.0(5)	9.0(6)	2.1(4)	3.2(5)	2.0(5)
C10	3.7(3)	7.5(7)	5.5(4)	-1.1(4)	2.2(3)	-2.2(4)
C11	5.0(4).	8.4(7)	4.9(4)	1.6(4)	2.9(4)	-0.9(4)
C12	6.9(6)	6.6(6)	11.1(8)	3.6(5)	5.1(6)	4.8(6)
C13	4.6(4)	4.3(5)	8.1(6)	0.6(4)	1.0(4)	-1.6(4)
C14	5.4(4)	5.9(5)	4.6(4)	-2.7(4)	1.3(3)	0.0(4)
C15	5.9(4)	4.3(4)	2.9(3)	-0.4(4)	0.4(3)	-0.4(3)
C16	4.8(4)	3.1(4)	4.2(3)	0.0(3)	2.0(3)	0.4(3)
C17	5.6(4)	5.5(5)	6.1(4)	-1.4(4)	3.3(4)	-2.2(4)
C18	4.4(4)	8.5(7)	4.7(4)	-0.8(4)	1.2(3)	-1.9(4)
C19	5.3(4)	8.7(8)	3.7(3)	2.2(5)	0.1(3)	0.0(4)
C20	4.7(4)	5.3(5)	4.2(4)	1.1(4)	1.5(3)	0.2(4)
C21	7.1(5)	4.6(5)	3.7(3)	-1.3(4)	1.5(3)	0.0(3)
C22	8.9(6)	3.8(4)	7.7(5)	1.4(4)	5.8(5)	1.3(4)
C23	9.1(8)	8.9(9)	15.1(11)	2.4(7)	9.0(8)	6.0(8)
C24	8.4(7)	6.3(6)	5.7(5)	-3.3(5)	-0.6(5)	0.5(5)
C25	6.5(6)	7.3(8)	14.6(11)	-2.7(6)	2.3(7)	3.5(8)
Li1	3.1(5)	3.9(6)	2.4(4)	0.3(4)	0.6(4)	0.3(4)

References

1. Strite, S. and Morkoc, H., *J. Vac. Technol. B*, **1992**, *10(4)*, p. 1237.

2. Cowley, A. H., *J. Organomet. Chem.*, **1990**, *400*, p. 71.

3. H. Isum and A. C. Rose-Innes, Semiconducting III-V Compounds, Pergamon Press, London (1961).

4. Pauling, The Nature of the Chemical Bond, Cornell University Press, Ithaca (1960).

5. Paciorek, K. J. L., Nakahara, J. H., and Masuda, S. R., *Inorg. Chem.*, **1990**, *29*, p. 4252.

6. Nutt, W. R., Anderson, J. A.,Odom, J. D., Williamson, M. M., and Rubin, B. H., *Inorg. Chem.*, **1985**, *24*, p. 159.

7. (a) Wells, R. L., *Coord. Chem. Rev.*, **1992**, *112*, p. 273. and references therein. (b) Wells, R. L., Pasterczyk, J. W., McPhail, A. T., Johanssen, J. D., and Alvanipour, A., *J. Organomet. Chem.*, **1991**, *407*, p. 17.

8. Wells, R. L., McPhail, and Speer, T. M., *Organometallics*, **1992**, *11*, p. 960.

9. Wells, R. L., McPhail, A. T, and Self, M. F., *Organometallics*, **1992**, *11*, p. 221.

10. Wells, R. L., Aubuchon, S. R., and Self, M. F., *Organometallics*, **1992**, *11*, p. 3370.

11. Buhro, W. E., *Polyhedron*, **1994**, *13*, p. 1131.

12. (a) Wells, R. L., Self, M. F., McPhail, A. T., and Aubuchon, S. R., *Organometallics*, **1993**, *12*, p. 2832. (b) Aubuchon, S. R., McPhail, A. T., and Wells, R. L., *Chem. Mater.*, **1994**, *6*, p. 82.

13. (a) Wells, R. L, Pitt, C. G., McPhail, A. T., Purdy, A. P., Schafieezad, S., Hallock, R. B., *Chem. Mater.*, **1989**, *1*, p. 4. (b) Wells, R. L, Pitt, C. G., McPhail, A. T., Purdy, A. P., Schafieezad, S., Hallock, R. B., *Mater. Res. Soc. Symp. Proc.*, **1989**, *131*, p. 45.

14. Olshavsky, M. A., Goldstein, A. N., Alivisatos, A. P., *J. Am. Chem. Soc.*, **1990**, *112*, p. 9438.

15. Wells, R. L, Hallock, R. B., McPhail, A. T., Pitt, C. G., and Johanssen, J. D., *Chem. Mater.*, **1991**, *3*, p. 381.

16. Wells, R. L, Aubuchon, S. R., Kher, S. S., Lube, M. S., *Chem. Mater.*, **1995**, *7*, p. 793.

17. (a) Healy, M. D., Laibinis, P. E., Stupik, P. D., and Barron, A. R., *Chem. Commun.*, **1989**, p. 359. (b) Healy, M. D., Laibinis, P. E., Stupik, P. D., and Barron, A. R., *Mat. Res. Soc. Symp. Proc.*, **1989**, *131*, p. 83.

18. Cowley, A. H., and Jones, R. A., *Angew. Chem. Int. Ed. Engl.*, **1989**, *28*, p. 1208. and references therein.

19. Wells, R. L, Purdy, A. P., McPhail, A. T.,and Pitt, C. G., *J. Organomet. Chem.*, **1986**, *308*, p. 281.

20. Golubinskaya, L. M., Golbinskii, A. V., Mastryukov, V. S., Vilkov, L. V., and Bregadze, V. I., *J. Organomet. Chem.*, **1976**, *117*, p. C4.

21. Bradley, D. C., Dawes, H. M., Frigo, D. M., Hursthouse, M. B., and Hussain, B., *J. Organomet. Chem.*, **1987**, *325*, p. 55.

22. Bradley, D. C., Dawes, H. M., Hursthouse, M. B., Smith, L. M., and Thornton-Pett, M., *Polyhedron*, **1990**, *9*, p. 343.

23. Atwood, D. A., Jones, R. A., Cowley, A. H., Bott, S. G., and Atwood, J. L., *J. Organomet. Chem.*, **1992**, *434*, p. 143.

24. Cowely, A. H., Harris, P. R., Jones, R. A., and Nunn, C. M., *Organometallics*, **1991**, *10*, p. 652.

25. Atwood, D. A., Cowely, A. H., Harris, P. R., Jones, R. A., Koschmieder, S. U., Nunn, C. M., Atwood, J. L., and Bott, S. G., *Organometallics*, **1993**, *12*, p. 24.

26. Interrante, L. V., Sigel, G. A., Garbauskas, M., Hejna, C., and Slack, G. A., *Inorg. Chem.*, **1989**, *28*, p. 252.

27. Hwang, J. W., Hanson, S. A., Britton, D., Evans, J. F., Jensen, K. F., and Gladfelter, W. L., *Chem. Mater.*, **1990**, *2*, p. 342.

28. Almond, M. J., Drew, M. G. B, Jenkins, C. E., and Rice, D. A., *J. Chem. Soc., Dalton Trans.*, **1992**, p. 5.

29. Sauls, F. C., Interrante, L. V., and Jiang, Z., *Inorg. Chem.*, **1990**, *29*, p. 2989.

30. Coates, G. E. and Whitecomb, R. A., *J. Chem. Soc.*, **1956**, p. 3351.

31. Bertolet, D. C. and Rogers, Jr., J. W., *J. Phys. Chem.*, **1991**, *95*, p. 4453.

32. (a) Jones, J. I., and McDonald, W. S., *Proc. Chem. Soc.*, **1962**, p. 366. (b) McDonald, T. R. R., and McDonald, W. S., *Acta Crystallogr. Sect. B*, **1972**, *28*, p. 1619.

33. Belgardt, T., Waezsada, S. D., Roesky, H. W., Gornitzka, L. H., and Stalke, D., *Inorg. Chem.*, **1994**, *33*, p. 6247. (b) Belgardt, T., Roesky, H. W., Noltemeyer, M., and Schmidt, H-G., *Angew. Chem. Int. Ed. Engl.*, **1993**, *32(7)*, p. 1056.

34. Stuczynski, S. M., Opila, R. L., Marsh, P., Brennan, J. G., and Steigerwald, M. L., *Chem. Mater.*, **1991**, *3*, p. 379.

35. Trentler, T. J., Hickman, K. M., Goel, S. C., Viano, A. M., Gibbons, P. C. and Buhro, W. E., *Science*, **1995**, *270*, p. 1791.

36. Aitchison, K. A., Backer-Dirks, J. D. J., Bradley, D. C., Faktor, M. M., Frigo, D. M., Hursthouse, M. B., Hussain, B., and Short, R. L., *J. Organomet. Chem.*, **1989**, *366*, p. 11.

37. Neumuller, B., *Chem. Ber.*, **1989**, *122*, p. 2283.

38. Neumayer, D. A., Cowley, A. H., Decken, A., Jones, R. A., Lakhotia, V., and Ekerdt, J. G., *J. Am. Chem. Soc.*, **1995**, *117*, p. 5893.

39. Lakhotia, V., Heitzinger, J. M., Cowley, A. H., Jones, R. A., and Ekerdt, J. G., *Chem. Mater.*, **1994**, *6*, p. 871.

40. Atwood, D. A., Atwood, V. O., Cowley, A. H., Jones, R. A., Atwood, J. L., and Bott, S. G., *Inorg. Chem.*, **1994**, *33*, p. 3251.

41. Burger, H., Cichon, J, Goetze, U., Wannagat, U.,und Wismar, U., *J. Organomet. Chem.*, **1977**, *33*, p. 1.

42. Petrie, M. A., Ruhlandt-Senge, K., Hope, H., and Power, P. P., *Bull. Soc. Chem. Fr.*, **1993**, *130*, p. 851.

43. Purdy, A. P., *Inorg. Chem.*, **1994**, *33*, p. 282.

44. Mehrotra R. C., and Rai, A. K., *Polyhedron*, **1991**, *10*, p. 1967.

45. Uchida, H., Matsunaga, T., Yoneyama, H., Sakata, T., Mori, H., and Sasaki, T., *Chem. Mater.*, **1993**, *5*, p. 716.

46. Byrne, E. B., Douglas, T., and Theopold, K. H., *Mater. Res. Soc. Symp. Proc.*, **1989**, *131*, p. 59.

47. Buhro, W. E. and Theopold, K. H., *Inorg. Chem.*, **1991**, *30*, p. 594.

48. Rogers, J. H., Apblett, A. W., Cleaver, W. M., Tyler, A. N., and Barron, A. R., *J. Chem Soc. Dalton Trans.*, **1992**, p. 3179. and references therein.

49. Healy, M. D., Ziller, J. W., and Barron, A. R., *Organometallics*, **1991**, *10*, p. 597.

50. Von Grosse, A., and Mavity, J. M., *J. Org. Chem.*, **1940**, *5*, p. 106.

51. Cleaver, W. M., Barron, A. R., McGufey, A. R., and Bott, S. G., *Polyhedron*, **1994**, *13*, p. 2831.

52. Tuck, D. G., Comprehensive Organometallic Chemistry (Ed: Wilkinson, G., Stone, F. G. A., and Abel, E. W.), Vol. 1, Pergamon Press, Oxford (1982).

53. Schmidbaur, H., und Schindler, F., *Chem. Ber.*, **1966**, *99*, 2178.

54. Petrie, M. A., Olmstead, M. M., and Power, P. P., *J. Am. Chem. Soc.*, **1991**, *113*, p. 8704.

55. Cleaver, W. M.and Barron, A. R., *Organometallics*, **1993**, *12*, p. 1001.

56. Bradley, D. C., Chudzynska, H., Frigo, D. M., Hursthouse, M. B., and Mazid, M. A., *J. Chem. Soc., Chem. Commun.*, **1988**, p. 1258.

57. Al-Juaid, S. S., Buttrus, N. H., Eaborn, C., Hitchcock, P. B., Roberts, A. T. L., Smith, D., and Sullivan, A. C., *J. Chem. Soc., Chem. Commun.*, **1986**, p. 908.

58. Power, M. B., Cleaver, W. M., Apblett, A. W., Barron, A. R., and Ziller, J. W., *Polyhedron*, **1992**, *11*, p. 477.

59. Cleaver, W. M.and Barron, A. R., *J. Am. Chem. Soc.*, **1989**, *111*, p. 8966.

60. Brindley, P. B., The Chemistry of Peroxides (Ed. S. Patai), Wiley, London, (1983).

61. MacInnes, A. N., Power, M. B., and Barron, A. R., *Chem. Mater.*, **1992**, *4*, p. 11.

62. Power, M. B. and Barron, A. R., *J. Chem. Soc., Chem. Commun.*, **1991**, p. 1315.

63. Chatterjee, S., Bindal, S. R., and Mehrotra, R. C., *J. Indian Chem. Soc.*, **1976**, *L3*, p. 867.

64. Schmidbaur, H., *Angew. Chem.*, **1965**, *4*, p. 169.

65. Bradley, D. C., Frigo, D. M., Hursthouse, M. B., and Hussain, B., *Organometallics*, **1988**, *7*, p. 1112.

66. Brothers, P. J., Wehmschulte, M. M. O., Ruhlandt-Senge, K., Parkin, S. R. and Power, P. P., *Organometallics*, **1994**, *13*, p. 2792.

67. Amonoo-Neizer, E. H., Shaw, R. A., Skovlin, D. O., and Smith, B. C., Inorganic Syntheses, (Ed. H. F. Holtzclaw, Jr.), McGraw-Hill, New York, 1966.

68. Wallwork, S. C. and Worrall, I. J., *J. Chem. Soc.*, **1965**, p. 1816.

69. Joint Committee for Powder Diffraction Data, Center for Diffraction Data, PA, Card No. 2-1078

70. Wells, R. L., Baldwin, R. A., White, P. S., Pennington, W. T., Rheingold, A. L., and Yap, G. P. A., *Organometallics*, **1996**, *15*, p. 91.

71. Joint Committee for Powder Diffraction Data, Center for Diffraction Data, PA, Card No. 32-397.

72. Kover, R. A., Derr, H., Brandau, D., and Callaway, J. O., *Inorg. Chem.*, **1975**, *14*, p. 2809.

73. Joint Committee for Powder Diffraction Data, Center for Diffraction Data, PA, Card No. 32-452.

74. Joint Committee for Powder Diffraction Data, Center for Diffraction Data, PA, Card No. 5-642.

75. Todt, E. *Z. Anorg. Alleg. Chem.*, **1963**, *321*, p. 120.

76. For an example, please see Beachley, O. T., Noble, M. J., Churchill, M. R., and Lake, C. H., *Organometallics*, **1992**, *11*, p. 1051.

77. Burger, Cichon, Goetz, Wannagat, and Wismar, *J. Organomet. Chem.*, **1971**, *33*, p. 1.

78. Funk. E. A., and Paul, T., *Zeit. Anorg. Allg. Chem.*, **1965**, *337*, p. 145.

79. Heller, S. R. and Milne, G. W. A., EPA/NIH Mass Spectral Data Base, Vol. 1, 1978.